New Challenges in Azole Resistance Selection in *Aspergillus fumigatus*

Yinggai Song

RADBOUD UNIVERSITY PRESS

Radboud Dissertation Series

New Challenges in Azole Resistance Selection in *Aspergillus fumigatus*

The work presented in this thesis was carried out within the Radboudumc Research Institute for Medical Innovation, Nijmegen, the Netherlands; Peking University First Hospital, Beijing, China.

During the research, Yinggai Song was supported by National Key Research and Development Program of China (Grant No: 2021YFC2300400) and National Natural Science Foundation of China (Grant No: 82272354). Parts of the study were supported by a grant from the Wellcome Trust (Grant No: 219551/Z/19/Z).

Financial support from Radboudumc Research Institute for Medical Innovation for printing this thesis is gratefully acknowledged.

New Challenges in Azole Resistance Selection in *Aspergillus fumigatus*
Yinggai Song

Radboud Dissertation Series
ISSN: 2950-2772 (Online); 2950-2780 (Print)

Published by RADBOUD UNIVERSITY PRESS
Postbus 9100, 6500 HA Nijmegen, The Netherlands
www.radbouduniversitypress.nl

Design: Yinggai Song
Cover:Yinggai Song
Printing: DPN Rikken/Pumbo

ISBN: 9789465152042
DOI: 10.54195/9789465152042
Free download at: https://doi.org/10.54195/9789465152042

RADBOUD
UNIVERSITY
PRESS

New Challenges in Azole Resistance Selection in *Aspergillus fumigatus*

Proefschrift ter verkrijging van de graad van doctor

aan de Radboud Universiteit Nijmegen

op gezag van de rector magnificus prof. dr. J.M. Sanders,

volgens besluit van het college voor promoties in het openbaar te verdedigen op

woensdag 4 februari 2026

om 12.30 uur precies

door

Yinggai Song

geboren op 5 december 1986

te Henan, China

Promotor:

Prof. dr. P.E. Verweij

Copromotoren:

Dr. W.J.G. Melchers

Prof. dr. G.S. de Hoog

Manuscriptcommissie:

Prof. dr. R.J.M. Brüggemann

Prof. dr. M. Lackner (Medizinische Universität Innsbruck, Oostenrijk)

Prof. dr. M. Richardson (The University of Manchester, Verenigd Koninkrijk)

Contents

Appendix

CHAPTER 1

General introduction and outline of the thesis

INTRODUCTION

The opportunistic fungal pathogen *Aspergillus fumigatus* presents a growing threat to immunocompromised populations, with rising resistance to first-line triazole antifungals. As the predominant etiological agent of invasive aspergillosis (IA), this pathogen's treatment efficacy is increasingly undermined by resistance mechanisms, particularly the characteristic *cyp51A* mutations TR_{34}/L98H and TR_{46}/Y121F/T289A that confer pan-azole resistance. While environmental selection pressure from agricultural azole fungicides remains the primary driver of resistance, concerning cases of host-adapted resistance are emerging in patients undergoing long-term azole therapy for chronic aspergillosis.

This thesis presents a comprehensive examination of the complex issue of azole resistance in *A. fumigatus*, integrating multidisciplinary approaches to explore its evolutionary pathways, underlying mechanisms, and clinical consequences. The study culminates in a synthesis of key findings that assess emerging challenges in resistance selection, discuss implications for clinical management and public health policy, and propose actionable strategies for future research. Together, these insights advance our understanding of the drivers of azole resistance and contribute to ongoing efforts to preserve the efficacy of antifungal agents in both medical and agricultural contexts.

A. fumigatus and aspergillosis

Aspergillus species are filamentous fungi that are ubiquitously present in the environment. Among them, *A. fumigatus* is a clinically significant opportunistic pathogen capable of causing a spectrum of diseases in humans and animals (Singh et al., 2025; Castro-Ríos et al., 2025; Dieste-Pérez et al., 2025). This saprophytic fungus thrives on decaying organic matter, producing vast quantities of airborne conidia that can be inhaled, leading to pulmonary infections in immunocompromised hosts.

Recognizing its global health impact, the World Health Organization (WHO) has classified *A. fumigatus* as one of the four fungal pathogens of highest public health concern, alongside *Candida albicans*, *Cryptococcus neoformans*, and *C. (Candidozyma) auris* (WHO fungal priority pathogens list). The most severe disease manifestation is IA, a life-threatening condition characterized by fungal tissue invasion and high mortality if untreated. High-risk populations including patients with hematological malignancies, solid organ or hematopoietic stem cell transplant recipients, critically ill individuals with severe influenza or COVID-19, those with chronic pulmonary diseases, and patients receiving immunosuppressive therapies

(Feys et al., 2024; van de Veerdonk et al., 2025; Verweij et al., 2021; Alanio et l., 2020; Verweij et al., 2020; Ullmann et al., 2018)

IA remains a challenging clinical management issue. Infection occurs through inhalation of environmentally dispersed conidia, which originate from *Aspergillus*'s natural reservoirs in compost. Despite hospital-based preventive measures to reduce fungal spore exposure, vulnerable patient groups continue to face significant infection risks (Singh et al., 2025).

Azole resistance in *Aspergillus fumigatus*

The management of aspergillosis primarily relies on azole antifungals, which target the fungal cytochrome P450 lanosterol 14α-demethylase (CYP51) - a key enzyme in ergosterol biosynthesis (Hagiwara et al., 2016; Chowdhary et al., 2017). Among the clinically available triazoles, itraconazole (1992), voriconazole (2002), posaconazole (2006), and isavuconazole (2015) have demonstrated potent activity against *Aspergillus* species, with voriconazole and isavuconazole being the recommended first-line treatments for IA.

Despite their clinical efficacy, treatment failures remain common due to multiple factors including the patient's refractory underlying conditions, constraints in reducing immunosuppressive therapy, and the presence of disseminated fungal infection.

A major contributing factor to therapeutic failure is azole resistance in *A. fumigatus*, which has become an increasing concern in both clinical and environmental settings (Barber et al., 2020). The primary mechanism of resistance involves mutations in the *cyp51A* gene encoding the CYP51 target enzyme. These mutations, particularly in the active site region, alter the enzyme's structural conformation and significantly reduce its binding affinity for azole drugs (Chowdhary et al., 2013, 2015; Bader et al., 2013). The emergence and global spread of azole-resistant *A. fumigatus* strains pose a severe and escalating threat to public health, rendering first-line treatments ineffective and significantly increasing morbidity and mortality rates.

The emergence of azole-resistant *A. fumigatus* has been increasingly documented in both agricultural and domestic environments. Resistance hotspots are particularly prevalent in agricultural/horticultural settings with intensive azole fungicide use (Schoustra et al., 2019), while resistant strains have also been detected in residential areas (Lavergne et al., 2017; Paluch et al., 2019). A nationwide citizen science initiative in the UK demonstrated that 14% of *A. fumigatus* isolates collected from residential gardens showed elevated minimum inhibitory concentrations (MICs) to

tebuconazole, indicating reduced azole susceptibility (Shelton et al., 2022). Whole-genome sequencing analyses have provided evidence for environmental acquisition of resistance, revealing striking genomic similarities between clinical isolates and azole-resistant strains from environmental sources.

Resistance Mechanisms in *Aspergillus fumigatus*

Environmental Origins as Primary Driver

Medical azole resistance in *A. fumigatus* is increasingly linked to environmental selection pressures, particularly the widespread agricultural use of structurally similar azole fungicides, surpassing clinical selection during long-term patient therapy (Snelders et al., 2009, 2012; Fisher et al., 2022). Resistant strains thrive in fungicide-contaminated environments like compost, plant matter, and even garden soil (14% UK samples positive for TR_{34}/L98H), creating significant reservoirs for human infection (Snelders et al., 2009; Shelton et al., 2022; Rhodes et al., 2022). Agricultural triazole fungicides (e.g., tebuconazole) exert cross-selection pressure; their residues persist in soil (>6 months) and correlate with ambient air prevalence of resistant spores (1–14%) (van Rhijn & Rhodes 2025).

Whole-genome sequencing confirms near-identical sequences between environmental hotspots and clinical isolates, establishing direct environment-to-patient transmission via inhalation of resistant spores as a primary route, rather than frequent de novo evolution during therapy (Rhodes et al., 2022; Snelders 2025).

Dominant genetic resistance mechanisms in *A. fumigatus* encompass three primary pathways: (1) Environment-selected mutations such as TR_{34}/L98H and TR_{46}/Y121F/T289A in *cyp51A*, which confer cross-resistance to medical triazoles (Snelders et al., 2009, 2012); (2) Novel hybrid mutations generated through recombination of environmental and clinical alleles (e.g., TR_{34}/L98H/T289A/I364V/G448S), enabling pan-azole resistance (MICs >16 mg L^{-1}) against all medical triazoles (Rhodes, 2022; Abdolrasouli, 2022); and (3) Non-*cyp51A* mechanisms including *cyp51* paralogue copy-number variation and aneuploidy, serving as rapidly inducible resistance strategies (van Rhijn & Rhodes, 2025).

Global Spread, Host Adaptation and Evolutionary Drivers

Chronic aspergillosis patients can harbor phenotypically diverse yet genetically clonal azole-resistant isolates (e.g., distinct morphotypes like altered pigmentation/sporulation but identical resistance genotypes) (Abdolrasouli &

Rhodes, 2022). This phenotypic diversity despite high genetic relatedness suggests roles for epigenetic regulation, stress adaptation, or gene expression changes (Abdolrasouli & Rhodes, 2022). Long-term azole therapy in chronic diseases (e.g., cystic fibrosis) provides strong selection pressure, driving microevolution and generating new resistance variants (including novel recombinant genotypes) within patients (Ballard et al., 2018; Rhodes et al., 2022; Abdolrasouli, 2022).

Four synergistic accelerators propel the rapid evolution and worldwide spread of azole-resistant *Aspergillus fumigatus*. First, intrinsic hyper-recombination—the highest reported meiotic crossover rate—works in concert with parasexual recombination within biofilms (e.g., cystic-fibrosis airways) to generate novel resistance haplotypes at unprecedented speed (Auxier et al., 2023; Engel et al., 2020). Second, multi-fungicide co-selection: TR_{34}/TR_{46} haplotypes not only withstand medical triazoles but also display cross-resistance to benzimidazoles, SDHIs, and QoIs, eroding the efficacy of triazole-centric stewardship programs (Snelders, 2012; Snelders, 2025). Third, environmental hotspots—compost heaps and azole-treated flower bulbs—maintain large fungal populations under sustained chemical pressure, providing fertile ground for adaptive mutations (Schoustra et al., 2019; Zhang et al., 2022). Finally, global clonal expansion has yielded more than 200 genetically streamlined clonal groups, exemplified by the TR_{34}/L98H lineage found across continents in both clinical and environmental samples (Sewell et al., 2019; Snelders, 2025). With negligible correlation between genetic and geographic distances, airborne spores and human-mediated transport disseminate these clones without geographic barriers, making single-source attribution virtually impossible (Sewell et al., 2019).

Diagnostic, Therapeutic, and One Health Challenges in Azole Resistance

Azole-resistant *Aspergillus fumigatus* poses severe clinical threats, driving 47% mortality in IA among immunocompromised patients (Lestrade et al., 2019). Diagnosis is hampered by low sensitivity of culture, which undermines culture-based methods and necessitates molecular tools like *cyp51A* sequencing and AsperGenius® PCR (Rhodes et al., 2022). Conventional PCR assays targeting only TR_{34}/L98H and TR_{46}/Y121F/T289A and changing azole phenotypes in TR_{34}/L98H and TR_{46}/Y121F/T289A isolates—including novel SNP variants and wild-type *cyp51A* strains with alternative resistance mechanisms, which hampers the use of current PCR-based resistance tests (Lestrade et al., 2020; Postina et al., 2018). While culture-based MIC determination remains the reference method, its low sensitivity in ICU patients and inability to resolve mixed infections highlight the

urgent need for next-generation sequencing and multi-locus amplicon panels to capture the expanding resistance spectrum.

Resistance complexity extends beyond genetic mutations: even azole-susceptible isolates form "persister" subpopulations that survive supra-MIC voriconazole exposure without genetic changes, confounding MIC-based diagnostics (Scott, 2023). Genetically identical colonies may exhibit morphological divergence in sputum, implying epigenetic or microenvironmental resistance modulation (Abdolrasouli, 2022). To address these challenges, novel assays like *TEF1α* metabarcoding detect cryptic resistance alleles at ≤2 genome copies in respiratory DNA and reveal silent reservoirs undetected by culture (Weaver, 2024). This underscores the transition from de novo resistance during therapy to environmentally acquired resistance, demanding integrated clinical-environmental surveillance.

Agricultural fungicide misuse directly compromises medical azole efficacy, necessitating sustainable stewardship (Snelders et al., 2012; Sewell et al., 2019). Resistance hotspots emerge where intensive farming overlaps with clinical populations, requiring integrated monitoring of air, water, plant waste, and hospital environments. Current surveillance underestimates environmental reservoirs; high-throughput *TEF1α* sequencing (Weaver, 2024) and air-sample qPCR (Kortenbosch, 2022) are proposed as complementary tools. Whole-genome epidemiology confirms clonal spread but cannot attribute individual infections due to ubiquitous spore dispersal via transnational networks (Snelders, 2025). Policy interventions must therefore target all fungicide classes and address cross-border dispersal.

This thesis, titled "New Challenges in Azole Resistance Selection in *Aspergillus fumigatus*", delves into the multifaceted nature of this crisis, moving beyond simply documenting resistance to dissecting its origins, mechanisms, dynamics, and clinical impact. We confront the novel challenges presented by this evolving landscape, particularly the environmental selection pressure and the remarkable adaptability of the pathogen itself. The central aim is to provide a deeper, more integrated understanding of azole resistance selection to inform effective surveillance, diagnostic, therapeutic, and environmental stewardship strategies.

OUTLINE OF THIS THESIS

This thesis is structured to systematically investigate key facets of the azole resistance challenge in *A. fumigatus*:

Chapter 2 presents a comprehensive genomic and phenotypic analysis of triazole-resistant *A. fumigatus* isolates collected in the Netherlands over nearly three decades (1994-2022). This longitudinal study tracks the emergence, evolution, and dissemination of resistance mechanisms, providing crucial insights into temporal trends and the rise of environmentally linked resistance genotypes.

Chapter 3 shifts focus to the functional impact of genetic variation within predominant resistance backgrounds. It specifically investigates how individual single nucleotide polymorphisms (SNPs) and combinations thereof modulate the azole resistance phenotype in strains harboring the widespread TR_{34}/L98H allele, revealing nuances beyond the core mutation that influence clinical resistance levels.

Chapter 4 directly addresses the critical link between agricultural fungicide use and clinical resistance. By characterizing the "agricultural fungicide resistance signature" in resistant isolates, this chapter provides evidence for the environmental selection hypothesis and explores the potential pathways connecting agrochemical use to human disease.

Chapter 5 explores an intrinsic factor contributing to the pathogen's adaptability: an accelerated mutator phenotype. This chapter investigates how increased mutation rates in specific *A. fumigatus* strains facilitate rapid adaptive evolution, potentially accelerating the development of resistance to azoles and other stressors within both environmental and clinical niches.

Chapter 6 broadens the perspective through a systematic review, analyzing susceptibility patterns and drug resistance not only in aspergillosis but also in mucormycosis patients. This comparative analysis highlights the specific challenges posed by Aspergillus resistance within the broader context of difficult-to-treat mold infections.

Chapter 7 integrates the findings from the preceding chapters into a General Discussion, critically evaluating the new challenges in azole resistance selection, discussing the implications for clinical practice and public health policy, and proposing directions for future research to combat this urgent threat.

Collectively, this thesis aims to advance our understanding of the complex forces driving azole resistance in *A. fumigatus*, emphasizing the novel challenges posed by environmental selection and pathogen evolution. By integrating genomic, phenotypic, environmental, evolutionary, and clinical perspectives, it strives to contribute significantly to the global effort to preserve the efficacy of our vital antifungal armamentarium.

REFERENCE

Alanio A, Dellière S, Fodil S, Bretagne S, Mégarbane B. Prevalence of putative invasive pulmonary aspergillosis in critically ill patients with COVID-19. *Lancet Respir Med.* 2020; 8: e48-e49.

Bader O, Weig M, Reichard U, Lugert R, Kuhns M, Christner M, et al. Cyp51A-based mechanisms of aspergillus fumigatus azole drug resistance present in clinical samples from Germany. *Antimicrob Agents Chemother*. 2013; 57:3513–3517.

Barber AE, Riedel J, Sae-Ong T, et al. Effects of agricultural fungicide use on *Aspergillus fumigatus* abundance, antifungal susceptibility, and population structure. *mBio.* 2020; 11: e02213-e02220.

Ballard E, Melchers WJG, Zoll J, Brown AJP, Verweij PE, Warris A. In-host microevolution of *Aspergillus fumigatus*: A phenotypic and genotypic analysis. *Fungal Genet Biol*. 2018; 113:1-13.

Castro-Ríos K, Buri MCS, Ramalho da Cruz AD, Ceresini PC. *Aspergillus fumigatus* in the Food Production Chain and Azole Resistance: A Growing Concern for Consumers. *J Fungi (Basel)*. 2025; 11:252.

Chowdhary A, Sharma C, Meis JF. Azole-resistant aspergillosis: epidemiology, molecular mechanisms, and treatment. *J Infect Dis*. 2017;216: S436–444.

Chowdhary A, Kathuria S, Xu J, Meis JF. Emergence of azole-resistant Aspergillus fumigatus strains due to agricultural azole use creates an increasing threat to human health. *PLoS Pathog*. 2013;9: e1003633.

Chowdhary A, Sharma C, Hagen F, Meis JF. Exploring azole antifungal drug resistance in Aspergillus fumigatus with special reference to resistance mechanisms. *Future Microbiol*. 2014;9:697–711.

Dieste-Pérez L, Holstege MMC, de Jong JE, Heuvelink AE. Azole resistance in *Aspergillus* isolates from animals or their direct environment (2013-2023): a systematic review. *Front Vet Sci*. 2025; 12:1507997.

Feys S, Carvalho A, Clancy CJ, Gangneux JP, Hoenigl M, Lagrou K, Rijnders BJA, Seldeslachts L, Vanderbeke L, van de Veerdonk FL, Verweij PE, Wauters J. Influenza-associated and COVID-19-associated pulmonary aspergillosis in critically ill patients. *Lancet Respir Med*. 2024; 12:728-742.

Fisher MC, Alastruey-Izquierdo A, Berman J, Bicanic T, Bignell EM, Bowyer P, Bromley

M, Brüggemann R, Garber G, Cornely OA, Gurr SJ, Harrison TS, Kuijper E, Rhodes J, Sheppard DC, Hagiwara D, Watanabe A, Kamei K, Goldman GH. Epidemiological and genomic landscape of azole resistance mechanisms in Aspergillus fungi. *Front Microbiol*. 2016; 7:1382.

Paluch M, Lejeune S, Hecquet E, Prévotat A, Deschildre A, Fréalle E. High airborne level of *Aspergillus fumigatus* and presence of azole-resistant TR_{34}/L98H isolates in the home of a cystic fibrosis patient harbouring chronic colonisation with azole-resistant H285Y *A. fumigatus*. *J Cyst Fibros.* 2019; 18: 364-367.

Rhodes J, Abdolrasouli A, Dunne K, Sewell TR, Zhang Y, Ballard E, Brackin AP, van Rhijn N, Chown H, Tsitsopoulou A, Posso RB, Chotirmall SH, McElvaney NG, Murphy PG, Talento AF, Renwick J, Dyer PS, Szekely A, Bowyer P, Bromley MJ, Johnson EM, Lewis White P, Warris A, Barton RC, Schelenz S, Rogers TR, Armstrong-James D, Fisher MC. Population genomics confirms acquisition of drug-resistant *Aspergillus fumigatus* infection by humans from the environment. *Nat Microbiol*. 2022;7:663-674.

Schoustra SE, Debets AJM, Rijs AJMM, et al. Environmental hotspots for azole resistance selection of *Aspergillus fumigatus*, the Netherlands. *Emerg Infect Dis.* 2019; 25: 1347–53.

Lavergne RA, Chouaki T, Hagen F, et al. Home environment as a source of life-threatening azole-resistant *Aspergillus fumigatus* in immunocompromised patients. *Clin Infect Dis.* 2017; 64: 76-8.

Lestrade PPA, Buil JB, van der Beek MT, Kuijper EJ, van Dijk K, Kampinga GA, Rijnders BJA, Vonk AG, de Greeff SC, Schoffelen AF, van Dissel J, Meis JF, Melchers WJG, Verweij PE. Paradoxal trends in azole-resistant *Aspergillus fumigatus* in a national multicenter surveillance program, the Netherlands, 2013-2018. *Emerg Infect Dis*. 2020; 26:1447-1455.

Postina P, Skladny J, Boch T, Cornely OA, Hamprecht A, Rath PM, Steinmann J, Bader O, Miethke T, Dietz A, Merker N, Hofmann WK, Buchheidt D, Spiess B. Comparison of two molecular assays for detection and characterization of *Aspergillus fumigatus* triazole resistance and *Cyp51A* mutations in clinical isolates and primary clinical samples of immunocompromised patients. *Front Microbiol*. 2018. 27;9:555.

Shelton JMG, Collins R, Uzzell CB, et al. Citizen science surveillance of triazole-resistant *Aspergillus fumigatus* in United Kingdom residential garden soils. *Appl Environ Microbiol.* 2022; 88: e0206121.

Singh A, Singh J, Kumar S. Aspergillosis: A comprehensive review of pathogenesis,

drug resistance, and emerging therapeutics. *J Food Drug Anal*. 2025;33:75-96.

Ullmann AJ, Aguado JM, Arikan-Akdagli S, et al. Diagnosis and management of *Aspergillus* diseases: executive summary of the 2017 ESCMID-ECMM-ERS guideline. *Clin Microbiol Infect.* 2018; 24: Suppl 1: e1-e38.

van de Veerdonk FL, Carvalho A, Wauters J, Chamilos G, Verweij PE. *Aspergillus fumigatus* biology, immunopathogenicity and drug resistance. *Nat Rev Microbiol*. 2025 May 2. doi: 10.1038/s41579-025-01180-z.

Verweij PE, Brüggemann RJM, Azoulay E, Bassetti M, Blot S, Buil JB, Calandra T, Chiller T, Clancy CJ, Cornely OA, et al. 2021. Taskforce report on the diagnosis and clinical management of COVID-19 associated pulmonary aspergillosis. *Intensive Care Med.* 47:819–834.

Verweij PE, Rijnders BJA, Brüggemann RJM, Azoulay E, Bassetti M, Blot S, Calandra T, Clancy CJ, Cornely OA, Chiller T, et al. Review of influenza-associated pulmonary aspergillosis in ICU patients and proposal for a case definition: an expert opinion. *Intensive Care Med*. 2020; 46:1524–1535.

Warris A, White PL, Xu J, Zwaan B, Verweij PE. Tackling the emerging threat of antifungal resistance to human health. *Nat Rev Microbiol*. 2022; 20:557-571.

World Health Organization. WHO fungal priority pathogens list to guide research, development and public health action [Internet]. 2022. Available from: https://www.who.int/publications/i/item/9789240060241.

Zhang J, Verweij PE, Rijs AJMM, Debets AJM, Snelders E. Flower Bulb Waste Material is a Natural Niche for the Sexual Cycle in *Aspergillus fumigatus*. *Front Cell Infect Microbiol*. 2022. 21; 11:785157.

CHAPTER 2

Triazole-resistant *Aspergillus fumigatus* in the Netherlands between 1994 and 2022: a genomic and phenotypic study

Yinggai Song • Jochem B Buil • Johanna Rhodes • Jan Zoll • Marlou Tehupeiory-Kooreman • Mehmet Ergün • Jianhua Zhang • Ruoyu Li • Thijs Bosch • Willem J G Melchers • Paul E Verweij

Lancet Microbe. 2025 Jun 20:101114. doi: 10.1016/j.lanmic.2025.101114.

Abstract

Objectives *Aspergillus fumigatus* is the main cause of invasive aspergillosis (IA) and triazole antifungals represent primary treatment options. The effectiveness of triazole therapy is hampered by the emergence of resistance, mainly caused by TR_{34}/L98H and TR_{46}/Y121F/T289A mutations in the *cyp51A*-gene, which correspond with signature triazole resistance phenotypes. We investigated the occurrence of triazole phenotype and genotype variation over a 29-year period in the Netherlands.

Methods 12,679 clinical *A. fumigatus* isolates from Dutch hospitals collected since Jan 6, 1994 were screened for resistance using agar-based methods, and characterized by sequencing of the *cyp51A*-gene and in vitro susceptibility testing using EUCAST reference method. Whole-genome sequencing (WGS) was performed on selected isolates, including those harboring TR_{34} variants, high-frequency SNPs, and wild-type strains. Clinical information was collected for Radboud University Medical Centre (RUMC) between January 1st 2017 and December 31st 2022.

Results In total, 1,979 (15·6%) *A. fumigatus* isolates harboured Cyp51A triazole resistance mutations, predominately TR_{34}/L98H *sensu stricto* (*ss*) in 67·6% and TR_{46}/Y121F/T289A *ss* in 16·8% of resistant isolates. Phenotype and genotype variations were observed in 325 (17·2%) triazole-resistant isolates harbouring a TR-resistance mechanism, including 12 *cyp51A*-genotype variants. WGS showed that isolates with combinations of TR_{34}- and TR_{46}-based polymorphisms seemed to be derived from separate populations, but there was some overlap. Fifty-nine cases of proven/probable IA were identified, including 13 triazole-resistant cases of which three were caused by genotype variants. Mixed genotype infection was observed in 11 of 13 patients and the number of antifungal treatment switches was higher compared with triazole-susceptible disease ($p<0·001$).

Conclusions Our study showed variation in triazole genotypes and phenotypes in clinical *A. fumigatus* isolates with *cyp51A*-mediated resistance, some of which were cultured from triazole-resistant IA cases. Triazole resistance variation and mixed *A. fumigatus* genotypes represents a major challenge in clinical management of *Aspergillus* diseases as our current molecular diagnostic tools will increasingly fail to predict the resistance phenotype, underscoring the need for improved detection methods.

Keywords: *Aspergillus fumigatus*, triazole resistance, *cyp51A* mutations, whole genome sequencing, phylogenetics

Research in context

Evidence before this study

Previous studies have identified signature *cyp51A*-gene mutations, i.e. TR_{34}/L98H and TR_{46}/Y121F/T289A, as dominant mechanisms in triazole-resistant *Aspergillus fumigatus* isolates. We reviewed the evidence between database inception and Jan 1, 2024, for the occurrence and frequency of variations in these signature resistance mutations by searching the National Library of Medicine article database and medRxiv for preprint publications, using the terms "*Aspergillus fumigatus*", "azole", "voriconazole", "itraconazole", "posaconazole" "isavuconazole", "resistance", and "*cyp51A*-gene". We found 186 studies that report variations of the two signature resistance mutations involving additional short nucleotide polymorphisms (SNPs) or variations in the tandem repeat (TR) sequence or copy number. Especially recent studies since 2021 involving environmental sampling reported many *cyp51A*-gene variants, but to our knowledge, there are no studies that have investigated the epidemiology of variants in triazole-resistant *A. fumigatus* recovered from patient samples.

Added value of this study

This study investigated a large collection of clinical *A. fumigatus* isolates, to determine variations in phenotypes and genotypes associated with *cyp51A*-mutations as well as the clinical implications thereof. Our study shows that phenotype variations occur in isolates with TR_{34}/L98H and TR_{46}/Y121F/T289A mutations, while additional SNPs in the *cyp51A*-gene may confer phenotype variations, but frequently not in all isolates harboring these additional SNPs. These observations underscore the complexity of triazole resistance mechanisms in *A. fumigatus*, pointing towards non-CYP51A- mediated (but unknown) mechanisms that contribute to the triazole phenotype. We furthermore show that variant isolates are involved in azole-resistant IA and that pulmonary IA is in principle caused by mixed genotypes. Although the clinical relevance of mixed genotype infection is limited in triazole susceptible infection, it challenges our ability to demonstrate or rule-out resistance in triazole-resistant disease. Indeed, resistance can easily be overlooked when single *A. fumigatus* colonies are used for MIC testing, which is recommended in protocols for in vitro susceptibility testing.

Implications of all the available evidence

Resistance phenotype and genotype variations may represent the next challenge in triazole resistance management in *A. fumigatus*, as we recovered resistance variants from patients with IA and observed frequent mixed genotype infections. The high frequency of novel drug-resistant polymorphism combinations may result from the exceptional cross-over rate which was observed in *A. fumigatus*. These variations challenge our ability to reliably predict the triazole phenotype in patients with *Aspergillus* diseases. Especially in culture-negative patients we rely on resistance *Aspergillus* PCR, which uses specific pre-selected markers to detect resistance. New diagnostic techniques, such as sequence-based approaches, are needed that enable detection of genotype variations, including mechanisms outside the *cyp51A*-gene. Our findings furthermore underscore the need for international One Health resistance surveillance programs for *A. fumigatus*.

Introduction

Aspergillus fumigatus can cause a broad-spectrum of diseases in humans, with emerging risk groups for invasive aspergillosis (IA) including severe influenza and COVID-19 (Ullmann et al., 2018; Alanio et al., 2020).The triazoles itraconazole (approved in 1992), voriconazole (2002), posaconazole (2006) and isavuconazole (2015), show activity against *Aspergillus* species, and voriconazole and isavuconazole are recommended first-line therapy for patients with IA (Ullmann et al., 2018). The clinical use of triazoles has improved the survival of patients with IA, but treatment failure remains common, which may be due to refractory underlying conditions, inability to reduce immunosuppression and disseminated *Aspergillus* disease. Furthermore, voriconazole resistance was shown to be associated with a 25% lower day-90 survival rate in *A. fumigatus* culture-positive IA patients compared to those with voriconazole-susceptible IA (Lestrade et al., 2019).

There are increasing reports on triazole-resistant *A. fumigatus* isolates recovered from the environment (Barber et al., 2020). In addition to environmental hotspots that are associated with agricultural fungicide applications (Schoustra et al., 2019), triazole-resistant *A. fumigatus* strains were also recovered from the home environment (Lavergne et al., 2017; Paluch et al., 2019). A recent citizen science study showed that 14% of *A. fumigatus* isolates cultured from residential garden samples in the United Kingdom with non-wildtype tebuconazole MICs (Shelton et al., 2022). Genomic epidemiological studies furthermore show closely related

environmental and clinical triazole-resistant *A. fumigatus* isolates, supporting an environment-to-patient transmission route (Rhodes et al., 2022).

Although TR_{34}/L98H and TR_{46}/Y121F/T289A remain the dominant genotypes in triazole-resistant *A. fumigatus* isolates recovered from clinical and environmental samples, variants that involve additional single nucleotide polymorphisms (SNPs) or additional tandem repeats (TRs) in the *cyp51A*-gene promoter have been reported. A TR_{34}/L98H/S297T/F495I variant was recovered from a clinical sample obtained in 1998 (Snelders et al., 2010), indicating that TR-variations were present when the TR_{34}/L98H mutation was first reported. Since then, this variant has been detected in various countries, and the F495I SNP was shown to be associated with resistance to imidazoles (Liu et al., 2015; Chen et al., 2018). The recent citizen science study in the United Kingdom reported 17 TR_{34}-variants, including TR_{34}, TR_{34}/L98H with various additional SNPs in the *cyp51A*-gene and one isolate with a TR_{34}-duplication in the gene promoter (Shelton et al., 2022). These observations indicate that over time the number of TR-variants may be increasing, although advances in molecular techniques may have also contributed to this increase.

We determined the presence of variants in a large collection of clinical *A. fumigatus* isolates from the Netherlands and investigated if the number of genotype and phenotype variants increased over time and if these variants were involved in triazole-resistant IA.

Methods

Study design and samples

The Radboud University Medical Centre (RUMC) serves as mycology reference laboratory for Dutch hospitals and has collected and stored clinical *A. fumigatus* isolates since 1994, including isolates cultured from patients admitted to our centre, isolates sent from hospitals for identification and in vitro susceptibility testing, and isolates sent by centres that contribute to the national *Aspergillus* resistance surveillance program. We included all *A. fumigatus* isolates collected between Jan 6, 1994, and Dec 31, 2022. Specimens were incubated at 28°C and 37°C and if the colony morphology was consistent with *A. fumigatus*, the isolate was incubated at 48°C. At this temperature growth of cryptic species is unlikely, but if there was concern regarding atypical colony morphology and microscopic morphology or growth rate a beta-tubulin sequence was performed to identify or rule out cryptic species. The surveillance protocol was submitted to the institutional Medical

Research Ethics Committee of RUMC (CMO) who indicated that the study was waived from the evaluation procedure as anonymous information was used (December 2020).

Triazole resistance screening and variant identification

When available up to five *A. fumigatus* colonies were subjected to azole-containing screening agar, initially Sabouraud agar containing 4 mg/l of itraconazole and later VIPcheck^{TM} screening agar (BMproducts, the Netherlands), which contains itraconazole, voriconazole and posaconazole. Isolates were stored at -70^{o}C in 10% glycerol and in vitro susceptibility testing was performed using the EUCAST microdilution reference method (EUCAST 2020). Minimal inhibitory concentrations (MICs) were determined for itraconazole, voriconazole, posaconazole, isavuconazole (since 2014) and olorofim (since 2018). The following triazole resistance breakpoints were used: MIC >0·25 mg/l for posaconazole, >1 mg/l for itraconazole and voriconazole, and >2 mg/l for isavuconazole (Arendrup et al., 2020). For *A. fumigatus* isolates with a triazole-resistant phenotype, the full *cyp51A*-gene including its promoter was analysed by PCR amplification and sequencing (Mellado et al., 2001). The *cyp51A* sequence (GenBank accession no. AF338659) was used for SNP analysis.

To investigate phenotype variation, we defined a core MIC-range that included the most prevalent triazole MIC +/- 2 dilution steps for isolates harbouring TR_{34}/L98H *sensu stricto (ss)* or TR_{46}/Y121F/T289A *ss* mutations. A phenotype variant was defined as a TR_{34}/L98H *ss* or TR_{46}/Y121F/T289A *ss* isolate with a non-core MIC for any of the triazoles. A genotype variant was defined as an isolate that harboured additional mutations in the *cyp51A*-gene or its promoter region in TR_{34}/L98H and TR_{46}/Y121F/T289A harbouring isolates. For F46Y harbouring isolates pT-335C/pC-70T/F46Y/iC7T/ iC66T/M172V/E427K was considered the *ss* genotype as these mutations were present in all genotypes. Single and multiple SNPs in the *cyp51A*-gene in the absence of TRs were counted as individual variants.

Genomic and phylogenetic analysis

Genome DNA extraction was followed by the cetyltrimethylammonium bromide (CTAB) protocol adapted from the RUMC mycology laboratory (Arentshorst et al., 2012). Genomic DNA libraries were constructed with NovoSeq NGS DNA Library Prep Set (Novogene, Cambridge, UK). Prepared whole-genome libraries were sequencing on an Illumina NovaSeq 6000 at Novogene (Cambridge, UK), generating 150 bp paired-end reads. Raw reads were aligned to the *A. fumigatus* reference genome Af293 (ASM265v1 GCF_000002655.1) using BWA mem v0.7.17. SAMtools v1.16.1

was used to post-process the alignment prior to variant calling with GATK HaplotypeCaller v4.2.6.1 to generate GVCFs excluding repetitive regions (identified by RepeatMasker v4.0.6) (Li et al., 2013; Li et al., 2009; Smit et al., 2023). Low-confidence variants were filtered if they met at least one of the criteria: QD < 2.0, FS > 60.0, MQ < 40.0, MQRankSum < -12.5, ReadPosRankSum < -8.0 SOR > 4.0 DP < 5 and GQ < 50. Filtered SNPs were mapped to genes using snpEff v5.1.

Phylogenetic analysis was carried out on whole genome SNP data were converted to presence/absence of a SNP that has been determined as high confidence in the filtering step with respect to reference. Any SNPs identified as low confidence in the variant filtration step were assigned to missing. These data were converted to FASTA format and maximum parsimony phylogenies were created using RAxML v8.2.9, with the GTRCAT model of rate heterogeneity. Maximum-likelihood phylogenies were also constructed using RAxML v8.2.9 using rapid bootstrap analysis over 750 replicates and GTRCAT model of rate heterogeneity. Final phylogenies were visualised in R v4.2.1 using the ggtree package v3.6.2.

To identify significant loci *treeWAS* was performed on isolates from four groups: TR_{34}/L98H *ss* with MICs within the core MIC (19 isolates) and outside the core MIC (20 isolates), and TR_{34}/L98H genotypic variants with MICs inside the core MIC (2 variants, 30 isolates) and with MICs outside the core MIC (3 variants, 13 isolates)(appendix p3-10) (Collins et al., 2018). All raw reads have been deposited to the European Nucleotide Archive (ENA) under project accession PRJEB74938.

Genetic similarity and population allocation was investigated *via* Principal Component Analysis (PCA) using whole-genome SNP data in R v4.3.2 using package *ade4* v1.7-22 (Ter et al., 2017). Plots were constructed in R v4.3.2 using package *mapmixture* v1.1.0 (Jenkins et al., 2024).

Clinical implications of triazole resistance

Clinical information was collected for isolates cultured between Jan 1, 2017, and Dec 31, 2022 at RUMC using microbiological records with one year follow-up. Initial selection criterion was a positive *A. fumigatus* culture from BAL, bronchial washings, and tissue biopsies. Subsequently, the presence of IA was determined using the EORTC/MSGERC and FUNDICU case definitions (Donnelly et al., 2020; Bassetti et al., 2024). Data collected for IA patients included underlying disease, initial and final IA classification, initial and follow-up antifungal therapy, ICU admission at diagnosis, survival, triazole phenotype and genotype, and the presence of mixed *A. fumigatus* infection. Mixed infection was defined as the recovery of multiple *A. fumigatus*

genotypes and phenotypes during the infection episode. IA patients were excluded if other molds were identified in BAL, bronchial washing, and tissue specimens. Patients with triazole-susceptible IA were excluded if any history of a triazole-resistant isolate was recorded.

Statistical analysis

We calculated geomean MICs with GraphPad Prism 8.02 (https://www.graphpad.com). For calculations, we recoded MICs >16 mg/L as 32 mg/L. Differences in MIC distributions were analysed using Kruskal-Wallis test, and Fisher exact test was used to detect differences in classification according to clinical breakpoints. Two-way ANOVA and linear regression were used to investigate the difference between the resistant and non-resistant isolates over time. A *p*-value cut-off of 0·01 for all three tests of association (subsequent, simultaneous, and terminal) between the triazole phenotype and genotype groups were used. Bonferonni *p*-value correction was also performed. Only the subsequent test results were used as this is the most effective at detecting subtle patterns of association. Overrepresented gene ontology (GO) and KEGG pathway terms were assessed using FungiDB (Alvarez-Jarreta et al., 2024). Triazole-resistant and triazole-susceptible IA groups were compared for number of switches in antifungal therapy using Mann-Whitney Test and survival using Kaplan-Meier estimates.

Role of the funding source

The funders of the study had no role in study design, data collection, data analysis, data interpretation, or writing of the report.

Results

Between 1994 and 2022, 12,679 *A. fumigatus* isolates from clinical samples were screened for triazole resistance and the presence of cyp51A-mediated mutations (Figure S1). Overall, 1,979 (15·6%) triazole-resistant *A. fumigatus* isolates were identified that harboured mutations in the *cyp51A*-gene, involving five groups: TR_{34} (1,432 isolates), TR_{46} (455 isolates), TR_{53} (1 isolate), F46Y (38 isolates) and single SNPs (52 isolates), and a single isolate harbouring pC-70T/G54E/iC7T/iC66T/M172V (Figure 1a, 1b). The first resistance mutation was detected in 1995 in an isolate harbouring pT-335C/pC-70T/F46Y/iC7T/iC66T/M172V/E427K (Figure 1a) and in 1998 two isolates harbouring TR_{34}/L98H/S297T/F495I. TR_{34}/L98H *ss* was first detected in 2000 and was since then recovered each year. This mutation was the most frequent resistant

mechanism among the triazole-resistant isolates (1,338 (67·6%) isolates) followed by TR_{46}/Y121F/T289A *ss* which was present in 332 (16·8%) isolates and first observed in 2009 (Table 1). The third most frequent resistance mutation was F46Y present in 38 isolates and first cultured in 1995, while single SNPs were first recovered in 2002 (Figure 1a). An increasing trend of triazole-resistant *A. fumigatus* isolates was noted, which significantly correlated with increasing number of isolates over time (Figure S1).

	Itraconazole	Voriconazole	Posaconazole	Isavuconazole*
TR_{34}/Leu98His sensu stricto (n=1338)				
Geometric mean MIC, mg/L	28·24	4·91	0·69	7·81
MIC_{50}, mg/L	32	4	0·5	8
MIC_{90}, mg/L	32	16	2	16
Range, mg/L	0·12 to >16	0·5 to >16	0·016 to >16	0·5 to >16
Resistant, % (n)	99·5% (1331)	99·0% (1324)	87·7% (1173)	97·0% (906)
ATU-resistant, % (n)	1·5% (20)	17·9% (239)	11·7% (156)	1·5% (20)
ATU-susceptible, % (n)	0	0	0	0·2% (2)
TR_{46}/Tyr121Phe/Thr289Ala sensu stricto (n=332)				
Geometric mean MIC, mg/L	5·95	26·68	0·62	24·45
MIC_{50}, mg/L	8	32	0·5	32
MIC_{90}, mg/L	32	32	1	32
Range, mg/L	0·25 to >16	1 to >16	0·125 to >16	2 to >16
Resistant, % (n)	71·7% (238)	99·7% (331)	80·1% (266)	99·7% (1)
ATU-resistant, % (n)	14·5% (48)	0	3·6% (12)	0·3% (1)
ATU-susceptible, % (n)	0	0	14·8% (49)	0

ATU=area of technical uncertainty. MIC=minimum inhibitory concentration. MIC_{50}=minimum inhibitory concentration that inhibits the growth of 50% of the tested microorganisms. MIC_{90}=minimum inhibitory concentration that inhibits the growth of 90% of the tested microorganisms. TR=tandem repeat. *Isavuconazole MICs were not measured before 2014.

Table 1: **Triazole phenotypes for TR_{34}/Leu98His sensu stricto and TR_{46}/Tyr121Phe/Thr289Ala sensu stricto isolates**

Triazole-resistant phenotypes

According to EUCAST clinical breakpoints, a pan-triazole-resistant phenotype was present in 916 of 1,338 (68·5%) TR_{34}/L98H *ss* isolates, in 106 of 332 (31·9%) TR_{46}/Y121F/T289A *ss* isolates and in 16 of 38 (42·1%) F46Y isolates. Overall, 1,920 of 1,979 (97·0%) triazole-resistant *A. fumigatus* isolates were voriconazole-resistant, including 308 isolates (15·6%) with a voriconazole MIC of 2 mg/l (ATU-resistant).

Underlying resistance *cyp51A* mutations detected in the 1,920 voriconazole-resistant isolates included TR_{34} (1,406; 71·0%), and TR_{46} (453 isolates; 22·9%). All voriconazole-resistant isolates were cross-resistant to isavuconazole, with exception of six isolates that were isavuconazole-susceptible (MIC 1 mg/l), including four TR_{34} isolates and one isolate with pC-70T/G54E/iC7T/iC66T/ M172V and pT-335C/pC-70T/F46Y/iC7T/iC66T/M172V/E427.

Phenotype variation

A broad range of MICs was observed for TR_{34}/L98H *ss* and TR_{46}/Y121F/T289A *ss* for all triazoles (Figure 2). For each triazole, a core MIC-range could be defined except for itraconazole in TR_{46}/Y121F/T289A *ss* isolates, where the MIC distribution indicated the presence of two populations (Figure 2). Among the TR_{34}/L98H *ss* isolates 99 (7·4%) exhibited a MIC outside the core MIC (Table S1). Itraconazole non-core phenotype variants (36 isolates) showed MICs <4 mg/l, while for voriconazole most variant isolates (15/24, 62·5%) showed MICs >16 mg/l (Table S1). For TR_{46}/Y121F/T289A *ss* isolates 9（2·7%）exhibited a MIC outside the defined core MIC (Table S1).

Genotype variation

In the TR_{34} genetic background, 6 (19·4%) genotype variants were observed, involving 94 (6·6%) isolates (Figure 1a). In the TR_{46} genetic background, 6 variants (16·1%) were found, involving 123 (27·0%) isolates. Unlike TR_{34} isolates, variations in TR_{46} duplication number were observed, including 17 (3·7%) isolates with three TRs (TR_{46}^3/Y121F/M172I/T289A/G448S) and one isolate with four TRs, together with two SNPs in the *cyp51A*-gene: TR_{46}^4/Y121F/M172I/T289A/G448S (Figure 1a).

Of 38 isolates with the F46Y genetic background 14 isolates harboured additional N248T/D255E SNPs and one isolate M220I (Figure 1a). Finally, 14 (45·2%) SNPs were observed in 52 (2·6%) isolates (Figure 1a).

G448S was relatively common and present in various genetic backgrounds, including

TR_{46} (5 variants) and TR_{34} (2 variants) (Figure S1). In addition to G448S, both TR_{34}-variants also harboured T289A, a substitution that is characteristic of the TR_{46} genotype. Mutations in the gene promoter were also frequent, with the T-67G substitution most often found in isolates harbouring TR_{34}/L98H (32 isolates) (Figure S2).

Figure 1: Number of cyp51A genotype variants in 1979 clinical triazole-resistant Aspergillus fumigatus isolates cultured between Jan 6, 1994, and Dec 31, 2022

(A) Plot showing the number of isolates for each genotype over the study period. Colours indicate the various genetic backgrounds. Blue represents TR_{34}, red represents TR_{46}, orange represents TR_{53}, green represents Phe46Tyr, and light blue

represents SNPs. (B) Line graph showing the mutations overtime for each overall genotype category (TR_{34}, TR_{46}, TR_{53}, Phe46Tyr, and SNPs). i=intron. p=promoter region. SNP=single-nucleotide polymorphism. TR=tandem repeat.

	Isolation date	Phenotype			
		Itraconazole, mg/L	Voriconazole, mg/L	Posaconazole, mg/L	Isavuconazole, mg/L
TR_{34}/Leu98His sensu stricto geometric mean MIC	..	28·24	4·91	0·69	7·81
Core MIC range	..	8 to >16	1 to 16	0·12 to 2	2 to >16
TR_{46}/Tyr121Phe/Thr289Ala sensu stricto geometric mean MIC	..	5·95	26·68	0·62	24·45
Core MIC range	..	..	8 to >16	0·12 to 2	8 to >16
TR_{34}/Leu98His/Thr289Ala/Ile364Val/Gly448Ser (10 [100%] of 10 isolates)					
Strain: V309-77	Jan 31, 2020	1*	>16*	1	>16
Strain: M010-39	Nov 04, 2020	2*	>16*	1	>16
Strain: M027-69	May 27, 2021	0·5*	>16*	0·5	>16
Strain: M029-04	June 08, 2021	2*	>16*	1	>16
Strain: M033-22	Aug 09, 2021	1*	>16*	1	>16
Strain: M037-21	Sept 29, 2021	1*	>16*	0·5	>16
Strain: M046-26	Dec 30, 2021	0·5*	>16*	1	>16
Strain: M061-48	Aug 04, 2022	2*	>16*	0·5	>16
Strain: M061-58	Aug 05, 2022	1*	16	0·5	>16
Strain: M062-29	Aug 16, 2022	1*	>16*	0·5	>16
TR_{34}/Leu98His/Thr289Ala/Gly448Ser (3 [100%] of 3 isolates)					
Strain: v165-63	June 27, 2014	1*	>16*	1	>16
Strain: v253-11	May 18, 2018	1*	>16*	0·25	>16
Strain: M072-67	Dec 15, 2022	2*	>16*	0·5	>16
TR_{34}/promoter-67T→G/Leu98His (6 [18·8%] of 32 isolates)					
Strain: v259-28	July 26, 2018	2*	2	0·5	2
Strain: v269-74	Nov 29, 2018	2*	2	0·25	4
Strain: v272-27	Dec 06, 2018	2*	2	0·25	2
Strain: v272-32	Dec 06, 2018	2*	2	0·5	2
Strain: v306-29	Dec 12, 2019	2*	2	0·5	4
Strain: M031-27	July 09, 2021	1*	2	0·25	2
TR_{34}/Leu98His/Ser297Thr/Phe495Ile (5 [10·6%] of 47 isolates)					
Strain: v085-79	Aug 23, 2009	>16	>16*	0·5	>16
Strain: v141-26	Oct 04, 2012	1*	>16*	0·5	>16
Strain: v206-01	Aug 10, 2016	>16	2	4*	>16
Strain: V255-19	May 31, 2018	>16	0·5*	0·5	16
Strain: M042-45	Nov 29, 2021	1*	>16*	0·5	>16
TR_{46}/Tyr121Phe/Thr289Ala/Ser363Pro/Ile364Val/Gly448Ser (4 [4·1%] of 78 isolates)					
Strain: v255-56	May 30, 2018	>16	>16	16*	>16
Strain: M005-25	Sept 04, 2020	>16	>16	4*	>16
Strain: M045-14	Dec 21, 2021	>16	4*	0·25	8
Strain: M052-47	April 05, 2022	>16	4*	0·25	8

MIC=minimum inhibitory concentration. TR=tandem repeat. *MICs outside of the core MIC distribution.

Table 2: **TR_{34} and TR_{46} genotype variants with triazole phenotypes that are not within the core MIC distribution of TR_{34}/Leu98His sensu stricto and TR_{46}/Tyr121Phe/Thr289Ala sensu stricto isolates**

Triazole phenotypes of genotype variants

Five *cyp51A*-variant genotypes (28 isolates) in TR_{34} and TR_{46} isolates conferred triazole phenotypes outside the TR_{34}/L98H *ss* and TR_{46}/Y121F/T289A *ss* core MIC distribution (Figure 2, Table 2). In TR_{34}-genotype variants, low itraconazole MICs (range 0·5 to 2 mg/l) were the most prevalent non-core phenotype (21 of 24 (87·5%) isolates), commonly combined with high voriconazole MICs (MIC >16 mg/l, 15 of 24

(62·5%) isolates)(Table 2). In TR_{46}-genotype variants, two isolates showed low voriconazole MICs, and two isolates high posaconazole MICs (Table 2). In two TR_{34}-genotype variants (TR_{34}/L98H/T289A/I364V/G448S and TR_{34}/L98H/T289A/G448S) a non-core phenotype was observed in all isolates, while in the remaining variants only a minority of isolates exhibited a non-core phenotype (Table 2).

Overall, 325 (17·2%) of 1,887 TR-isolates showed triazole phenotype and/or *cyp51A*-genotype variation. Cyp51A genotype and phenotype variants increased over time and correlated with increasing TR-isolate numbers (Figure S3).

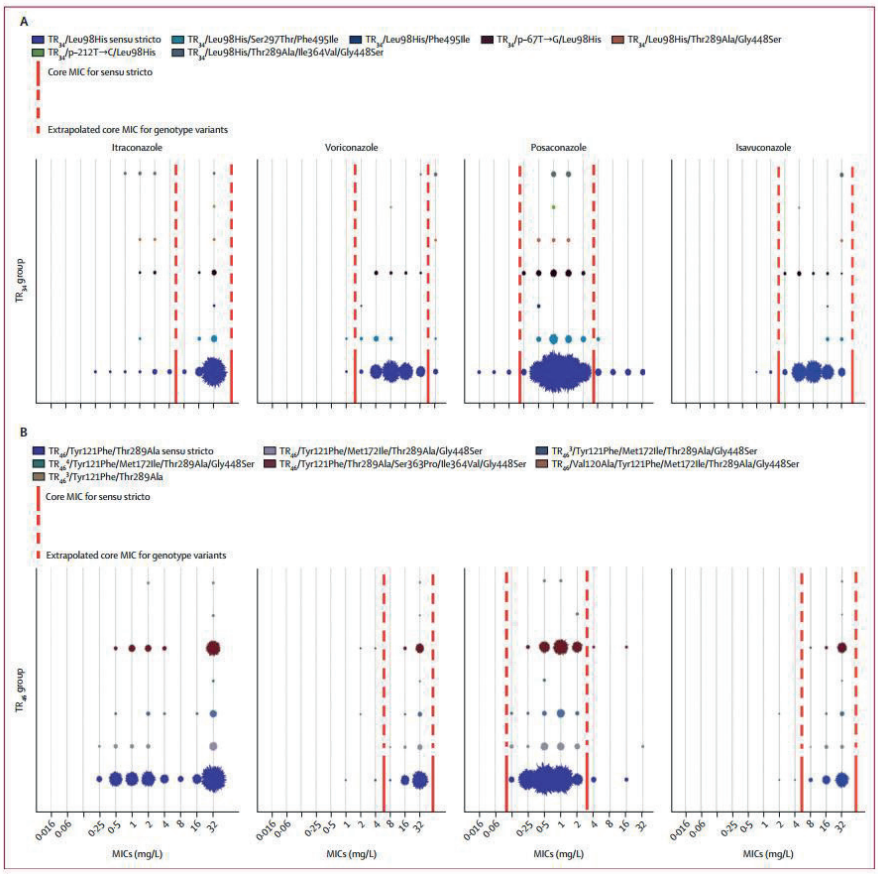

Figure 2: Triazole phenotypes of TR_{34}/Leu98His sensu stricto isolates and TR_{34} genotype variants (A), and TR_{46}/Tyr121Phe/Thr289Ala sensu stricto isolates TR_{46} genotype variants (B)The size of the dots corresponds with the proportion of isolates

with that specific MIC. The red lines indicate the core MIC values. TR_{34}/Leu98His sensu stricto and TR_{46}/Tyr121Phe/Thr289Ala sensu stricto isolates with MICs outside the range shown in the figure were considered non-core phenotype variants. *cyp51A*-genotype variants are indicated in other colours. For these isolates the core MIC values were derived from the TR_{34}/Leu98Hissensustricto and TR_{46}/Tyr121Phe/Thr289Alasensustricto, indicated with the red dotted lines. MIC=minimal inhibitory concentration. p=promoter region. TR=tandem repeat.

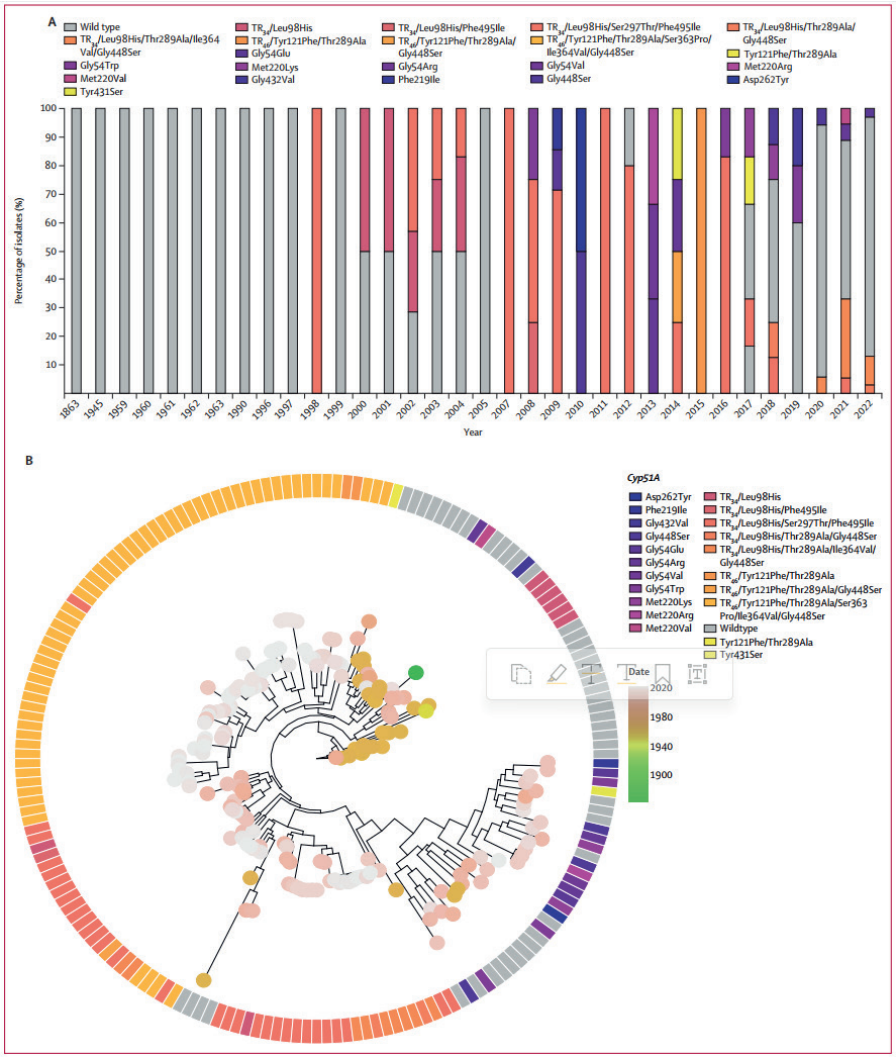

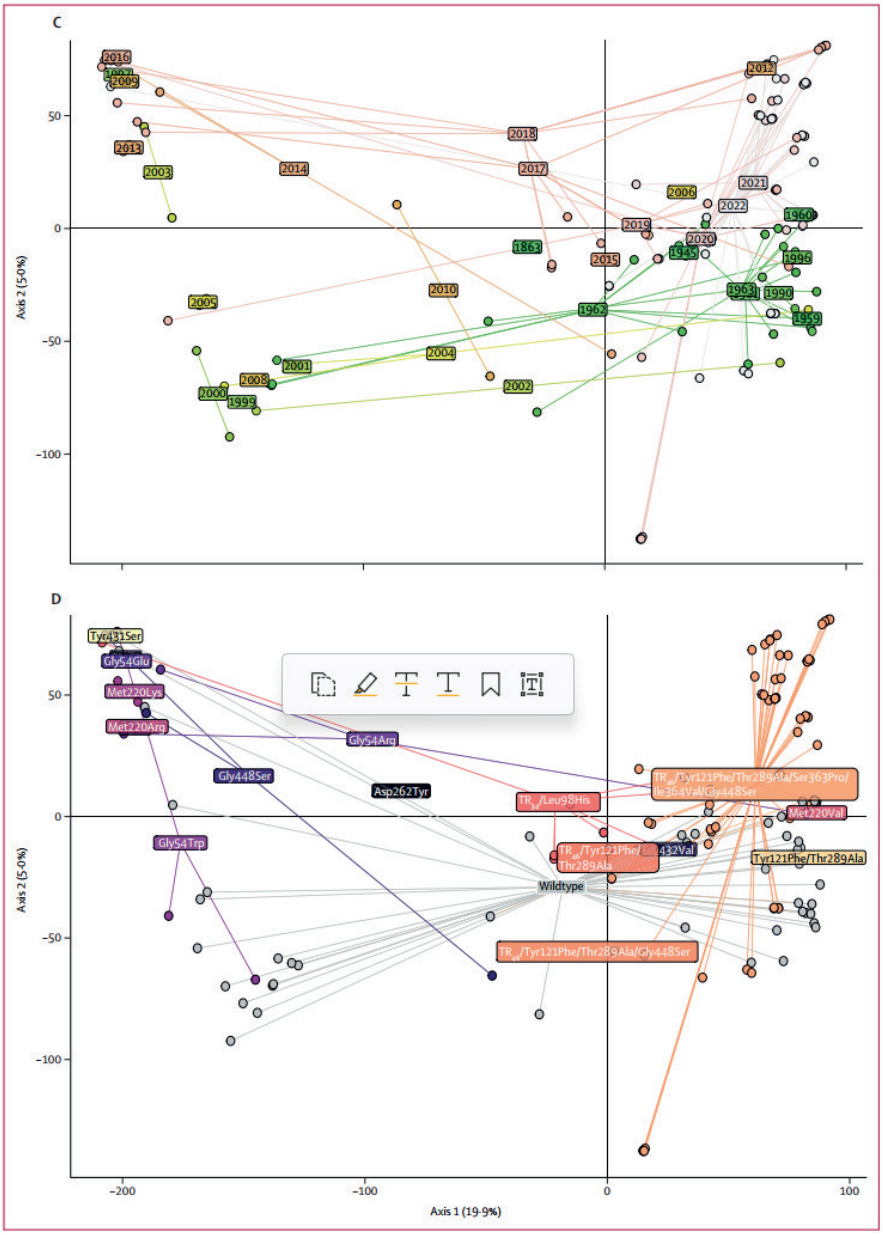

Figure 3: Whole-genome sequencing of 181 triazole susceptible and triazole resistant *Aspergillus fumigatus* isolates (A) Normalized bar plot of percentage of 181 isolates along time according to *cyp51A* polymorphism. (B) Maximum parsimony phylogeny and *cyp51A* phenotypic variation of 181 isolates. (C) Principal component analysis of the year of isolation. The first two principal components show no distinction on time.

(D) Principal component analysis based on *cyp51A* genotype shows TR_{34} and TR_{46} isolates are drawn from different backgrounds, with some overlap. Scale bar represents an approximate number of single nucleotide polymorphisms.

Genomic diversity and evolutionary patterns

WGS was performed on 213 *A. fumigatus* isolates, of which 47 contained no polymorphisms in the coding or promoter regions of *cyp51A* and were classified as wildtype (Figure 3a). The remaining 166 isolates displayed either polymorphisms in the coding or promoter regions of *cyp51A*, or both. Phylogenetic analysis revealed that most of the wildtype isolates clustered together, whilst TR_{34}- and TR_{46} isolates also clustered together (Figure 3b). Whilst there was no distinction observed based on PCA of the date of isolation (Figure 3d), confirming the observation in the phylogenetic analysis, there was some distinction along the second PCA observed between isolates with combinations of TR_{34}- and TR_{46}-based polymorphisms (Figure 3c).

TreeWAS identified 552 significant loci using the subsequent test as associated non-core MICs in TR_{34}/L98H variant isolates. No significant loci were found associated with core/non-core MIC phenotypes in TR_{34}/L98H *ss* isolates. These 552 loci map to 109 genes, which were overrepresented for KEGG pathway terms chlorocyclohexane and chlorobenzane degradation (*p*-value $3{\cdot}25e^{-02}$) and diterpenoid biosynthesis (*p*-value $4{\cdot}523e^{-02}$) (Table 3); these are components of azoles, suggesting certain pathways are more upregulated in isolates with additional *cyp51A* polymorphisms. Additionally, GO terms associated with recombination were also overrepresented in these 109 genes, suggested recombination is crucial in determining core vs. non-core triazole phenotype in TR_{34}/L98H variant isolates.

Clinical implications of triazole resistance

Between 2017 and 2022 2,010 cultures yielded *A. fumigatus* obtained from 1,189 patients. Most cultures were from sputum (1,296) and bronchial aspirates (258), while 210 patients had positive cultures from BAL, bronchial washings, and tissue. IA could be classified in 59 patients, including 17 proven and 42 probable cases. Although the FUNDICU case definition requires a CT scan to classify probable IPA in non-neutropenic patients, this criterion was omitted as many ventilated ICU patients do not undergo CT imaging. Thirteen (22·0%) patients had triazole-resistant IA (Table 4). Compared with 46 patients with triazole-susceptible IA (Table S2), the proportion

of ICU patients was similar for both groups (9/13 (69·2%) and 32/46 (69·6%) for triazole-resistant IA and triazole-susceptible IA, respectively), as was the overall mortality (7/13 (53·8%) and 23/46 (50·0%), respectively)(Figure 4).

	Single-nucleotide polymorphism type	Gene	Description
Chromosome 1			
Position: 4 707 904	Upstream	AFUA_1G17210	Protein of unknown function; orthologs are F-box containing proteins
Position: 4 707 979	Upstream	AFUA_1G17210	Protein of unknown function; orthologs are F-box containing proteins
Position: 4 708 022	Upstream	AFUA_1G17210	Protein of unknown function; orthologs are F-box containing proteins
Chromosome 2			
Position: 2 050 524	Missense (Arg355Cys)	AFUA_2G08000	Orthologs are transmembrane proteins
Position: 2 050 607	Missense (Gly327Glu)	AFUA_2G08000	Orthologs are transmembrane proteins
Position: 2 052 509	Upstream	AFUA_2G08000	Orthologs are transmembrane proteins

*The four groups are TR_{34}/Leu98His sensu stricto with MICs within the core MIC (19 isolates) and outside the core MIC (20 isolates), and TR_{34}/Leu98His genotypic variants with MICs inside the core MIC (two variants, 30 isolates) and with MICs outside the core MIC (three variants, 13 isolates).

Table 3*: Significant loci identified by treeWAS as associated with the four groups

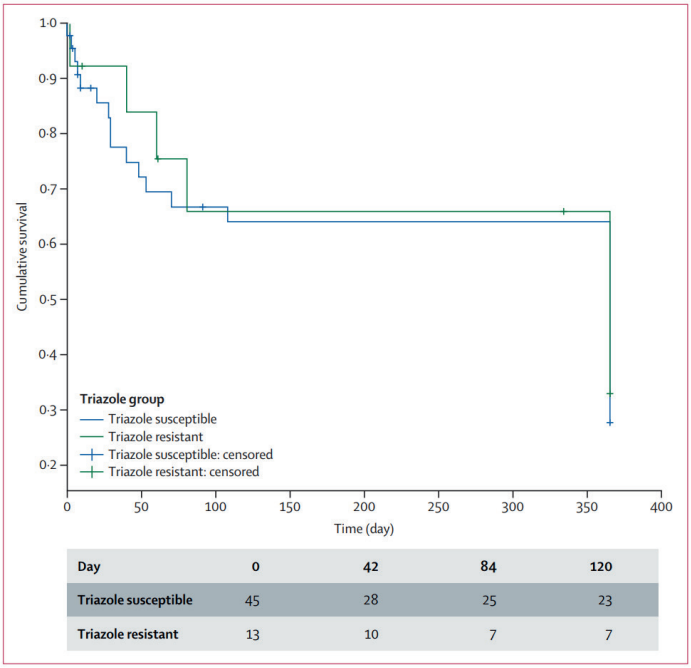

Day	0	42	84	120
Triazole susceptible	45	28	25	23
Triazole resistant	13	10	7	7

Figure 4: Kaplan–Meier survival analysis of patients with triazole-resistant invasive aspergillosis and triazole-susceptible invasive aspergillosis

This analysis estimated the survival function from lifetime data to compare survival distributions between the two groups.

TR-mediated resistance genotypes were involved in 12 of 13 (92·3%) patients with triazole-resistant IA, including three genotype variants (Table 4). Furthermore, mixed infection was observed in 11 of 13 (84·6%) patients, including four patients with multiple resistance genotypes. The two patients without mixed infection were diagnosed through biopsy of a single lesion (Table 4). In both patient groups, most patients received initial antifungal therapy that covered triazole resistance (i.e. triazole and echinocandin or L-AmB, or L-AmB monotherapy), which is recommended by the Dutch National Invasive Mycoses Guideline published in December 2017 (9 of 10 (90·0%) triazole-resistant IA cases since 2018 and 34 of 39 (87·2%) triazole-susceptible cases since 2018). Compared with triazole susceptible IA, significant more antifungal treatment switches were made in patients with triazole-resistant infection (mean rank 25.98 for triazole-susceptible compared with 44.23 for triazole-resistant; $p<0.0001$). Olorofim showed low MICs against both triazole-susceptible and triazole-resistant *A. fumigatus* isolates (Table 4 and Table S2).

	Year	Age, years	Underlying disease	Initial classification	Final classification	ICU	Initial therapy	Follow-up therapy	Outcome	Mixed infection	Resistance genotype	Resistance phenotype					
												AmB, mg/L	ITZ, mg/L	VCZ, mg/L	POS, mg/L	ISA, mg/L	OLO, mg/L
Patient 1	2017	67	Oropharynx carcinoma	Probable IPA	Probable IPA	Yes	VCZ	VCZ and AFG; VCZ	Died 60 days after therapy	S; R	TR_{34}/Leu98His	0·5	16	2	0·5	4	··
Patient 2	2017	73	CLL (ibrutinib), COPD, and NTM	Probable IPA	Probable IPA	Yes	VCZ and AFG	AFG; L-AmB and AFG; VCZ and AFG	Died 40 days after therapy	S; R; R	WT; TR_{34}/Leu98His	0·5; 0·5	>16; >16	4; 2	0·5; 0·5	4; 4	0·031; <0·016
Patient 3	2017	58	Legionella pneumonia	Unclassified	Proven IPA	Yes	VCZ	None	Died 2 days after therapy	S; R; R	WT; TR_{46}/Tyr121Phe/Thr289Ala	0·25; 0·5	>16; 2	2; >16	0·5; 1	4; >16	0·031; 0·063
Patient 4	2018	55	Rheumatoid arthritis and COPD	Probable IAPA	Probable IAPA		VCZ and CAS	VCZ; VCZ and CAS; VCZ, L-AmB, and nL-AmB; VCZ and nL-AmB	Died 10 days after therapy	S; R	TR_{34}/Leu98His	0·5	>16	2	0·5	8	0·016
Patient 5	2019	38	Rheumatoid arthritis	Probable IAPA	Probable IAPA	Yes	VCZ and AFG	VCZ and L-AmB	Alive	S; R	TR_{46}/Tyr121Phe/Met172Ile/Thr289Ala/Gly448Ser	0·25	0·5	>16	0·25	>16	0·031
Patient 6	2020	62	None	Proven osteomyelitis following mastoidectomy	Proven osteomyelitis	No	L-AmB and tL-AmB	AFG; AFG and ISA; VCZ, AFG, and tVCZ	Alive	No	TR_{34}/Leu98His	1	>16	4	1	4	0·031
Patient 7	2020	67	Diabetes and hypertension	Probable CAPA and TBA	Probable CAPA+TBA	Yes	VCZ and AFG	VCZ, AFG, and nL-AmB; L-AmB and nL-AmB	Died 81 days after therapy	S; R	TR_{34}/Leu98His	0·5	>16	4	0·5	8	0·063
Patient 8	2021	58	Primary hyperaldosteronism	Probable CAPA	Probable CAPA	Yes	VCZ and AFG	L-AmB; POS and AFG	Alive	S; R	TR_{46}/Tyr121Phe/Thr289Ala	1	0·5	>16	0·25	>16	0·031
Patient 9	2021	61	None	Probable CAPA	Probable CAPA	Yes	VCZ and AFG	L-AmB	Alive	R; R; R	TR_{34}/promoter–67T→G/Leu98His; WT; TR_{34}/Leu98His	0·5; 0·5; 0·5	>16; >16; >16	4; 2; 4	1; 0·25; 0·5	8; 4; 8	0·063; 0·031; 0·031
Patient 10	2021	73	Diabetes	Probable CAPA	Probable CAPA	Yes	VCZ and AFG	ISA and AFG	Alive	S; R	TR_{34}/Leu98His	0·25	>16	8	1	16	0·063
Patient 11	2021	33	Kidney transplant	CAPA (unclassified)	Proven disseminated IA	Yes	POS and AFG	OLO; OLO and L-AmB	Died 334 days after therapy	R; R	TR_{46}/Tyr121Phe/Thr289Ala/Ser363Pro/Ile364Val/Gly448Ser; TR_{34}/Leu98His	0·5; 1	>16; >16	4; 8	0·25; 0·5	8; 16	0·031; 0·031
Patient 12	2022	54	AML and MUD alloSCT	Proven IPA	Proven IPA	No	VCZ	ISA; L-AmB; MFG; L-AmB; ISA and MFG	Alive	No	TR_{34}/Leu98His	1	>16	4	1	8	0·016
Patient 13	2022	31	CGD	Proven IPA	Proven disseminated IA	No	ISA and OLO	OLO and AFG; OLO, AFG, and L-AmB	Died 61 days after therapy	S; R	WT	0·5	2	2	0·25	4	0·125

AFG=anidulafungin. alloSCT=allogeneic stem cell transplantation. AmB=amphotericin. AML=acute myeloid leukaemia. CAPA=COVID-19-associated pulmonary aspergillosis. CAS=caspofungin. CGD=chronic granulomatous disease. CLL=chronic lymphoblastic leukaemia. COPD=chronic obstructive pulmonary disease. IA=invasive aspergillosis. IAPA=influenza-associated pulmonary aspergillosis. ICU=intensive care unit. IPA=invasive pulmonary aspergillosis. ISA=isavuconazole. L-AmB=liposomal amphotericin B. MFG=micafungin. MUD=matched unrelated donor. nL-AmB=nebulized liposomal amphotericin B. NTM=non-tuberculous mycobacteria. OLO=olorofim. POS=posaconazole. R=triazole-resistant. S=triazole susceptible. TBA=invasive tracheobronchial aspergillosis. tL-AmB=topical liposomal amphotericin B. TR=tandem repeat. tVCZ=topical voriconazole. VCZ=voriconazole. WT=wildtype.

Table 4: **Characteristics of 13 patients with proven or probable triazole-resistant invasive aspergillosis**

Discussion

Analysis of a large collection of clinical *A. fumigatus* isolates collected over a period of 29 years showed that *cyp51A*-genotype and triazole phenotype variation was frequent in resistant isolates. Non-core MICs were observed both in TR_{34}/L98H *ss* and TR_{46}/Y121F/T289A *ss* isolates, and in *cyp51A*-genotype variants. Furthermore, triazole phenotype variations may be more frequent in isolates collected since 2017 compared with those collected in the earlier period from 1994 to 2004, which was also observed in genomic comparisons.

Our data indicate that over time *A. fumigatus* acquires mutations, some of which may alter the triazole resistance phenotype. These mutations are detectable when *Cyp51A* is involved, but we hypothesize that mutations outside *cyp51A* are likely responsible for part of the phenotypic variation we observed. With the generation of de novo mutations in asexual reproducing *A. fumigatus* and continued triazole selection pressure in the environment, our observation is not unexpected. WGS showed that despite isolates with combinations of TR_{34}- and TR_{46}-based polymorphisms in *cyp51A* seem to be derived from separate populations, there is some overlap. One possible explanation is (sexual) recombination between isolates with these distinct genetic backgrounds, creating new combinations of triazole resistance polymorphisms e.g. TR_{34}/L98H/T289A; more combinations have been observed recently during the period of this study (Table S2). The high cross-over rate in *A. fumigatus* (Auxier et al., 2023), alludes to a future with more novel drug-resistant polymorphism combinations being observed. Recombination was also seen to be involved in the determination of core vs non-core MIC phenotypes in isolates included in this study; many significant loci in TR_{34}/L98H *cyp51A*-variant isolates being overrepresented for GO terms associated with recombination, suggesting this is driving phenotypic variation and potentially patient infection experience. It is therefore crucial to routinely perform susceptibility testing of novel resistance polymorphism combinations as part of surveillance programs, and to assess patient outcomes.

We recovered resistance variants from patients with proven/probable IA underscoring the potential of these variants to cause invasive disease. Most patients were admitted to the ICU, which might be due to culture-positivity as selection criterion. In patients with haematological malignancy and neutropenia, IA diagnosis is frequently based on biomarkers, while positive cultures are infrequent. Mortality in triazole-resistant and triazole-susceptible IA was similar, which may be due to initial antifungal therapy that covered triazole resistance as recommended in our

national guideline. Although our previous cohort study showed significant higher mortality in patients with voriconazole-resistant IA compared to those with voriconazole-susceptible IA, the mortality in both groups was similar for patients admitted to the ICU (Lestrade et al., 2019). Other factors likely have greater impact on survival in critically ill patients in addition to triazole resistance. Nevertheless, the high number of antifungal drug changes in patients with triazole-resistant IA underscores the challenges faced, including the need for high triazole exposure (especially posaconazole) and continued combination therapy with associated drug toxicity and interactions.

Our study indicates that pulmonary IA in principle involves multiple *A. fumigatus* genotypes, as lung nodules originate from genetically distinct spores (Kolwijck et al., 2016). Indeed, both patients with one genotype, had been biopsied from a single lesion in lung and bone (Table 4). Multiple resistance genotypes/phenotypes including resistant isolates with a wildtype *cyp51A*-sequence as well as *cyp51A*-genotype variants is a concern for resistance detection. *Aspergillus* resistance PCR assays use predefined markers (e.g., TR_{34}, L98H, Y121F and T289A) to detect resistance, but will fail to detect *cyp51A*-genotype/phenotype variants as well as non-*cyp51A*-mediated resistance. Phenotypic resistance detection through agar-based screening of multiple *A. fumigatus* colonies and MIC-testing will be the most reliable method to detect MIC-variation. However, many patients are culture-negative and rely on molecular testing to detect resistance. Other techniques, such as sequence-based approaches, will be required in clinical microbiology to enable reliable detection of resistance. However, gene editing experiments will be needed to understand the role of individual SNPs in the *cyp51A*-gene as well as identifying new resistance hotspots. The TR_{34}/L98H/T289A/G448S variant incorporates two mutations that are known to confer triazole resistance (Abdolrasouli et al., 2022). TR_{34}/L98H confers high itraconazole MICs and isolates with a G448S point mutation show high MICs for both voriconazole and itraconazole (Pelaez et al., 2012). The T289A mutation is not associated with increased triazole MICs but confers triazole resistance when combined with Y121F and/or TR_{46} (Snelders et al., 2015). Therefore, each SNP will need to be investigated individually and in combination using, to understand the associated phenotype.

Our study was limited by using cultures as denominator and variation in resistance detection methods over time. Multiple isolates from the same patient could impact on the resistance frequency and variation. We were unable to retrieve patient data for all isolates as some of them were collected anonymously for our resistance surveillance program. However, the data collected for our centre provide an

indication regarding sample types and clinical implications of triazole resistance.

Our study showed phenotype/genotype variation in 17.2% of clinical triazole-resistant *A. fumigatus* isolates, and involvement of these variants in triazole-resistant IA. Mixed infections involving resistance variants represents the next major challenge in triazole resistance management as our current molecular diagnostic tools will increasingly fail to accurately predict the triazole phenotype. New approaches are needed to detect resistance variants in clinical specimens.

Authors contributions

PV, JB and WM conceived and designed the study; YS, JR and PV performed the data analysis and have verified the data reported in the study; YS, JZ, MTK and ME conducted all experiments and performed the statistical analysis of the data; YS, PV, JB, JZ, RL, TB, JR, ME and WM discussed the experiments and results. All authors had full access to all the data in the study and had final responsibility for the decision to submit for publication. YS, JR and PV wrote the draft manuscript; all authors reviewed the different drafts and approved the final version of the manuscript.

Declaration of interests

JBB received research grants from Gilead Sciences and F2G Ltd. PEV received grants for research and consultancy from Gilead Sciences, Mundipharma, Shionogi, and F2G Ltd. YS, JR, JZ, MT-K, ME, JZ, RL, TB, WJGM declare no conflict of interests.

Data sharing

All genotypic variants are shown in Figure 1a. All data requests should be submitted to PEV (paul.verweij@radboudumc.nl). Requests will be assessed for scientific rigour before being granted and a data-sharing agreement might be required.

Funding

This study was supported by National Key Research and Development Program of China [2021YFC2300400] and National Natural Science Foundation of China [82272354] supporting YS and RL. Parts of the study were supported by a grant from Wellcome Trust [no. 219551/Z/19/Z] to JR and PEV.

References

Alanio A, Dellière S, Fodil S, Bretagne S, Mégarbane B. Prevalence of putative invasive pulmonary aspergillosis in critically ill patients with COVID-19. *Lancet Respir Med.* 2020; 8: e48-e49.

Abdolrasouli A, Rhodes JL. Phenotypic variants of azole-resistant *Aspergillus fumigatus* that co-exist in human respiratory samples are genetically highly related. *Mycopathologia.* 2022; 187: 497-508.

Arendrup MC, Friberg N, Mares M, Kahlmeter G, Meletiadis J, Guinea J. How to interpret MICs of antifungal compounds according to the revised clinical breakpoints v. 10.0 European committee on antimicrobial susceptibility testing (EUCAST). *Clin Microbiol Infect.* 2020; 26: 1464–72.

Arentshorst M, Ram AF, Meyer V. Using non-homologous end-joining-deficient strains for functional gene analyses in filamentous fungi. *Methods Mol Biol.* 2012; 835: 133-50.

Alvarez-Jarreta J, Amos B, Aurrecoechea C, et al. VEuPathDB: the eukaryotic pathogen, vector and host bioinformatics resource center in 2023. *Nucleic Acids Res.* 2024; 52: D808-D816.

Auxier B, Debets AJM, Stanford FA, et al. The human fungal pathogen *Aspergillus fumigatus* can produce the highest known number of meiotic crossovers. *PLoS Biol.* 2023; 21: e3002278.

Bassetti M, Giacobbe DR, Agvald-Ohman C, et al. Invasive Fungal Diseases in Adult Patients in Intensive Care Unit (FUNDICU): 2024 consensus definitions from ESGCIP, EFISG, ESICM, ECMM, MSGERC, ISAC, and ISHAM. *Intensive Care Med.* 2024; 50: 502-515.

Barber AE, Riedel J, Sae-Ong T, et al. Effects of agricultural fungicide use on *Aspergillus fumigatus* abundance, antifungal susceptibility, and population structure. *mBio.* 2020; 11: e02213-20.

Collins C, Didelot X. A phylogenetic method to perform genome-wide association studies in microbes that accounts for population structure and recombination. *PLoS Comput Biol.* 2018; 14: e1005958.

Chen Y, Li Z, Han X, et al. Elevated MIC values of imidazole drugs against *Aspergillus fumigatus* isolates with TR_{34}/L98H/S297T/F495I mutation. *Antimicrob Agents Chemother.* 2018; 62: e01549-17.

Donnelly JP, Chen SC, Kauffman CA, et al. Revision and update of the consensus definitions of invasive fungal disease From the European Organization for Research and Treatment of Cancer and the Mycoses Study Group Education and Research Consortium. *Clin Infect Dis.* 2020; 71:1367-1376.

European Committee on Antimicrobial Susceptibility Testing, Antifungal Susceptibility Testing. [(accessed on 4 December 2020)]; Available online: https://www.eucast.org/ast_of_fungi/.

Jenkins T. mapmixture: Spatial Visualisation of Admixture on a Projected Map. R package version 1.1.0. (2024).

Kolwijck E, van der Hoeven H, de Sévaux RG, et al. Voriconazole-susceptible and voriconazole-resistant *Aspergillus fumigatus* coinfection. *Am J Respir Crit Care Med.* 2016; 193: 927-29.

Lestrade PP, Bentvelsen RG, Schauwvlieghe AFAD, et al. Voriconazole resistance and mortality in invasive aspergillosis: a multicenter retrospective cohort study. *Clin Infect Dis.* 2019; 68: 1463–71.

Liu M, Zeng R, Zhang L, et al. Multiple cyp51A-based mechanisms identified in azole-resistant isolates of *Aspergillus fumigatus* from China. *Antimicrob Agents Chemother.* 2015; 59: 4321-5.

Li H. Aligning sequence reads, clone sequences and assembly contigs with BWA–MEM. *arXiv*, (2013).

Li H, Handsaker B, Wysoker A, et al., The Sequence Alignment/Map format and SAMtools. *Bioinformatics.* 2009; 25: 2078–79.

Lavergne RA, Chouaki T, Hagen F, et al. Home environment as a source of life-threatening azole-resistant *Aspergillus fumigatus* in immunocompromised patients. *Clin Infect Dis.* 2017; 64: 76-8.

Mellado E, Diaz-Guerra TM, Cuenca-Estrella M, Rodriguez-Tudela JL. Identification of two different 14-alpha sterol demethylase-related genes (cyp51A and cyp51B) in *Aspergillus fumigatus* and other *Aspergillus* species. *J Clin Microbiol.* 2001; 39: 2431-8.

Paluch M, Lejeune S, Hecquet E, Prévotat A, Deschildre A, Fréalle E. High airborne level of *Aspergillus fumigatus* and presence of azole-resistant TR_{34}/L98H isolates in the home of a cystic fibrosis patient harbouring chronic colonisation with azole-resistant H285Y *A. fumigatus*. *J Cyst Fibros.* 2019; 18: 364-7.

Pelaez T, Gijón P, Bunsow E, et al. Resistance to voriconazole due to a G448S substitution in *Aspergillus fumigatus* in a patient with cerebral aspergillosis. *J Clin Microbiol.* 2012; 50: 2531e4.

Rhodes J, Abdolrasouli A, Dunne K, et al. Population genomics confirms acquisition of

drug-resistant *Aspergillus fumigatus* infection by humans from the environment. *Nat Microbiol.* 2022; 7: 663-74.

Shelton JMG, Collins R, Uzzell CB, et al. Citizen science surveillance of triazole-resistant *Aspergillus fumigatus* in United Kingdom residential garden soils. *Appl Environ Microbiol.* 2022; 88: e0206121.

Snelders E, Karawajczyk A, Schaftenaar G, Verweij PE, Melchers WJ. Azole resistance profile of amino acid changes in *Aspergillus fumigatus* CYP51A based on protein homology modeling. *Antimicrob Agents Chemother.* 2010; 54: 2425-30.

Smit AFA, Hubley R, Green P. *RepeatMasker Open-4.0*.

Schoustra SE, Debets AJM, Rijs AJMM, et al. Environmental hotspots for azole resistance selection of *Aspergillus fumigatus*, the Netherlands. *Emerg Infect Dis.* 2019; 25: 1347–53.

Ter Braak CJ, Peres-Neto P, Dray S. A critical issue in model-based inference for studying trait-based community assembly and a solution. *Peer J.* 2017; 5: e2885.

Snelders E, Camps SM, Karawajczyk A, et al. Genotype-phenotype complexity of the TR_{46}/Y121F/T289A cyp51A azole resistance mechanism in *Aspergillus fumigatus*. *Fungal Genet Biol.* 2015; 82: 129-35.

Ullmann AJ, Aguado JM, Arikan-Akdagli S, et al. Diagnosis and management of *Aspergillus* diseases: executive summary of the 2017 ESCMID-ECMM-ERS guideline. *Clin Microbiol Infect.* 2018; 24: Suppl 1: e1-e38.

Supplementary material

Figure S1 Cyp51A variants resistant rate and triazole susceptible isolates

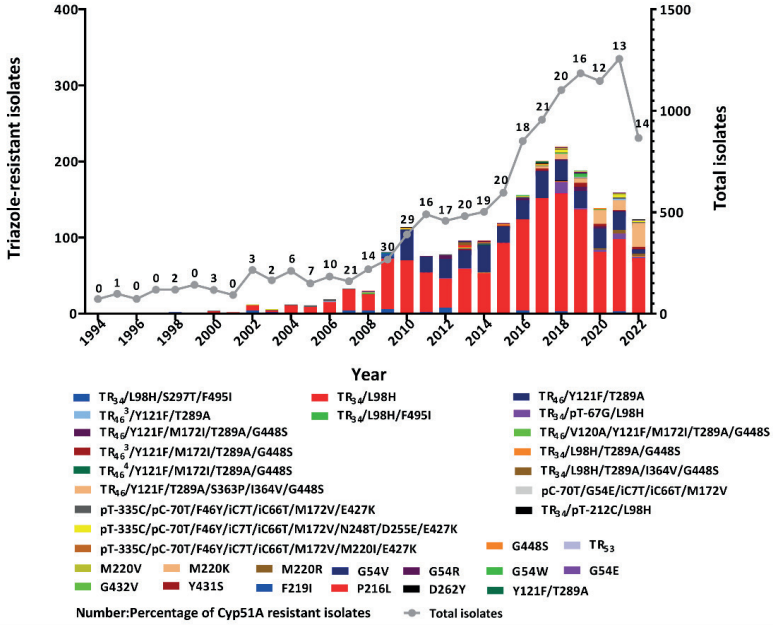

Figure S2 The difference between the resistant and non-resistant isolates over time

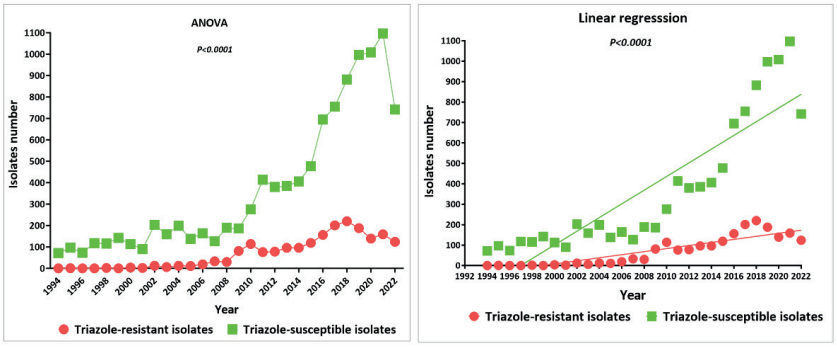

Figure S3 TR isolates and variants

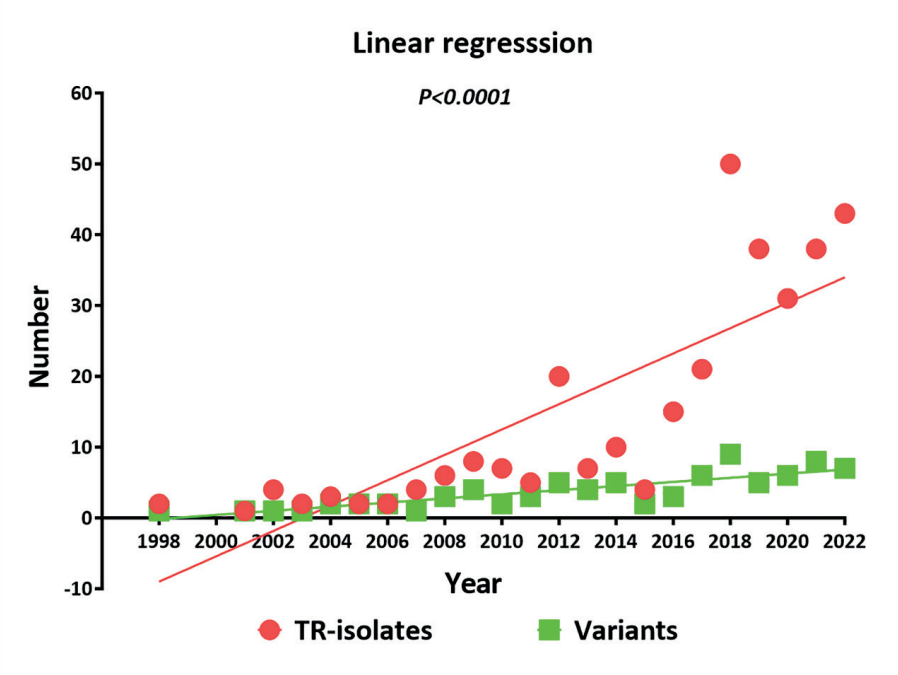

Table S1 TR_{34}/L98H and TR_{46}/Y121F/T289A *ss* isolates outside the core MIC

ID	Date	ITC	VOR	POS	ISA	Mutation
V028-78	2004	4	4	0·5	-	TR_{34}/L98H
V034-78	2004	4	4	0·25	-	TR_{34}/L98H
v041-27	2005	8	0·5	0·125	-	TR_{34}/L98H
V048-21	2006	2	2	0·5	-	TR_{34}/L98H
V050-54	2006	4	8	0·5	-	TR_{34}/L98H
V050-55	2006	2	4	0·25	-	TR_{34}/L98H
v068-18	2008	>16	>16	1	-	TR_{34}/L98H
v080-17	2009	>16	>16	1	-	TR_{34}/L98H
v099-29	2010	>16	8	>16	-	TR_{34}/L98H
v099-30	2010	>16	8	>16	-	TR_{34}/L98H
v099-43	2010	>16	4	8	-	TR_{34}/L98H
v099-44	2010	>16	16	8	-	TR_{34}/L98H
v107-38	2010	>16	16	>16	-	TR_{34}/L98H
v111-02	2010	>16	4	>16	-	TR_{34}/L98H
v097-62	2010	>16	>16	4	-	TR_{46}/Y121F/T289A
v111-55	2011	>16	>16	1	-	TR_{34}/L98H
v122-46	2011	>16	>16	1	-	TR_{34}/L98H
v133-26	2012	4	2	0·25	-	TR_{34}/L98H
v141-76	2012	>16	>16	2	-	TR_{34}/L98H
v136-02	2012	>16	16	8	-	TR_{34}/L98H
v142-80	2012	>16	16	4	-	TR_{34}/L98H
v133-53	2012	>16	>16	4	-	TR_{46}/Y121F/T289A
v140-57	2012	>16	>16	4	-	TR_{46}/Y121F/T289A
v147-31	2013	>16	>16	2	-	TR_{34}/L98H

v153-31	2013	>16	>16	1	-	TR_{34}/L98H
v157-11	2013	>16	>16	1	-	TR_{34}/L98H
v148-81	2013	>16	16	>16	-	TR_{34}/L98H
v162-73	2014	>16	16	4	-	TR_{34}/L98H
v166-42	2014	>16	8	16	16	TR_{34}/L98H
v168-31	2014	>16	4	16	8	TR_{34}/L98H
v170-20	2014	>16	8	0·031	-	TR_{34}/L98H
v171-42	2014	>16	8	>16	8	TR_{34}/L98H
v159-67	2014	>16	4	0·5	-	TR_{46}/Y121F/T289A
v159-72	2014	>16	4	0·25	-	TR_{46}/Y121F/T289A
v173-18	2015	>16	>16	2	>16	TR_{34}/L98H
v178-08	2015	>16	>16	2	>16	TR_{34}/L98H
v185-56	2015	>16	>16	0·5	>16	TR_{34}/L98H
v207-06	2016	2	2	0·25	4	TR_{34}/L98H
v197-19	2016	>8	4	4	>8	TR_{34}/L98H
v199-37	2016	>8	8	4	>8	TR_{34}/L98H
v200-50	2016	>8	8	8	>8	TR_{34}/L98H
v201-21	2016	>8	8	8	>8	TR_{34}/L98H
v202-16	2016	>16	4	8	16	TR_{34}/L98H
v206-39	2016	>16	4	4	>16	TR_{34}/L98H
v213-15	2016	>16	4	4	>8	TR_{34}/L98H
v215-38	2017	4	4	1	4	TR_{34}/L98H
v219-39	2017	4	2	0·5	4	TR_{34}/L98H
v230-06	2017	2	2	0·5	4	TR_{34}/L98H
v230-69	2017	2	2	0·25	4	TR_{34}/L98H
v234-09	2017	4	2	0·5	4	TR_{34}/L98H

v236-74	2017	4	2	0·5	8	TR_{34}/L98H
v216-08	2017	>16	8	>8	8	TR_{34}/L98H
v222-67	2017	>16	8	4	>4	TR_{34}/L98H
v224-58	2017	>16	8	4	>4	TR_{34}/L98H
v237-31	2017	>16	>8	>8	>16	TR_{34}/L98H
v224-08	2017	>16	2	0·25	1	TR_{34}/L98H
v221-06	2017	>16	16	16	16	TR_{46}/Y121F/T289A
v221-81	2017	>16	16	4	16	TR_{46}/Y121F/T289A
v256-62	2018	2	1	1	2	TR_{34}/L98H
v257-66	2018	4	1	0·25	4	TR_{34}/L98H
v261-13	2018	2	2	0·5	4	TR_{34}/L98H
v261-31	2018	4	2	0·25	2	TR_{34}/L98H
v261-51	2018	4	8	1	8	TR_{34}/L98H
v262-54	2018	4	2	0·5	4	TR_{34}/L98H
v265-39	2018	4	2	0·5	4	TR_{34}/L98H
v268-34	2018	2	2	0·5	4	TR_{34}/L98H
v268-60	2018	4	4	0·5	4	TR_{34}/L98H
v268-62	2018	4	4	0·5	4	TR_{34}/L98H
v273-32	2018	2	2	0·25	4	TR_{34}/L98H
v264-20	2018	>16	>16	1	>16	TR_{34}/L98H
v264-29	2018	>16	>16	0·5	>16	TR_{34}/L98H
v265-12	2018	>16	>16	0·5	>16	TR_{34}/L98H
v265-56	2018	>16	>16	1	>16	TR_{34}/L98H
v269-23	2018	16	>16	0·5	2	TR_{34}/L98H
v238-07	2018	>16	8	4	>16	TR_{34}/L98H
v255-81	2018	>16	8	16	>16	TR_{34}/L98H

v256-46	2018	2	1	16	2	TR46/Y121F/T289A
v257-17	2018	0·5	16	0·25	4	TR_{46}/Y121F/T289A
v278-04	2019	4	4	0·5	4	TR_{34}/L98H
v278-46	2019	2	2	0·25	4	TR_{34}/L98H
v279-09	2019	2	2	0·25	8	TR_{34}/L98H
v279-10	2019	2	2	0·5	4	TR_{34}/L98H
v279-18	2019	2	2	0·25	8	TR_{34}/L98H
v282-25	2019	2	2	0·5	8	TR_{34}/L98H
v300-25	2019	2	2	0·5	2	TR_{34}/L98H
v305-69	2019	2	2	0·5	4	TR_{34}/L98H
v307-55	2019	2	4	0·5	4	TR_{34}/L98H
v284-36	2019	>16	>16	>8	>8	TR_{34}/L98H
v284-37	2019	>16	>16	>8	>8	TR_{34}/L98H
v295-08	2019	>16	>16	2	>8	TR_{34}/L98H
v298-23	2019	>16	>16	1	>8	TR_{34}/L98H
v305-66	2019	>16	>16	0·5	>16	TR_{34}/L98H
v284-36	2019	>16	>16	>8	>8	TR_{34}/L98H
v284-37	2019	>16	>16	>8	>8	TR_{34}/L98H
v298-24	2019	>16	2	0·25	1	TR_{34}/L98H
v299-20	2019	>16	2	0·25	1	TR_{34}/L98H
v299-21	2019	>16	4	0·25	1	TR_{34}/L98H
v309-03	2020	2	4	0·5	4	TR_{34}/L98H
M009-63	2020	>16	4	4	8	TR_{34}/L98H
M024-08	2021	2	1	0·25	2	TR_{34}/L98H
M035-15	2021	2	2	0·25	4	TR_{34}/L98H
M022-51	2021	>16	0·5	> 8	1	TR_{34}/L98H

M030-72	2021	>16	>16	1	>16	TR_{34}/L98H
M037-35	2021	>16	>16	0·5	>16	TR_{34}/L98H
M045-08	2021	>16	>16	1	>16	TR34/L98H
M022-51	2021	>16	0·5	>8	1	TR_{34}/L98H
M052-30	2022	>16	>16	0·125	>16	TR34/L98H
M052-66	2022	>16	>16	0·5	>16	TR34/L98H

Table S2 Characteristics of 46 patients with proven/probable triazole-susceptible IA

year	age	Underlying disease	Initial classification	Final classification	ICU	Initial therapy	Follow-up therapy	outcome	Azole phenotype					
									AmB	ITZ	VCZ	POS	ISA	OLO
2017	59	Auto immune disease	Probable IPA	Probable IPA	Yes	VCZ+AFG	VCZ	Alive	0·5	0·125	0·5	0·063	1	-
2017	45	NHL	Probable IPA	Proven disseminated IA	No	L-AmB	VCZ	Alive	0·5	0·25	0·5	0·125	1	-
2017	67	Kidney Tx	Proven skull base osteomyelitis	Proven skull base osteomyelitis	No	VCZ	ISA, VCZ	Alive	0·25	0·25	0·5	0·063	0·5	-
2017	68	None	Proven endophthalmitis	Proven endophthalmitis	No	AmB_{iv}	VCZ+tVCZ+AmB_{iv}	Alive	0·5	0·5	0·5	0·125	0·5	-
2017	17	ALL	Probable IPA	Probable IPA	No	VCZ+L-AmB	VCZ	Alive	-	S	S	S	-	-
2017	54	Hypertension	Proven rhino cerebral	Proven rhino cerebral	Yes	VCZ+L-AmB	VCZ	Alive	0·5	0·5	0·5	0·125	1	-
2017	12	Autoimmune disease	Proven disseminated IA	Proven disseminated IA	Yes	-	-	Died (+0)	-	S	S	S	-	-
2018	36	HIV, disseminated tuberculosis	Probable IPA	Probable IPA	Yes	L-AmB		Alive	0·25	0·125	0·25	0·031	0·5	0·016

2018	59	Adenocarcinoma	Probable IPA	Probable IPA	Yes	VCZ+ANF		Died (+5)	-	S	S	S	-	-
2018	8	ALL	Probable IAPA	Probable IAPA	Yes	VCZ+L-AmB	VCZ	Alive	0·125	0·5	1	0·125	1	0·031
2018	27	None	Probable IAPA	Probable IAPA	Yes	VCZ+AFG	VCZ	Alive	0·25	0·125	0·25	0·063	0·5	0·016
2018	34	Trauma	Probable IPA	Probable IPA	Yes	VCZ+AFG		Died (+108)	0·5	0·5	0·5	0·125	2	0·063
2018	18	Relapse ALL	Proven IPA + CNS	Proven IPA + CNS	No	VCZ+L-AmB	ISA+L-AmB; ISA	Alive	0·25	0·25	0·25	0·063	1	0·063
2018	44	Liver cirrhosis, pancreatitis	Probable IPA	Probable IPA	Yes	VCZ+AFG	VCZ	Died (+29)	1	0·5	0·25	0·063	1	0·063
2018	74	Live Tx	Probable IAPA	Probable IAPA	Yes	VCZ+AFG		Died (+3)	-	S	S	S	-	-
2019	67	Multiple myeloma	Probable IAPA	Probable IAPA	No	VCZ		Alive	0·25	0·25	0·25	0·016	0·5	0·031
2019	55	Kidney TX, Larynx carcinoma	Probable IAPA	Probable IAPA	Yes	VCZ+AFG	VCZ	Alive	0·5	0·5	1	0·063	1	0·031
2019	45	Diabetes Mellitus	Probable IAPA	Probable IAPA	Yes	VCZ+AFG	VCZ	Alive	0·5	0·25	0·25	0·031	0·5	0·031
2019	57	Liver cirrhosis	Probable IPA	Probable IPA	Yes	VCZ+AFG		Died (+9)	-	S	S	S	-	-
2019	58	Kidney Tx	Proven CNS	Proven CNS	No	VCZ+L-AmB	VCZ	Alive	1	0·125	0·25	0·031	0·25	<0·016

2020	71	AML, MUD alloSCT	Proven sinusitis	Proven sinusitis	No	L-AmB	ISA	Died (+48)	0·5	0·25	0·5	0·063	0·5	<0·016
2020	64	Kidney Tx	Probable CAPA	Probable CAPA	Yes	VCZ+AFG		Died (+20)	1	0·25	0·5	0·063	0·5	0·016
2020	67	Relapse AML	Proven sinusitis	Proven sinusitis	No	L-AmB	VCZ	Died (+70)	0·5	0·25	0·5	0·063	0·5	0·016
2020	60	AML	Proven sinusitis	Proven sinusitis	No	L-AmB	VCZ	Died (+40)	1	0·5	0·5	0·125	1	0·063
2020	60	COPD	Probable IAPA+TBA	Probable IAPA+TBA	Yes	VCZ+AFG+nL-AmB		Alive	0·5	0·5	0·5	0·063	1	0·031
2020	63	M. Crohn, abdominal sepsis	Probable IPA +TBA	Proven IPA + TBA	Yes	VCZ+AFG+nL-AmB	VCZ+nL-AmB	Died (+53)	1	0·5	1	0·125	1	0·063
2020	76	Diabetes mellitus, hypertension, obesity	Probable CAPA	Probable CAPA	Yes	VCZ+AFG	VCZ	Died (+28)	-	S	S	S	-	-
2020	78	None	Proven osteomyelitis sphenoid	Proven osteomyelitis sphenoid	No	VCZ		Alive	0·5	0·063	0·125	0·063	0·125	<0·016
2020	69	CVA	Probable IAPA	Probable IAPA	Yes	VCZ+AFG	VCZ; L-VCZ+AmB+nL-AmB;	Alive	0·25	0·25	0·5	0·063	1	0·031
2020	65	Kidney Tx	Probable IAPA	Probable IAPA	Yes	VCZ+AFG	ISA+AFG	Alive	1	0·125	0·5	0·063	0·5	0·016

2020	75	Colitis ulcerosa, diabetes mellitus, abdominal sepsis	Probable IPA + TBA	Probable IPA + TBA	Yes	VCZ+AFG+nL-AmB		Died (+7)	0·5	0·5	1	0·125	1	0·031
2020	74	Myasthenia gravis	Probable CAPA	Probable CAPA	Yes	VCZ+AFG		Died (+16)	0·5	0·5	1	0·125	1	0·016
2020	58	Rheumatoid arthritis, pancytopenia	Probable IPA	Proven IPA + TBA	Yes	VCZ+AFG		Died (+1)	1	0·5	0·5	0·063	0·5	0·031
2021	68	Diabetes Mellitus	Probable CAPA	Probable CAPA	Yes	VCZ+AFG		Died (+9)	1	0·5	0·5	0·125	0·5	0·016
2021	75	myasthenia gravis	Probable CAPA	Probable CAPA	Yes	VCZ+AFG		Died (+3)	0·5	0·5	1	0·125	1	0·016
2021	74	Coronary sclerosis, obesity, hypertension	Probable CAPA	Probable CAPA	Yes	VCZ+AFG		Died (+2)	0·5	0·5	1	0·063	1	0·031
2021	66	Coronary sclerosis, hypertension	Probable CAPA	Probable CAPA	Yes	VCZ+AFG	VCZ, ISA	Alive	0·5	1	1	0·125	1	0·125
2021	74	Rheumatoid arthritis	Probable CAPA	Probable CAPA	Yes	VCZ+AFG		Died (+4)	0·25	0·5	1	0·125	1	0·031
2021	67	None	Probable CAPA	Probable CAPA	Yes	VCZ+AFG	ISA+AFG	Died (+9)	0·5	0·25	1	0·063	1	0·016

2021	71	Diabetes Mellitus	Probable CAPA	Proven CAPA + TBA	Yes	VCZ+AFG	VCZ+AFG+nL-AmB	Alive	1	0·25	0·5	0·125	0·5	0·016
2021	67	Hypercholesterolemia, hypertension	Probable CAPA	Probable CAPA	Yes	VCZ+AFG	VCZ	Died (+7)	0·5	0·25	0·25	0·063	0·5	0·031
2022	61	B-ALL, allo SCT	Probable IPA	Probable IPA	No	VCZ		Died (+29)	0·5	0·25	0·5	0·063	1	0·016
2022	58	Multiple Myeloma	Proven CNS	Proven CNS		VCZ	ISA, VCZ	Alive	0·5	0·5	1	0·125	1	0·031
2022	69	Type A dissection	Probable IPA + TBA	Probable IPA + TBA	Yes	VCZ+AFG	VCZ+AFG+nL-AmB; ISA+nL-AmB	Alive	0·25	0·25	0·5	0·125	0·5	0·063
2022	17	Trauma	Proven osteomyelitis	Proven osteomyelitis	No	VCZ	VCZ+AFG; VCZ; ISA	Alive	0·5	0·25	0·5	0·063	1	0·031
2022	64	Lung carcinoma, neutropenia	Probable IPA	Probable IPA	Yes	VCZ+AFG	VCZ	Died (+91)	0·5	0·5	0·5	0·125	1	0·031

NHL, non-Hodgkin lymphoma; Tx, transplant; ALL, acute lymphoblastic leukaemia; HIV, human immunodeficiency virus; AML, acute myeloid leukaemia; MUD, matched unrelated donor; allSCT, allogeneic stem cell transplantation;COPD, chronic obstructive pulmonary disease; CVA, cerebral vascular accident.

IPA, invasive pulmonary aspergillosis; IAPA, influenza-associated pulmonary aspergillosis; CAPA, COVID-19-associated pulmonary aspergillosis; CNS, central nervous system; TBA, invasive tracheobronchial aspergillosis; IA, invasive aspergillosis.

VCZ, voriconazole; tVCZ, topical voriconazole; POS, posaconazole; ISA, isavuconazole; AFG, anidulafungin; AmB_{iv} intravitreal amphotericin B; L-AmB, liposomal amphotericin B; nL-AmB, nebulized liposomal amphotericin B; OLO, olorofim.

For isolates where no MIC values were available, results of agar-based screening using VIPcheck™ is shown. S indicates that there was no growth on agar supplemented with a triazole, which is consistent with a triazole wildtype phenotype.

CHAPTER 3

Characteristics of individual *cyp51A* SNPs and combinations thereof impacting the azole phenotype in TR34-mediated resistance *Aspergillus fumigatus*

Yinggai Song • Jochem B Buil • Jan Zoll • Marlou Tehupeiory-Kooreman • Hanka Venselaar • Ruoyu Li • Willem J G Melchers • Paul E Verweij

Manuscript Submitted

Abstract

The World Health Organization has flagged the rise of drug resistance in *A. fumigatus* as a critical concern. Elevated mutation rates in this pathogen contribute to the rapid development of resistance, complicating treatment efforts. We conducted a study on the prevalence of azole resistance among clinical *Aspergillus fumigatus* isolates in the Netherlands from 1994 to 2022 and identified 34 *cyp51A* variants. To investigate the impact of individual SNPs and combinations thereof on the azole phenotype in TR_{34}-mediated resistance genotypes, we focus on novel, recent mutations and explore the effects of these SNPs: L98H, T289A, I364V, G448S and the combination of these mutations TR_{34}/L98H, TR_{34}/L98H/T289A/G448S, TR_{34}/L98H/T289A/I364V/G448S, on azole affinity and susceptibility. We created the three-dimensional protein model of the CYP51A protein with azoles, and the mutation was introduced to the wildtype-*cyp51 A. fumigatus* strain by the CRISPR-Cas9 gene editing technique. Finally, *in vitro* susceptibility testing of *A. fumigatus* strains carrying the mutations was conducted to confirm the azole phenotypes observed in clinical isolates. The MICs of all four azoles against the mutated *cyp51A* strains harbored combination mutations were higher than that of the wild type, with highly elevated MICs of itraconazole, voriconazole, and isavuconazole. The TR_{34}/L98H, and L98H/T289A strains were resistant to the highest tested itraconazole concentration (16 mg/L). GenotypesTR_{34}/L98H/T289A/I364V/G448S showed consistent phenotype to the clinical strains, which are highly resistant to voriconazole but susceptible to Itraconazole. In this study, we show that molecular dynamics simulations amino acid substitutions in the *cyp51A* gene, correlate to the structure–function relationship of in vitro phenotype.

Keywords: *Aspergillus fumigatus*, azole-resistant, *cyp51A*, SNPs, molecular docking

Introduction

Aspergillus fumigatus, a globally distributed opportunistic pathogen, can cause a broad-spectrum of diseases, including invasive aspergillosis (IA), a life-threatening disease in immunocompromised patients (Ullmann et al., 2018). Patients at risk for invasive aspergillosis include patients with hematologic malignancy, solid organ transplant recipients, and patients receiving corticosteroids. In addition, new risk groups are being recognized, including patients treated with ibrutinib (Ullmann et al., 2018) and patients with severe influenza and COVID-19 (Latgé et al., 2019; Yong et al., 2018). The fungus might also cause chronic pulmonary infections, chronic lung colonization, and allergic syndromes (Alanio et al., 2020).

Triazole drugs (itraconazole, voriconazole, posaconazole, and isavuconazole) have become the cornerstone of the prevention and treatment of aspergillus diseases. Unfortunately, azole-resistant *A. fumigatus* (ARAF) has been increasingly found in patients who receive long-term azole treatment, azole-naive patients, and in the agricultural environment (Latgé et al., 2019; Verweij et al., 2022). The emergence of ARAF isolates has been a significant concern, with increasing resistance rates in some countries (Cuypers et al., 2025). The emergence of resistance to azole drugs arises primarily through two genetic mechanisms: point mutations in the *cyp51A* open reading frame (with or without tandem repeats [TR_{34}/ TR_{46}] in the promoter region) and overexpression of the *cyp51A* gene. These alterations confer varying levels of resistance to triazole antifungals. Although the TR_{34}/L98H and TR_{46}/Y121F/T289A are the dominant resistance mechanisms found worldwide, genotype variations have been frequently reported. G54, G138, M220, Y121, G448, and P216 are common hot spot mutations that have been detected in ARAF from the patients under long-term antifungal treatment (Snelders et al., 2010; Chowdhary et al., 2014). Additionally, resistance can involve upregulation of sterol 14α-demethylase due to *cyp51A* overexpression or reduced intracellular drug concentrations resulting from efflux pump gene overexpression (Chowdhary et al., 2014; Alvarez-Moreno et al., 2017; Chowdhary et al., 2017).

Although resistance might be selected during azole therapy, resistance selection in the environment through exposure to azole fungicides has been shown to be the main route in *A. fumigatus* (Verweij et al., 2016; Rhodes et al., 2022). Point mutations typically emerge from clinical azole exposure (prophylaxis or therapy). In contrast, TR-associated mutations TR_{34}/L98H and TR_{46}/Y121F/T289A are linked to environmental selection pressure from agricultural azole fungicides, widely used in

crop protection (Verweij et al., 2013; Schoustra, et al., 2019). These TR strains can disseminate via airborne conidia, infecting azole-naïve patients. Similar trends are observed globally. Two resistant *A. fumigatus* soil isolates harboring mutations of TR_{34}/L98H/S297T/F495I were identified in Beijing and Fuzhou, respectively (Chen et al., 2016). Ren et al. (2017) reported the emergence of ARAF the mutations TR_{46}/Y121F/T289A and TR_{34}/L98H/S297T/F495I in agricultural fields. Multi-azole resistant strains with these complex mutations have increasingly been isolated in the environment worldwide since 2020. Because there is a concern that their prevalence will likely increase in clinical settings, these strains must continue to be monitored and investigated (Uehara et al., 2025). Alongside known resistance polymorphisms, a novel *cyp51A* genotype associated with azole-resistance within the UK, the TR-associated polymorphism, TR_{34}/L98H/T289A/I364V/G448S, which was collected in 2016 from a sputum sample of one patient with necrotizing aspergillosis, manifesting a multi-azole resistant phenotype, demonstrated by high MIC values for itraconazole, voriconazole (both ≥ 16 mg/L) and posaconazole (4 mg/L), and this phenotypic and genotypic variant was only recovered in patient and was not found in the environment (Rhodes et al., 2022; Abdolrasouli et al., 2022). Given the threat of environmental and clinical resistance spread—exacerbated by intensive fungicide use (in Brazil, where pesticide consumption rose 190% by 2010)—monitoring ARAF epidemiology and mechanisms is critical for managing aspergillosis.

To elucidate how characteristics of the individual SNPs and combinations thereof impact the azole phenotype within the complex TR_{34}/L98H/T289A/I364V/G448S resistance background, this study employed the CRISPR-Cas9 gene editing technique to systematically introduce and evaluate the effects of these specific mutations, both singly and in various combinations.

Materials and Methods

Screening of azole-resistance *A. fumigatus* clinical isolates

We collected 12,679 Clinical *A. fumigatus* isolates from 1994 to 2022 preserved at Radboud University Medical Centre. MIC testing was performed according to the European Committee on Antimicrobial Susceptibility Testing (EUCAST) broth microdilution reference method for amphotericin B (AmB), itraconazole (ITR), voriconazole (VOR), posaconazole (POS), and isavuconazole (ISA) (from 2015 when the drug was clinically licensed). An agar plate containing only RPMI1640 with 2% glucose gar was used as growth control. Triazoles with activity against *A. fumigatus*

include itraconazole, voriconazole, posaconazole, and isavuconazole. Azole resistance was defined as resistance to >1 azole drug, according to EUCAST clinical breakpoints (itraconazole, >2 mg/L; voriconazole, >2 mg/L; posaconazole, >0.25 mg/L, and isavuconazole, >1 mg/L). EUCAST broth microdilution plates were made at Radboud UMC in batches of 96-well plates and complied with the recommended quality control standards.

Isolates with resistance genotype and phenotype

For four *A. fumigatus* isolates with a confirmed azole-resistant phenotype, the full c*yp51A* gene was analyzed by PCR amplification and sequencing. The c*yp51A* sequence (GenBank accession no. AF338659) was used for mutation analysis. A spore suspension of all isolates was stored at –80°C in 10% glycerol. Clinical information regarding underlying disease and classification of *Aspergillus* disease was not collected.

CRISPR/Cas9 lab strain and culture preparation

The parental strain used in this experiment was the *cyp51A*-wildtype *A. fumigatus* A1160ΔakuB^{ku80} pyrG^{+}, a derivative of the CEA10 clinical lineage which lacks a nonhomologous end-joining (NEHJ) DNA repair pathway (Zhao et al., 2019). This strain has been commonly employed in studies that performed genetic manipulation by integrating exogenous DNA using homologous recombination. The parental strain was taken from the freezer stock of the Radboudumc Mycology Research Group and cultured twice on SDA (Sabouraud Dextrose Agar, Oxoid) media to activate sporulation. The desired *cyp51A*-wildtype genotype was confirmed by sequencing. A new culture from the freezer stock was done after every three transformations.

Construction of the repair template and the dual Cas9-gRNAs system

All primers sequences and crRNAs designs are listed in Table 1.

The hygromycin B phosphotransferase (*hph*) cassette was integrated into the 3’ UTR of the *cyp51A* repair template with a 117-bp spacer from the ORF as the selection marker for Cas9-mediated gene replacement. The integration was checked transcriptomically to avoid influencing the adjacent gene. 2695-bp hph sequence was amplified from pAN7-1 plasmid with hyg-F and hyg-R primers using PCR. The plasmid remnants were digested by the DpnI enzyme (New England BioLabs). (Figure S1)

The *cyp51A* repair templates with four desired *cyp51A* genotypes: (1) wildtype-*cyp51A*, (2) TR_{34}/L98H, (3) TR_{34}/L98H/T289A/G448S, and (4) TR_{34}/L98H/T289A/I364V/G448S were isolated from the clinical strains. These

genotypes were first confirmed by Sanger sequencing before the PCR amplification step. The primers used for the *cyp51A* amplification were designated as cyp-F 5' and cyp-R 3', targeting the 5'UTR and 3'UTR, respectively (Table 1). cyp-R 3' and hygF shared a 21-bp overlapping sequence (annotated in blue), which would function as a linker for the fusion of the *cyp51A* and the hph cassette. The hyg-R primer was designed to insert 46bp of flanking microhomology region for the *cyp51A* 3'UTR. The resulting *hph* and *cyp51A* fragments were purified using QIAquick Gel Purification Kit (Thermo Fisher Scientific) and fused by Gibson Assembly Master Mix. The fused fragments were further amplified by PCR using a shorter set of primers: fusion-F and fusion-R. The final PCR products were purified and utilized as repair templates.

Table 1. Sequences of primers and crRNAs used in CRISPR/Cas9 system

Name	**Sequence (**5' -3'**)**
cyp-F 5'	GGCTTTCATATGTTGCTCAGCGGCAGCATTCTGAAACACGTGCGTAGCAAGCGAGAAGGAAAGAAGCAC
cyp-R 3'	GGTCTGAATAAGGGTTCAATACAGTCATTTATTAGGCGCTCGAGGGGCTGAATTAAGTATAA
hyg-F	TATTGAACCCTTATTCAGACCACGGCGTAACCAAAAGTCACACAACACAAGCTGTAAG
hyg-R	CAAATACTCATACTCAGTATAGGCAACAACACTTCAGGGCCAGTAATCTTGACGACCGTTGATCTG
fusion-F	TATTGAACCCTTATTCAGACCACGGCGTAACCAAAAGTCACACAACACAAGCTGTAAG
fusion-R	CAAATACTCATACTCAGTATAGGCAACAACACTTCAGGGCCAGTAATCTTGACGACCGTTGATCTG
hyg-cyp51F	GGCTTTCATATGTTGCTCAGCG
hyg-cyp51R	CAAATACTCATACTCAGTATAGGCAACAACAC
5' gRNA	TCTGAAACACGTGCGTAGCA
3' gRNA	ATACTTAATTCAGCCCCTCG

We replaced the parental *cyp51A* gene with the desired *cyp51A* genotypes. To knock out the whole open reading frame (ORF) and the prospective tandem repeat region, two crRNAs targeting the 5'-UTR and the 3'-UTR of the *cyp51A* gene were designed using the web-based guide RNA designing tool EuPaGDT (Nicolas et al., 2014). The genomic sequence of the 5'-UTR and the 3'-UTR from the genomic database were then uploaded to the EuPaGDT website. The program was run with the SpCas9

selection, microhomology search, and conserved region search setting. The generated crRNA would be chosen if it was close to the ORF and had the highest QC score (Figure 2). Alt-R™ CRISPR-Cas9 crRNA (2nmol), Alt-R™ CRISPR-Cas9 tracRNA (5nmol), and Alt-R™ s.p. Cas9 Nuclease (100µg) were ordered from Integrated DNA Technology (IDT). A 100µM stock solution of the crRNA and tracRNA each was made by resuspending the RNA oligos in a nuclease-free duplex buffer supplied by the IDT. For each gRNA (3' gRNA and 5' gRNA), a 33 µM RNA duplex solution was prepared by mixing an equimolar concentration of the crRNA and tracRNA in the nuclease-free duplex buffer. The solution was then heated at 95°C for 5 minutes and cooled to room temperature gradually in a thermal cycler for 10 minutes (0.1°C/s). The Cas9-nuclease was diluted ten times in the Cas9 working buffer (20mM HEPES; 150mM KCl, pH 7.5) to reach a final concentration of 1µg/µl. All the prepared molecular reagents were stored at -20°C.

Protoplast transformation

The procedure was established mostly based on the methodology of Zhao et al. (2019) approximately $1x10^6$ fresh conidia of the parental *A. fumigatus* were inoculated in 50mL Sabouraud Dextrose Broth (Thermo Fisher Scientific) at 37°C with shaking at 130rpm. After 16 hours, the mycelia were harvested by filtration through sterile Miracloth and resuspended in 20mL Yeast extract Glucose solution (YG; 0.5% yeast extract, 2% glucose) with protoplast solution (2g VinoTaste Pro [Lamothe-Abiet] in 20mL 1M KCl and 0.1M Citric Acid). After approximately two hours, the protoplasts were checked for proper size and harvested through a sterile Miracloth filter to discard the mycelial debris. The protoplast solution was centrifuged for 10 minutes at 2000 x g at 4°C. Following discarding the supernatant, the protoplast pellet was washed twice and resuspended in 0.6M KCl and 50mM CaCl2. The protoplast solution was kept on ice before use. Five minutes before the transformation, the Cas9: crRNA: tracRNA ribonucleotide complex (RNP) was assembled by mixing 1.5 µl of the 3' gRNA, 5' gRNA, and Cas9-nuclease (1 µg/µl) in 22 µl Cas9 working buffer (total volume of 26.5µl). After five minutes of incubation at room temperature, the RNP complex solution, 20µl dsDNA repair template, and 25µl PEG solution (60% wt/vol PEG3350, 50mM CaCl2, 450mM Tris-HCl, pH 7.5) was added to 50µl protoplast solution. The mixture was incubated on ice for 50 minutes before supplementing an additional 1mL PEG solution, followed by another 25 minutes of incubation at room temperature. The entire transformation solution was plated over five SMM agar plates (GMM supplemented with 1M sorbitol and 1.5% [wt/vol] agar) containing hygromycin B (150µg/ml). The plates were incubated at room temperature for the first 24 hours and then moved to the 37°C incubator for 48-72

hours.

Validation of CRISPR/Cas9 transformants

Single colonies on SMM agar plates supplemented with hygromycin B were selected and transferred to Sabouraud Dextrose Agar (Thermo Fisher Scientific). After two days of incubation at 37°C, the conidia were collected for DNA extraction. The conidia were first suspended in 250µl breaking buffer (2% Triton X-200, 1% SDS, 100mM NaCl, 10mM Tris-HCl pH=8, 1mM EDTA pH = 8) and shaken with glass beads (0.4 – 0.6 mm diameter) at maximum speed for 30 minutes at 70°C. Afterward, 200 µl PCI (phenol-chloroform-isoamyl alcohol) was added, followed by a 5-minute shake at maximum speed at room temperature. The mixture was centrifuged for 5 minutes at 11000 x g. The upper phase containing the DNA was collected. The recombinant isolates were first checked for the position of integration. To check whether the repair template was integrated into the correct position, a set of two primers designated as hyg-cyp51-F and hyg-cyp51-R was used, which covered an upstream region of the *cyp51A* 5'UTR and a part of the hph cassette, respectively. If the recombination happened correctly, a PCR product of around 3kb would be obtained. Isolates with correct integration positions had their *cyp51A* sequenced by Sanger sequencing to validate the genotypes of interest.

Growth testing and antifungal susceptibility testing of *A. fumigatus* recombinants

Growth measurements of the recombinants compared to the transformation recipient isolate and transformation control cassette isolate. The average diameter of three independent experiments was used to determine the radial growth rate. The azole-phenotype was illustrated as the minimum inhibitory concentration (MIC) of the medical azole compounds for *A. fumigatus*, which was determined according to the EUCAST E.Def 9.4 methodology for broth microdilution susceptibility testing, the novel antifungal olorofim and the fungicides susceptibility testing were performed against tebuconazole, difenoconazole, prochloraz, pyraclostrobine, benomyl, carbendazim, boscalid, and fluopyram. We also conducted testing for fungicides on the recombinants, covering five distinct targets, including agricultural triazole, Imidazole, Qol, MBC, and SDHI.

Three-dimensional protein model of the Cyp51A protein with azoles

Since no experimentally solved 3D-structure for *A. Fumigatus* Cyp51a exists, a homology model using the YASARA & WHAT IF Twinset software was created (Krieger et al., 2002; Vriend,1990). The standard YASARA modelling protocol with default settings was used. As possible templates the previously solved structures were

chosen *A. fumigatus* Cyp51b (PDB file 6CR2 64% sequence identity), *S. cerevisiae* Cyp51 (PDB files 5ESM and 8DL4, 49% sequence identity). The best parts of the created models were selected by the automatic modelling script to create a final hybrid model which was used for further analysis. The azole structures used in this study were obtained from PDB files 4UYM (Voriconazole), 5ESL (Itraconazole), 6E8R (Posaconazole) and 6UX0 (Isavuconazole). These molecules were superposed on the VNI-derivative molecule present in the hybrid CYP51 model followed by an energy minimization run using the standard YASARA script. The four different azole/protein combinations were compared and analyzed.

This 3D homology model visualizes *A. fumigatus* Cyp51A, the target of medical triazoles, with engineered point mutations at critical residues (L98, T289, I364, G448) fully solvent-exposed and labeled—key sites for azole resistance (e.g., TR_{34}/L98H). The substrate access channels, and binding regions are highlighted in green, revealing steric constraints for antifungal drugs. Experimentally docked azole ligands include itraconazole (visible, 4,167 atoms) and voriconazole (visible, 12,640 atoms), while isavuconazole and posaconazole are inactive. Real-time structural metrics are enabled for bond lengths, angles, and dihedrals, facilitating analysis of mutation-induced conformational changes in substrate channels and ligand-binding efficiency. This model directly correlates residue exposure with clinical resistance mechanisms, providing a mechanistic basis for azole treatment failures.

Results

Phenotypes of Clinical *A. fumigatus* isolates harbored TR_{34}/L98H/T289A/I364V/G448S

The desired mutations were introduced in the *A. fumigatus* A1160ΔakuB^{ku80} pyrG^{+} by the CRISPR-Cas9 method, which was further utilized for azole susceptibility testing. The recent variant TR_{34}/L98H/T289A/I364V/G448S, was identified by the 29-year genotype and phenotype screening in our center (Table S1, S2; Table 2). The azole profiles are showed in Table 3, The TR_{34}/L98H/T289A/I364V/G448S showed a consistent phenotype for the clinical strains, which are highly resistant to voriconazole but susceptible to Itraconazole, and the I364V introduction did not change the phenotype.

Compared with the *senso stricto* mutation TR_{34}/L98H (GM: ITR, 27.53 mg/L, VOR 4.87 mg/L, POS 0.70mg/L, ISA>7.59 mg/L), the variant TR_{34}/L98H/T289A/I364V/G448S showed the reverse changes against the ITR and VOR, we predicted the T289A or

G448S contribute to the phenotype changes, and from the following two mutations TR_{46}/Y121F/T289A/G448S and TR_{46}/Y121F/T289A azole phenotypes (Table S1), which show the T289A or G448S act differently when combined with the TR_{34} and TR_{46} groups.

Based on the above phenotype changes, we constructed the important mutants by CRISPR/Cas9 genome editing to explore the mechanism of different mutations: TR_{34}/L98H/T289A/I364V/G448S, TR_{34}/L98H/T289A/G448S, TR_{34}/L98H, L98H, G448S, T289A, and WT cyp51A.

Table 2. TR_{34}-variants with triazole phenotypes that are not within the core MIC distribution of TR_{34}/L98H *ss* isolates.

		Phenotype			
Variants	**Isolation date**	**Itraconazole**	**Voriconazole**	**Posaconazole**	**Isavuconazole**
TR_{34}/L98H *ss* GM-MIC		27.53	4.87	0.7	7.59
Mean log_2 MIC±3SD		4.78±2.34	2.28±2.95	-0.52±3.18	2.92±2.77
TR_{34}/L98H/S297T/F495I	23/08/2009	>16	>16	0.5	>16
TR_{34}/L98H/S297T/F495I	07/06/2011	>16	4	2	>16
TR_{34}/L98H/T289A/G448S	18/05/2018	1	>16	0.25	>16
TR_{34}/L98H/T289A/G448S	31/01/2020	1	> 16	1	>16
TR_{34}/L98H/T289A/G448S	04/11/2020	2	> 16	1	>16
TR_{34}/L98H/T289A/I364V/G448S	27/05/2021	0.5	> 16	0.5	>16
TR_{34}/L98H/T289A/I364V/G448S	08/06/2021	2	> 16	1	>16
TR_{34}/L98H/T289A/I364V/G448S	09/08/2021	1	> 16	1	>16
TR_{34}/L98H/T289A/I364V/G448S	29/09/2021	1	> 16	0.5	>16

Note: Red color, outside of the core MIC distribution; green color, within the core MIC distribution.

cyp51A transformation using CRISPR/Cas9 system

In total, three transformations were conducted to create *cyp51A* recombinants of (1) TR_{34}/L98H/T289A/I364V/G448S, (2) TR_{34}/L98H/T289A/G448S, (3) TR_{34}/L98H, (4)

L98H, (5) G448S, (6) T289A, and (7) WT cyp51A, with the selective marker. Several single colonies were chosen from the transformation plates and were sub-cultured on SDA slants. By PCR testing, three the full combination isolates, three TR_{34}/L98H isolates, and three *cyp51A* wildtype and SNPs isolates were confirmed to have the recombination occur at the correct location. Subsequently, streaking was performed for all isolates to obtain the pure strains. Sanger sequencing was carried out to validate the locus's sequence of the successful recombinants (Figure 1). The insertion of a 34-bp tandem repeat and the substitution of leucine to histidine at position 98 were present in three prospective TR_{34}/L98H. Likewise, two wildtype transformants were confirmed to have wildtype cyp51A locus. Four desired mutations were successfully introduced in three prospective TR_{34}/L98H/T289A/I364V/G448S isolates.

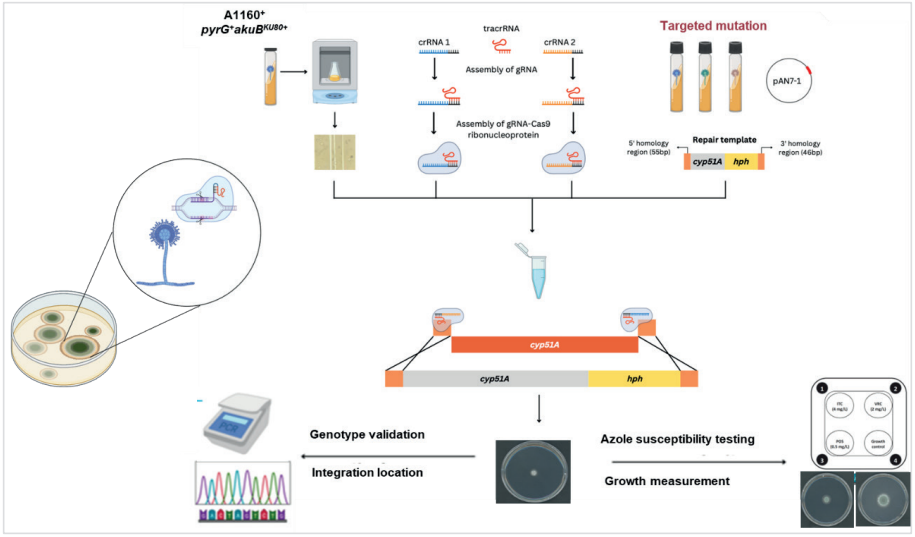

Figure 1. Overview of the microhomology-mediated cyp51A transformation using CRISPR-Cas9 gene editing. The overall workflow entails four main sections: (1) strain and culture preparation, (2) construction of the repair template and the dual Cas9-gRNAs system, (3) protoplast transformation, and (4) validation of transformation.

Baseline susceptibility and single mutations of *Aspergillus fumigatus* recombinants

The MICs of four medical azoles – itraconazole, voriconazole, posaconazole, and

isavuconazole against the recombined *A. fumigatus* strains were determined. The wild-type *A. fumigatus* strain ($A1160^{+}$ wt) and its genetically modified control (WT *cyp51A*) show baseline susceptibility to most antifungals (Table 3). Introducing single point mutations shows specific resistance profiles: the L98H mutation confers significant resistance to itraconazole, voriconazole, isavuconazole, and tebuconazole, while the G448S mutation drives strong resistance to voriconazole and isavuconazole. Mutations T289A and I364V cause only minor, clinically insignificant changes in susceptibility for the tested drugs.

Combined mutations and high-level resistance

The MICs of all four medical azoles against the mutated *cyp51A* strains harbored combination mutations were higher than that of the wild type, with highly elevated MICs of itraconazole, voriconazole, and isavuconazole. Combining mutations generates clinically relevant, high-level multi-azole resistance.

The TR_{34}/L98H recombinant exhibits high-level resistance to itraconazole (>16mg/L) alongside reduced susceptibility to voriconazole, posaconazole, isavuconazole, and tebuconazole. Further combining mutations into the TR_{34}/L98H/T289A/G448S background results in high-level resistance to isavuconazole (>16 mg/L) and voriconazole (16 mg/L), significant resistance to Prochloraz (4 mg/L), and reduced susceptibility to other azoles. Adding the I364V mutation to create Full TR_{34}/L98H/T289A/I364V/G448S exacerbates resistance, causing high-level resistance to voriconazole (16 mg/L), isavuconazole (>16 mg/L), tebuconazole (16 mg/L), difenoconazole (16 mg/L), and boscalid (>16 mg/L), while maintaining reduced susceptibility to posaconazole and itraconazole.

Non-azole antifungals and olorofim susceptibility

Most non-azole agricultural fungicides retain activity across mutants. Pyraclostrobine, benomyl, and carbendazim show consistently low MICs with no observable resistance. Fluopyram MICs remain high but stable. Boscalid resistance emerges only in the full combination with I364V mutant. Crucially, the novel antifungal olorofim (DHODH inhibitor) maintains very low MICs (0.016-0.03 mg/L) against all strains, including the complex pan-azole resistant mutants (TR_{34}/L98H, Full combination with or without I364V), demonstrating no cross-resistance and highlighting its value in managing multi-resistant pathogens.

High-frequency SNPs G448S and T289A

Two hotspot mutations with high-frequency SNPs: G448S and T289A, it can be combined with different groups and also changes the phenotype (ITR vs VOR). The MICs of all four azoles against the mutated *cyp51A* strains harbored combination

mutations were higher than that of the wild type, with highly elevated MICs of itraconazole, voriconazole, and isavuconazole. The L98H mutants and G448S mutants showed high voriconazole (8 mg/L) and Isavuconazole (4 mg/L), and high Agricultural Triazole. T289A mutant and I364V mutant showed susceptible phenotype to all medical azoles, and Agricultural Triazole. All mutants are susceptible to olorofim (≤0.03 mg/L) but resistant to Fluopyram (≥16 mg/L).

Phenotypes changes vary from mutations

The degree of resistance varies across different mutations, presumably owing to the intrinsic allele diversity of each isolate. Phenotypic differences between clinical isolates involve many thousands, to tens of thousands of SNPs. The average diameter of three independent experiments was used to determine the radial growth rate. G448S and full mutations combinations decreased the growth. The quintuple mutant (TR_{34}/L98H/T289A/I364V/G448S) exhibits severely impaired growth, indicating a significant *fitness cost* from accumulating multiple resistance mutations, particularly I364V in combination with TR_{34}/L98H/G448S. In contrast, control strains (recipient isolate, cassette control) and single mutants (T289A, G448S, I364V) show robust, near-normal growth. The double mutant (TR_{34}/L98H) displays only a mild growth reduction, confirming that fitness loss escalates with mutation complexity.

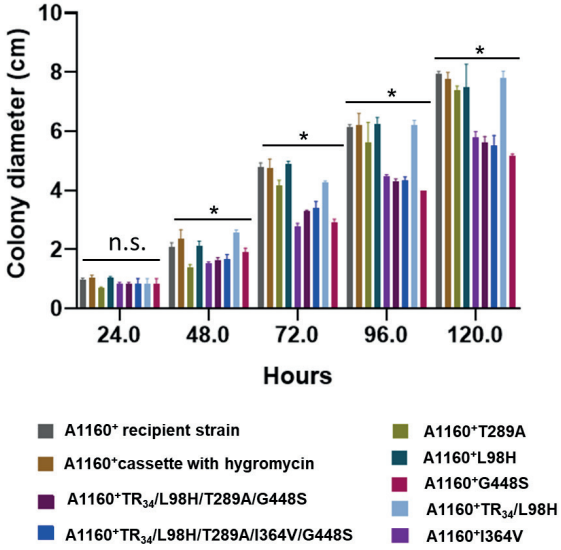

Figure 2. Growth measurements of the transformants

Colony diameter was measured over time to assess the growth rate. The strains analyzed

include the wild-type A1160^{+} recipient, a control strain with a hygromycin resistance cassette, and various mutant strains carrying single (T289A, L98H, G448S, I364V) or combined (TR_{34}/L98H, TR_{34}/L98H/T289A/G448S, TR_{34}/L98H/T289A/I364V/G448S) resistance-associated mutations.

Colony diameter was measured over time to assess the growth rate. The strains analyzed include the wild-type A1160^{+} recipient, a control strain with a hygromycin resistance cassette, and various mutant strains carrying single (T289A, L98H, G448S, I364V) or combined (TR_{34}/L98H, TR_{34}/L98H/T289A/G448S) resistance-associated mutations.

Molecule alignments and docking

Molecular dynamics simulations form a systematic atlas that pairs wild-type Cyp51A snapshots with close-up views of key resistance mutations found in two multi-azole–resistant *A. fumigatus* haplotypes. They are arranged so that each set of "close-up" panels highlights the exact residue, side-chain orientation, and local pocket changes introduced by the mutations. The 3D structural analysis of *Aspergillus fumigatus* Cyp51A mutants reveals how combinatorial mutations in the TR_{34}/L98H backbone synergistically confer pan-azole resistance while preserving enzymatic function (Figure 3). The L98H mutation destabilizes heme binding while increasing BC-loop flexibility, narrowing the ligand entry channel. T289A disrupts hydrogen-bond networks near the heme, compromising triazole coordination. G448S creates steric hindrance at the substrate channel entrance, blocking bulky azoles (isavuconazole). I364V compresses the hydrophobic cavity, restricting accommodation of hydrophobicity-dependent azoles (voriconazole/posaconazole). These mutations form a complementary defense barrier—L98H and T289A target the catalytic core, G448S guards the channel gateway, and I364V remodels the binding cavity—collectively dismantling the binding foundations of diverse azoles (Figure S2). The combinatorial mutations in *A. fumigatus* Cyp51A (L98H/T289A/I364V/G448S) confer pan-azole resistance through precise spatial reorganization. Despite these resistance-conferring changes, lanosterol (natural substrate) maintains binding through: Conformational flexibility of the BC loop, compensating for mutation-induced distortions; Minimal impact of T289A/L98H on substrate orientation; Tolerated geometry shifts at G448S/I364V due to hydrophobic stacking adaptability. This functional duality—simultaneous azole resistance and sustained lanosterol 14α-demethylation—explains both the high MICs (>16 mg/L) observed clinically and the environmental fitness of TR_{34}-harboring strains in fungicide-exposed niches.

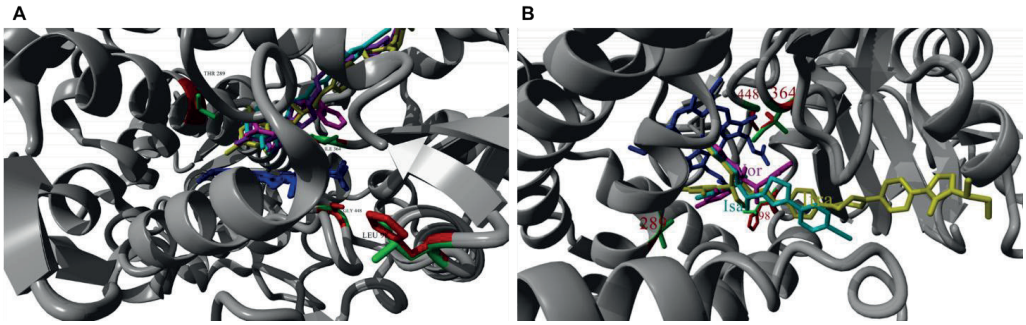

Figure 3. Homology model of *Aspergillus fumigatus* CYP51A

Three-dimensional protein model of the Cyp51A protein with four azoles, the amino acids L98, T289, I364, and G448 (A) are fully exposed and labeled, with engineered point mutations at critical residues (L98H, T289A, I364V, G448S) TR_{34}/L98H/T289A/I364V/G448S fully solvent-exposed and labeled (B). Red: isavuconazole, Yellow: Itraconazole, Purple: posaconazole, Magenta: voriconazole

Table 3. The susceptibility of medical antifungals and agricultural fungicides

Mutants	ITR	VOR	POS	ISA	TEB*	DIF*	PRO*	PYR*	BEN*	CAR*	BOS*	FLUO*	olorofim*
A1160$^+$ recipient strain	0.5	0.5	0.12	0.5	0.25	2	0.06	0.016	2	2	16	16	0.016
A1160$^+$ cassette hph	0.5	0.5	0.12	0.5	0.5	1	0.06	0.06	2	1	16	32	0.03
A1160$^+$ L98H	1	1	0.5	2	2	8	0.25	0.03	4	2	16	32	0.03
A1160$^+$ T289A	1	0.5	0.12	0.5	0.5	0.5	0.06	0.06	2	1	16	32	0.03
A1160$^+$ I364V	0.25	0.5	0.12	0.5	0.5	0.5	0.12	0.06	2	1	16	32	0.016
A1160$^+$ G448S	1	8	0.25	4	2	0.12	0.06	0.03	1	1	16	32	0.016
A1160$^+$ TR_{34}/L98H	>16	4	1	4	4	8	0.06	0.03	1	2	16	32	0.03
A1160$^+$ TR_{34}/L98H/T289A/G448S	0.5	16	0.25	>16	8	4	4	0.06	2	1	8	16	0.03
A1160$^+$ TR_{34}/L98H/T289A/I364V/G448S	0.5	>16	1	>16	16	16	4	0.12	2	1	>16	32	0.03

*Fungicides read out the MIC50;

TEB: Tebuconazole, DIF: Difenoconazole, PRO: Prochloraz, PYR: Pyraclostrobine, BEN: Benomyl, CAR: Carbendazim, BOS: Boscalid, FLUO: Fluopyram

Discussion

Drug resistant fungal infections are a major concern and challenge for the medicines and agriculture (Fisher et al., 2022). Resistance in *A. fumigatus* is linked to the accumulation of agricultural azoles in its natural habitats, such as decaying plant material, which amplifies resistant genotypes. Cross-resistance between agricultural azoles (e.g., tebuconazole) and medical azoles (e.g., voriconazole) complicates treatment, with resistant isolates often harboring signature mutations like TR_{34}/L98H and TR_{46}/Y121F/T289A (Debergh et al., 2024). Genomic studies confirm overlap between environmental and clinical resistant populations, highlighting the role of agricultural practices in clinical resistance (Rhodes et al., 2022).

The CRISPR-engineered *cyp51A* mutants reveal synergistic resistance mechanism of combinatorial mutations in *A. fumigatus*. In this study, we employed the CRISPR-Cas9 gene editing technique to investigate the effects of individual SNPs and combinations thereof on the azole phenotype in TR_{34}/L98H/T289A/I364V/G448S-mediated resistance genotypes. Our CRISPR-Cas9 mutagenesis reveals that G448S is the primary driver of voriconazole and isavuconazole resistance in single-mutant *A. fumigatus* strains. Combinatorial mutations within the TR_{34}/L98H backbone, however, induce synergistic high-level resistance. The TR_{34}/L98H/T289A/G448S confers MIC>16 mg/L for VOR/ISA, while adding I364V (TR_{34}/L98H/T289A/I364V/G448S) amplifies pan-azole resistance. Structural analyses explain these profiles: G448S sterically occludes large triazoles (VOR/ISA) at the substrate channel entrance; I364V contracts the hydrophobic cavity, restricting voriconazole/posaconazole; T289A disrupts hydrogen-bond networks critical for smaller triazoles; and L98H impairs heme-binding stability. This hierarchy establishes G448S as the linchpin mutation, potentiated by epistatic interactions. Our findings directly support the establishment of a national surveillance network to monitor trends in the frequency of azole resistance in *A. fumigatus* and to better understand the underlying resistance mechanisms.

Critically, these mutations preserve lanosterol 14α-demethylase activity through compensatory mechanisms. By maintaining membrane biosynthesis through uninterrupted lanosterol demethylation while excluding exogenous drugs, the mutations achieve a sophisticated molecular-level equilibrium between pan-resistance and ecological survival. These clinical resistance patterns extend to agricultural fungicides: All mutants retain susceptibility to fluopyram (MIC_{50}≤0.25 mg/L), carbendazim resistance is universal (MIC_{50}=16 mg/L), cross-resistance to SDHIs emerges in combinatorial mutants. Structural correlations explain these

profiles: G448S sterically occludes large triazoles (VOR/ISA) in the substrate channel, T289A disrupts hydrogen bonds critical for smaller azoles (ITR), I364V cooperatively contracts the binding pocket when paired with G448S. This suggests that while high-level pan-azole resistance evolves in complex mutants, their environmental persistence may be limited by reduced vegetative competitiveness compared to fitter, less resistant strains.

Despite increased *A. fumigatus* isolation during the COVID-19 pandemic, azole resistance rates remained stable—a phenomenon potentially reflecting diagnostic biases or ecological equilibria in TR_{34} genotype distribution. While azoles remain first-line therapy, combinatorial resistance undermines efficacy: high-dose isavuconazole shows limited utility against G448S strains, and co-infections (azole-susceptible + resistant strains) complicate diagnostics. The accumulation of diverse *cyp51A* mutations over time drives fluctuating resistance patterns, making treatment and antifungal stewardship challenging. Current culture/PCR methods fail to detect cryptic SNPs and heteroresistance, underscoring the urgent need for NGS-based diagnostic panels (e.g., *TEF1α* metabarcoding) and monitoring air/soil/clinical matrices using molecular tools (Weaver et al., 2024; de Groot T et al., 2019).

Clinical isolates harbor complex resistance mutations. Diversity mutations of *cyp51A* accumulated over time and resistant variants in clinical isolates are related to variation in the environment. Azoles resistance fluctuates vary from mutations and treatment option and antifungal stewardship is also challenging. Mutations compensatory evolution of resistant *A. fumigatus* is to overcome any potential fitness costs. The presence and clinical implications of compensatory evolution in *A. fumigatus* is largely unknown. Multidisciplinary and intersectoral collaborations are needed to counter the spread of antifungal resistance, diagnostic stewardship in healthcare and antifungal stewardship in the environment.

This study moves beyond correlation to establish causality and quantify the individual and interactive roles of key mutations within a new variant - multi-drug resistant fungal genotype and illustrates how specific *cyp51A* mutations confer targeted azole resistance, while combinations involving the TR_{34} promoter and multiple mutations drive broad, high-level pan-azole resistance, mirroring challenging clinical isolates. The sustained potent activity of olorofim against all resistant strains highlights its distinct mechanism of action and significant therapeutic potential for treating multi-drug-resistant *A. fumigatus* infections. It provides fundamental mechanistic knowledge crucial for combating the growing threat of azole-resistant fungal infections through improved diagnostics, drug

discovery, and treatment strategies.

Reference

Alanio A, Dellière S, Fodil S, et al. Prevalence of putative invasive pulmonary aspergillosis in critically ill patients with COVID-19. *Lancet Respir Med*. 2020,8(6): e48-e49.

Abdolrasouli A, Rhodes JL. Phenotypic variants of azole-resistant Aspergillus Fumigatus that co-exist in human respiratory samples are genetically highly related. *Mycopathologia*. 2022;187(5-6):497-508.

Alvarez-Moreno C, Lavergne RA, Hagen F, Morio F, Meis JF, Le Pape P. Azole-resistant Aspergillus fumigatus harboring TR34/L98H, TR46/Y121F/T289A and TR53 mutations related to flower fields in Colombia. *Sci Rep*. 2017; 7:45631.

Chowdhary A, Sharma C, Kathuria S, Hagen F, Meis JF. Exploring azole antifungal drug resistance in Aspergillus fumigatus with special reference to resistance mechanisms. *Future Microbiol*. 2014; 9:697–711.

Chowdhary A, Sharma C, Meis JF. Azole-resistant aspergillosis: epidemiology, molecular mechanisms, and treatment. *J Infect Dis*. 2017;216: S436–S444.

Chen Y, Lu Z, Zhao J, Zou Z, Gong Y, Qu F, Bao Z, Qiu G, Song M, Zhang Q, Liu L, Hu M, Han X, Tian S, Zhao J, Chen F, Zhang C, Sun Y, Verweij PE, Huang L, Han L. Epidemiology and molecular characterizations of azole resistance in clinical and environmental *Aspergillus fumigatus* isolates from China. *Antimicrob Agents Chemother.* 2016; 60:5878–5884.

Cuypers L, Aerts R, Van de Gaer O, Vinken L, Merckx R, Gerils V, Vande Velde G, Reséndiz-Sharpe A, Maertens J, Lagrou K. Doubling of triazole resistance rates in invasive aspergillosis over a 10-year period, Belgium, 1 April 2022 to 31 March 2023. *Euro Surveill*. 2025;30(18):2400559.

Debergh H, Castelain P, Goens K, Lefevere P, Claessens J, De Vits E, Vissers M, Blindeman L, Bataille C, Saegerman C, Packeu A. Detection of pan-azole resistant Aspergillus fumigatus in horticulture and a composting facility in Belgium. *Med Mycol*. 2024;62(7): myae055.

de Groot T, Meis JF. Microsatellite Stability in STR Analysis *Aspergillus fumigatus* Depends on Number of Repeat Units. *Front Cell Infect Microbiol*. 2019; 9:82.

Fisher MC, Alastruey-Izquierdo A, Berman J, Bicanic T, Bignell EM, Bowyer P, Bromley M, Brüggemann R, Garber G, Cornely OA, Gurr SJ, Harrison TS, Kuijper E, Rhodes J, Sheppard DC, Warris A, White PL, Xu J, Zwaan B, Verweij PE. Tackling the emerging threat of antifungal resistance to human health. *Nat Rev Microbiol*. 2022;20(9):557-571.

Krieger E, Koraimann G, Vriend G. Increasing the precision of comparative models with YASARA NOVA--a self-parameterizing force field. *Proteins*. 2002;47(3):393-402.

Latgé JP, Chamilos G. *Aspergillus fumigatus* and Aspergillosis in 2019. *Clin Microbiol Rev*. 2019;33(1): e00140-18.

Nicolas AG, Serero A, Legoix-Né P, Jubin C, Loeillet S. Mutational landscape of yeast mutator strains. *Proc Natl Acad Sci*. 2014;111(5):1897–902.

Ren J, Jin X, Zhang Q, Zheng Y, Lin D, Yu Y. Fungicides induced triazole-resistance in Aspergillus fumigatus associated with mutations of TR46/Y121F/T289A and its appearance in agricultural fields. *J Hazard Mater*. 2017;15; 326:54-60.

Rhodes J, Abdolrasouli A, Dunne K, et al. Population genomics confirms acquisition of drug-resistant Aspergillus fumigatus infection by humans from the environment. *Nat Microbiol*. 2022;7(11):1944.

Snelders E, Karawajczyk A, Schaftenaar G, Verweij PE, Melchers WJ. Azole resistance profile of amino acid changes in Aspergillus fumigatus CYP51A based on protein homology modeling. *Antimicrob Agents Chemother*. 2010;54(6):2425-30.

Schoustra SE, Debets AJM, Rijs AJMM, Zhang J, Snelders E, Leendertse PC, Melchers WJG, Rietveld AG, Zwaan BJ, Verweij PE. Environmental Hotspots for Azole Resistance Selection of Aspergillus fumigatus, the Netherlands. *Emerg Infect Dis*. 2019;25(7):1347-1353.

The Subcommittee on Antifungal Susceptibility Testing (AFST) of the ESCMID European Committee for Antimicrobial Susceptibility Testing (EUCAST). Method for the determination of broth dilution minimum inhibitory concentrations of antifungal agents for conidia forming moulds. EUCAST E.DEF 9.4, 2022.

Uehara S, Takahashi H, Nishino Y, Takahashi Y, Chiba T, Yokoyama K, Miyake H, Sadamasu K, Hagiwara D. Genetic analysis of azole-resistant Aspergillus fumigatus isolated from domestic and imported tulip bulbs in Japan. *J Glob Antimicrob Resist*. 2025; 44:306-313.

Ullmann AJ, Aguado JM, Arikan-Akdagli S, et al. Diagnosis and management of

Aspergillus diseases: executive summary of the 2017 ESCMID-ECMM-ERS guideline. *Clin Microbiol Infect*. 2018,24 Suppl 1: e1-e38.

Verweij PE, Arendrup MC, Alastruey-Izquierdo A, Gold JAW, Lockhart SR, Chiller T, White PL. Dual use of antifungals in medicine and agriculture: How do we help prevent resistance developing in human pathogens? *Drug Resist Updat*. 2022; 65:100885.

Verweij PE, Zhang J, Debets AJM, Meis JF, van de Veerdonk FL, Schoustra SE, Zwaan BJ, Melchers WJG. In-host adaptation and acquired triazole resistance in Aspergillus fumigatus: a dilemma for clinical management. *Lancet Infect Dis*. 2016;16(11): e251-e260.

Verweij PE, Kema GH, Zwaan B, Melchers WJ. Triazole fungicides and the selection of resistance to medical triazoles in the opportunistic mould Aspergillus fumigatus. *Pest Manag Sci*. 2013;69(2):165-70.

Vriend G. WHAT IF: a molecular modeling and drug design program. *J Mol Graph*. 1990;8(1):52-6, 29.

Weaver D, Novak-Frazer L, Palmer M, Richardson M, Bromley M, Bowyer P. Development of a novel mycobiome diagnostic for fungal infection. *BMC Microbiol*. 2024;24(1):63.

Yong MK, Slavin MA, Kontoyiannis DP. Invasive fungal disease and cytomegalovirus infection: is there an association? *Curr Opin Infect Dis*. 2018,31(6):481-9.

Zhao C, Fraczek MG, Dineen L, Lebedinec R, Macheleidt J, Heinekamp T, et al. High-Throughput Gene Replacement in Aspergillus fumigatus. *Curr Protoc Microbiol*. 2019;54(1): e88.

Supplementary Figures and Tables

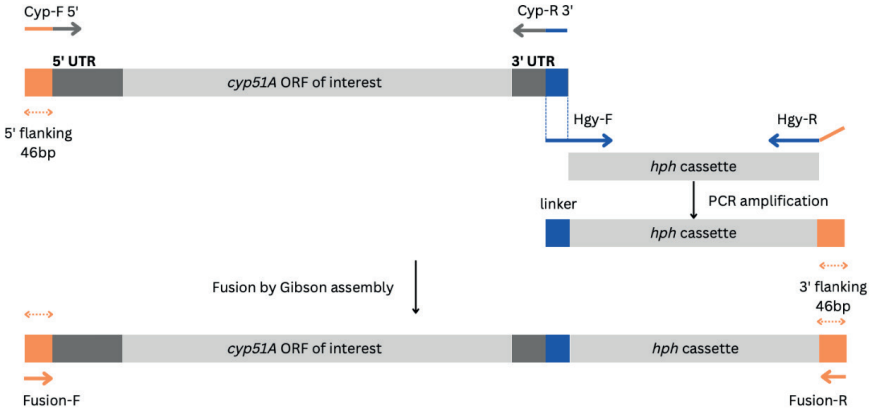

Figure S1: Schematic overview of the repair template construct. The hph cassette was added in the 3'-UTR of the cyp51A gene. The cyp51A fragment was amplified with primers cyp-F 5' and cyp-R 3'. The hph cassette was amplified from the pAN7-1 plasmid using hyg-R and hyg-F primers. Primers cyp-R 3' and hyg-F were designed to share an overlapping sequence, serving as a linker for the fusion of cyp51A template and hph cassette. fusion-F and fusion-R were used to amplify the final repair templates.

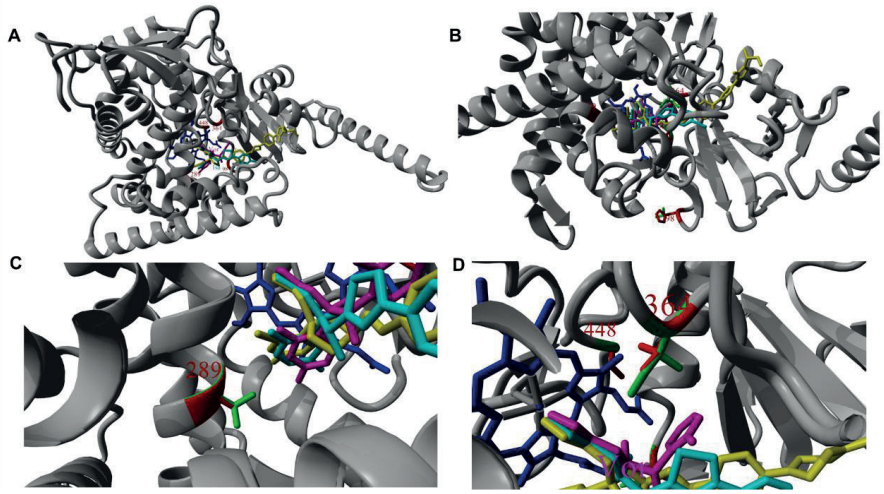

Figure S2: Homology model of *Aspergillus fumigatus* Cyp51A

Three-dimensional protein model of the Cyp51A protein with four azoles, the amino acids L98, T289, I364, and G448 (A) are fully exposed and labeled, with engineered point mutations at critical residues (L98H, T289A, I364V, G448S) exposed and labeled separately (B, C,D). Red: isavuconazole, Yellow: Itraconazole, Purple: posaconazole, Magenta: voriconazole

Table S1 The antifungal susceptibility overview of *Aspergillus fumigatus*

Genotype (N)	Itraconazole MIC*(mg/L)			Voriconazole MIC*(mg/L)			Posaconazole MIC*(mg/L)			Isavuconazole MIC*(mg/L)		
	GM	MIC_{50}	Range	GM	MIC_{50}	Range	GM	MIC_{50}	Range	GM	MIC_{50}	Range
TR_{34}/L98H (1621)	6.46	16	0.125-64	6.02	8	0.25->16	0.25	0.5	0.002->16	6.03	8	0.5->16
TR_{46}/Y121F/T289A (321)	2.807	2	0.25->64	13.71	16	8->64	0.288	0.5	0.002->8	12.179	16	4->16
TR_{34}/T-67G/L98H (16)	8.354	16	1->16	2.828	2	2-8	0.5	0.25	0.125-1	3.513	4	2-8
TR_{34}/L98H/S297T/F495I (38)	12.39	16	0.5->16	2.4	2	0.5->8	0.51	0.5	0.008-16	16	16	>=16
TR_{34}/L98H/T289A/I364V/G448S (5)	1.74	1	0.5->16	16	16	>16	0.76	1	0.5-1	16	16	>16
TR_{46}/Y121F/M172I/T289A/G448S (9)	9.332	16	1->16	11.758	16	4->16	0.250	0.125	0.063-2	2.333	2	0.25->16
TR_{46}/Y121F/T289A/S363P/I364V/G448S (33)	6.088	16	0.5->16	15.023	16	8->16	0.959	1	0.5-4	15.667	16	8->16
TR_{46}/Y121F/T289A/G448S (11)	2.573	1	0.5->16	13.244	16	8->16	0.828	1	0.12-16	11.676	16	8->16
TR_{92}/Y121F/M172I/T289A/G448S (14)	4.876	4	0.5->16	12.491	16	2->16	0.609	0.5	0.031->16	11.314	16	2->16

Table S2 The antifungal susceptibility of *Aspergillus fumigatus* isolated from each year

Genotype	Itraconazole MIC*(mg/L)			Voriconazole MIC*(mg/L)			Posaconazole MIC*(mg/L)			Isavuconazole MIC*(mg/L)		
(N)	GM	MIC_{50}	Range	GM	MIC_{50}	Range	GM	MIC_{50}	Range	GM	MIC_{50}	Range
TR_{34}/L98H												
2021(n=70)	13.52	16	0.25->16	4.97	4	0.5->16	0.80	1	0.125->8	7.17	8	0.5->16
2020(n=83)	15.22	16	2->16	3.84	4	2-16	0.64	0.5	0.25-4	5.97	4	0.5-16
2019(n=127)	14.11	16	2->16	3.73	4	2-8	0.46	0.5	0.12-2	5.75	8	4->16
2018(n=149)	14.17	16	0.25->16	3.17	4	0.5->16	0.61	0.5	0.063-16	5.75	8	0.5->16
2017(n=150)	14.93	16	2->16	3.61	4	2->8	0.75	1	0.125->8	6.12	8	1->16
2016 (n=114)	0.89	1	0.25-8	9.54	8	4->16	0.01	0.008	0.002-0.125			
2015 (n=93)	0.76	1	0.25-1	10.54	8	4->16	0.01	0.008	0.002-1			
2014 (n=52)	4	16	0.25->16	6.82	8	4->16	0.15	0.5	0.016->16			
2013 (n=60)	16	16	>16	7.20	8	2->16	1.03	1	0.25->16			
2012 (n=39)	15.17	16	4->16	8	8	2->16	1.13	1	0.25-8			
2011 (n=52)	14.38	16	1->16	7.69	8	2->16	0.83	1	0.031-2			
2010 (n=70)	16.32	16	16-64	6.50	8	2-16	1.15	1	0.25->16			

2009 (n=66)	14.56	16	0.125->64	5.26	4	1->16	0.35	0.25	0.06-1			
2008 (n=20)	16	16	>16	8.88	8	2-16	0.37	0.5	0.016-1			
2007 (n=24)	12.70	16	0.125->16	5.99	8	0.25-16	0.55	0.5	0.031-2			
2006 (n=13)	11.02	16	2->16	5.81	4	4-8	0.38	0.5	0.25-0.5			
2005 (n=8)	14.67	16	8->16	3.36	4	0.5-16	0.5	0.5	0.12-1			
2004 (n=10)	11.31	16	4->16	4	4	4	0.35	0.5	0.25-0.5			
2002 (n=6)	16	16	>16	4.49	4	0.5-1	0.63	0.5	2-8			
TR_{46}/Y121F/T289A												
2021 (n=18)	2.25	1	0.25->16	16	16	>16	0.5	0.5	0.25-2	16	16	>16
2020 (n=28)	5.12	4	0.25->16	16	16	>16	0.54	0.5	0.25-2	16	16	>16
2019 (n=23)	2.87	2	0.5->16	16	16	>16	0.37	0.5	0.12-1	10.81	8	8->16
2018 (n=22)	2	2	0.25->16	8.79	8	8->16	0.57	0.5	0.12-1	15.02	16	4->16
2017 (n=35)	3.41	2	0.5->16	8	8	>8	0.85	1	0.25->8	8	8	4->16
2016 (n=26)	0.71	0.5	0.25-2	10.73	8	8-16	0.01	0.008	0.002-0.125			
2015 (n= 22)	0.5	0.5	0.25-1	16	16	>16	0.01	0.004	0.002-0.031			
2014 (n=36)	1.82	1	0.25->16	14.75	16	4->16	0.14	0.25	0.004-2			
2013 (n=23)	6.68	16	0.5->16	16	16	>16	0.79	1	0.25-2			

2012 (n=27)	10.61	16	1->16	16	16	>16	0.93	1	0.5-4
2011 (n=22)	16	16	1->16	17.15	16	2->16	0.84	1	0.031-2
2010 (n=40)	1.90	1	0.25->16	16	16	>16	0.5	0.25	0.25-4

CHAPTER 4

The agricultural fungicide resistance signature in azole-resistant *Aspergillus fumigatus* isolates

Yinggai Song • Jochem B Buil • Jan Zoll • Marlou Tehupeiory-Kooreman • Jianhua Zhang • Ruoyu Li • Auke de Jong • Willem J G Melchers • Paul E Verweij

Manuscript Submitted

Abstract

Objectives: The emergence of triazole resistance in *Aspergillus fumigatus* poses a growing threat to public health. This study investigates the role of agricultural fungicide use in driving the evolution of pan-azole-resistant strains and examines the associated cross-resistance to non-azole fungicides.

Methods: A total of 198 *A. fumigatus* isolates were analyzed, including 79 pre-fungicide era (pre-FE, ≤1970s) strains and 109 fungicide era (FE) strains (49 *A. fumigatus* isolates with single resistance mutations, 40 TR_{46} and TR_{34} isolates, and 20 wild-type clinical strains). In vitro susceptibility testing was performed using EUCAST methodology, covering four medical azoles (itraconazole, posaconazole, voriconazole, and isavuconazole) and five distinct target classes: tebuconazole and difenoconazole (agricultural triazole), prochloraz (imidazole), Pyraclostrobin (QoI), benomyl and carbendazim (MBC), and boscalid and fluopyram (SDHI). We also determined the upper limits of wild-type (WT) MIC (UL-WT) based on the 97.5% and 99% MICs against the fungicides. Whole-genome sequencing and phylogenetic analyses were conducted on 128 isolates to track resistance evolution and spread.

Results: FE wild-type isolates showed significantly reduced susceptibility to medical and agricultural azoles compared to pre-FE isolates. TR_{34} and TR_{46} mutants exhibited not only pan-azole resistance but also broad co-resistance to SDHIs, QoIs, and MBCs. Prochloraz shows the highest percentage of Non-Wild-Type isolates (43.2%), even when using the 99% cut-off. Tebuconazole also shows a notable percentage of NWT isolates (8.4%). Pyraclostrobin and Benomyl have the lowest percentages of NWT isolates (2.1% and 3.4% respectively at the 97.5% cut-off). For Difenoconazole and Carbendazim, the percentage of NWT isolates is lower when using the 99% cut-off (0.9% and 1.6%) compared to the 97.5% cut-off (3.2% and 14.3%). Phylogenomics revealed that TR mutations emerged monophyletically after the 1970s, coinciding with agricultural triazole deployment. TR_{34} spread 4.2 times faster than genomic evolution and was disseminated across clinical and environmental reservoirs via clonal expansion and horizontal transfer.

Conclusion: This study demonstrates that agricultural triazole use has selected for multidrug-resistant *A. fumigatus* lineages capable of rapid cross-environmental spread. The convergence of resistance across fungicide classes underscores the urgent need for integrated One Health strategies to mitigate further resistance development.

Keywords: *Aspergillus fumigatus*, triazole resistance, agricultural fungicides, cross-

resistance, phylogenomics

Introduction

The emergence of drug-resistant fungal infections represents a critical challenge across agriculture, healthcare, and natural ecosystems, with profound implications for global food security, public health, and environmental stability. Fungi, as essential contributors to nutrient cycling and decomposition, also include pathogens that threaten human, animal, and plant health.

In agriculture, fungal pathogens are responsible for significant pre- and post-harvest crop losses, amounting to nearly $200 billion annually. Food security mainly relies on fungicides that help to reduce crop loss (Steinberg et al., 2020). Modern fungicides introduced after 1970 include various modes of action such as benzimidazoles, morpholines, piperazines, imidazoles, pyrimidines, triazoles, anilides and strobilurines (Beckerman et al., 2023). Despite advances in plant disease management, fungicides remain the primary method for controlling crop diseases, (Sparks et al.,2025; Beckerman et al., 2023) and climate change is expected to exacerbate crop losses by increasing fungal disease risks and crop yield variability (IPPC Secretariat. 2021).

In the past decades azole fungicides have been implicated as cause of cross resistance selection to medical azoles in human pathogenic fungi, including *Candida* and *Aspergillus* species. These fungi have large population sizes in their environmental habitats and resistance selection may occur when fungicides are introduced into the fungal habitat. This has been shown for *A. fumigatus*, where signature mutations in the *cyp51A*-gene (e.g. TR_{34}/L98H and TR_{46}/Y121F/T289A) have emerged that confer cross resistance to the medical azoles. Azole resistance complicates patient management and was shown to be associated with excess mortality in patients with voriconazole-resistant invasive aspergillosis (Lestrade et al., 2019).

However, recently other effects have been noted in *A. fumigatus* isolates that harbor TR-mediated resistance mutations and have been exposed to agricultural fungicides. An increased mutation rate was found in *A. fumigatus* harboring TR_{34}/L98H, which was found to be due to mutations in the DNA mismatch repair system (MMR) (Bottery et al., 2024). Furthermore, resistance selection was not only noted against

azole fungicides, but also against other fungicides that do not share their mode of action with medical antifungals (Kanellopoulos et al., 2025). The isolates were found to simultaneously harbor target-site mutations that confer resistance to benzimidazoles (benA F219Y) and quinone-outside inhibitors (cytB G143A) (Kang et al., 2022).

The present study was conducted to assess if the clinical resistant strain of *A. fumigatus* and its associated mutations in *cyp51A* could be induced by triazole fungicides and the distribution characteristics of *A. fumigatus* against different targeted agricultural fungicides, addressing the critical link between agricultural fungicide use and clinical resistance.

Materials and Methods

Study design

Definitions of cohorts of isolates

Pre-fungicide era isolates (Pre-FE; ≤ 1970s**):** These *A. fumigatus* isolates were cultured prior to the introduction of ketoconazole into clinical practice (1981) and the authorization of the first azole fungicides (Imazalil in 1973). We assume that these isolates have not been exposed to azoles.

Fungicide era isolates (FE; after the 1970s): This group includes clinical and environmental isolates that were cultured when azoles were in use in medicine and agriculture/horticulture. The isolates include various phenotypes/genotypes; wildtype isolates (FE-WT), isolates harboring tandem repeat resistance mechanisms (FE-TR_{34} and FE-TR_{46}), which are associated with environmental resistance selection; and isolates harboring single resistance mutations (FE-SNP), which are mainly associated with in host resistance selection.

Strain sources and genomic dataset

To trace the evolutionary trajectory of *A. fumigatus* before and during fungicide use, we assembled 188 isolates from clinical and environmental sources across France, the Netherlands and Germany over a 159-year period (1863–2022). The Radboud University Medical Center Fungal Culture Collection provided the core set: 79 wild-type strains isolated prior to 1965 (two German soil isolates from 1926, six French clinical isolates from 1863, and 71 Dutch clinical isolates from 1945–1965 held at the Westerdijk Fungal Biodiversity Institute); 59 clinical isolates carrying single resistance mutations (1995–2022); 40 TR_{46} or TR_{34} clinical azole-resistant isolates (1995–2005 and 2017–2022); and 20 wild-type clinical isolates from the contemporary FE (2017–

2022).

Strains for genomic difference analysis

From this collection, we generated whole-genome sequences for 128 representative isolates: 27 pre-FE genomes and 101 FE genomes (including 28 TR_{34} isolates, 28 TR_{46} isolates, 23 single-nucleotide mutations isolates, and 22 wild-type isolates), supplemented with publicly available environmental genomes to ensure comprehensive temporal and genetic coverage. Together 128 *A. fumigatus* genomes spanning 1863-2022 were analyzed and arranged into five genetic groups: pre-FE group with azole susceptibility, FE-TR_{34}, TR_{46} clades carrying canonical tandem-repeat-plus-SNP haplotypes, single nucleotide mutations, and environmental or susceptible “FE-WT” group.

The collection is geographically centered on the Netherlands (96 clinical and 6 soil isolates), with one clinical isolate from France, and a German soil sample subset (23 isolates), allowing direct comparison of hospital and environmental reservoirs.

Antifungal susceptibility testing of *A. fumigatus*

We collected *A. fumigatus* isolates preserved in Radboud University Medical Centre. In vitro susceptibility testing was performed according to the EUCAST microdilution reference method. Medical azoles phenotype was determined based on the EUCAST E.Def 9.4 standard for broth microdilution susceptibility testing (Guinea et al., 2022). Resistant isolates were further characterized by sequencing the *cyp51A* gene.

The following fungicides were tested, covering five distinct target classes: tebuconazole and difenoconazole (agricultural triazole), prochloraz (imidazole), Pyraclostrobin (QoI - Quinone outside Inhibitor), benomyl and carbendazim (MBC - Methyl Benzimidazole Carbamate), and boscalid and fluopyram (SDHI - Succinate Dehydrogenase Inhibitor)

All compounds were dissolved in DMSO and sterilized by autoclaving at room temperature for 30 minutes. The minimal inhibitory concentration (MIC) was determined using a microbroth dilution format, with incubation at 37 °C for 48 hours. MIC endpoints were determined spectrophotometrically as a 50% reduction in optical density at 450 nm (OD_{450}) compared to the growth control. MIC_{50}, MIC_{90} and geometric means (GMs) were calculated. Experiments were performed in triplicate on separate days. The upper limit of wild-type (UL-WT) was calculated by the 2010 updated version of the ECOFFinder program which is available from the CLSI website (https://clsi.org/resources/ecoffinder/).

Whole-genome sequencing and phylogenetics of *A. fumigatus* lineages

The isolates were genotyped using whole-genome sequencing (Illumina platforms), with a focus on azole-resistance markers (TR_{34}/TR_{46} *cyp51A* mutations) and genome-wide SNPs. Variants were called against the Af293 reference (GATK v4.2), filtered for depth (≥10×) and minor allele frequency (>5%), and stratified into pre-FE and FE cohorts.

Phylogenetic reconstruction was performed via maximum-likelihood (IQ-TREE v2.1.2) with temporal calibration (TempEst v1.5) and divergence dating (BEAST v1.10.4). Spatiotemporal spread was modeled using discrete diffusion, while temporal trends in resistance were quantified via kernel density estimation and linear regression against fungicide usage data. Statistical validation included node-specific bootstrap support (≥70% for TR groups) and Fisher's exact tests for source (clinical/environmental) associations, implemented in R v4.3.1.

Evolutionary relationships of taxa

The evolutionary history was inferred using the Neighbor-Joining method (Saitou et al., 1987). The optimal tree is shown. The percentage of replicate trees in which the associated taxa clustered together in the bootstrap test (1000 replicates) are shown next to the branches (Felsenstein et al., 1985). The tree is drawn to scale, with branch lengths (next to the branches) in the same units as those of the evolutionary distances used to infer the phylogenetic tree. The evolutionary distances were computed using the Maximum Composite Likelihood method (Tamura et al., 2004) and are in the units of the number of base substitutions per site. This analysis involved 133 nucleotide sequences. All positions with less than 50% site coverage were eliminated, i.e., fewer than 50% alignment gaps, missing data, and ambiguous bases were allowed at any position (partial deletion option). There was a total of 474 positions in the final dataset. Evolutionary analyses were conducted in MEGA X (Kumar et al., 2018).

Statistical analysis

Susceptibility data were analyzed using non-parametric methods due to non-normal MIC distributions (Shapiro-Wilk $p < 0.05$). GM-MICs were calculated for each antifungal-genotype combination to normalize variance. Group comparisons (Pre-FE vs. FE-WT vs FE-SNPs vs. TRs) were performed using the Kruskal-Wallis test with Dunn's post-hoc correction for multiple comparisons. Pairwise differences in GM-MICs between genotypes were quantified via fold-change ratios (resistant GM-MIC/ wild-type GM-MIC). For medical azoles (voriconazole, itraconazole, posaconazole, isavuconazole), agricultural azoles (tebuconazole, difenoconazole, prochloraz), and

non-azole fungicides (carbendazim, pyraclostrobin, boscalid, fluopyram), class-specific trends were evaluated using Spearman's rank correlation (ρ) to assess cross-resistance. Statistical significance was defined as $p < 0.01$ (two-tailed) to account for multiple hypothesis testing. All analyses were conducted in R v4.3.1 and GraphPad Prism v9.0.

Results

Medical-agricultural azole and non-azole susceptibility profiles of five groups

All tested agents showed high activity against pre-FE isolates (Table 1). The MIC_{50} and MIC_{90} values were uniformly low. GM MICs were lowest for medical azoles (itraconazole GM=0.15, voriconazole GM=0.42), prochloraz (GM=0.02), and carbendazim (GM=0.06). The narrow MIC ranges indicate a homogenous, susceptible wild-type population.

Antifungal activity was lower in FE-WT isolates compared with the Pre-FE isolates, particularly of the seven fungicides (TEB, DIF, PRO, PYR, BEN, CAR, BOS, $p<0.001$) except Fluopyram ($p=0.130$). Activity of medical azoles was also lower (ITR, VOR and POS, $p<0.001$) except isavuconazole ($p=0.130$).

The FE-SNPs group demonstrated significantly reduced activity against four medical azoles compared to the FE-WT group ($p < 0.001$). Additionally, this group exhibited a broad MIC range against most fungicides tested. Significantly higher resistance was observed for tebuconazole ($p = 0.049$), prochloraz ($p = 0.010$), benomyl ($p = 0.008$), and boscalid ($p < 0.001$) relative to the FE-WT group.

TRs group is characterized by high-level, pan-azole resistance. TR_{46} group displayed pan-azole resistance, with high MICs for VOR (GM: 30.91 mg/L) and ITR. It also showed strong cross-resistance to all other classes, including SDHIs (BOS, FLUO), QoIs (PYR), and MBCs (BEN, CAR), indicating a potent multidrug resistance (MDR) phenotype. TR_{34} group Also exhibited pan-azole resistance but with a distinct profile—extreme ITR resistance (GM: 24.25 mg/L) but lower VOR resistance (GM: 3.03 mg/L) compared to TR_{46} group. It also demonstrated substantial cross-resistance to agricultural azoles and non-azole fungicides, confirming a broad-spectrum MDR profile associated with this genotype (Table 1).

Table1 Medical triazole and agriculture fungicides phenotypes for Pre-FE and FE *A. fumigatus* isolates

Group		ITR	VOR	POS	ISA	TEB	DIF	PRO	PYR	BEN	CAR	BOS	FLUO
Pre-FE	MIC_{50}	0.25	0.5	0.03	1	0.25	0.12	0.03	0.06	1	0.5	2	4
(n=79)	MIC_{90}	0.25	0.5	0.03	1	0.5	0.25	0.06	0.25	2	2	16	32
	MIC range	0.06-0.25	0.25-0.5	0.016-0.06	0.5-1	0.03-2	0.016-0.5	0.03-0.06	0.016-0.5	0.12-8	0.12-8	0.06->16	0.12->32
	GM	0.15	0.42	0.02	0.85	0.23	0.12	0.04	0.06	0.95	0.63	1.60	3.32
FE-WT	MIC_{50}	0.25	1	0.06	1	0.5	0.25	0.06	0.12	2	1	32	8
(n=20)	MIC_{90}	0.25	1	0.12	1	0.5	0.1	0.12	0.25	2	1	32	32
	MIC range	0.12-1	0.5-2	0.03-0.12	0.5-1	0.25-0.5	0.5-1	0.06-0.25	0.03-0.5	1-4	0.5-4	1->16	1->32
	GM	0.26	0.78	0.09	0.90	0.42	0.44	0.09	0.11	1.93	1.04	14.42	6.28
SNPs	MIC_{50}	>16	2	2	4	0.5	0.25	0.06	0.06	2	1	2	4
(n=59)	MIC_{90}	>16	8	>16	4	2	1	0.5	1	2	2	16	32
	MIC range	0.25->16	0.12->16	0.12->16	0.12->16	0.06-8	0.016-8	0.016-16	0.016-16	0.5->32	0.016->16	0.06->16	0.06->32
	GM	14.89	1.84	3.24	2.25	0.70	0.25	0.11	0.13	1.86	1.13	2.21	4.08
TR_{46}	MIC_{50}	32	32	1	32	8	16	8	16	32	>16	8	8
(n=20)	MIC_{90}	32	32	2	32	>16	>16	16	>16	>32	>16	>16	32
	MIC range	1->16	16->16	0.25-4	16->16	0.12->16	0.5->16	0.06-32	0.016->16	1->32	1->16	0.5->16	1-32
	GM	10.93	30.91	0.97	28.84	8.86	8.57	4.59	8.86	28.84	18.38	9.19	9.51
TR_{34}	MIC_{50}	32	4	0.5	4	4	4	0.12	0.25	2	2	8	16
(n=20)	MIC_{90}	32	4	0.5	4	8	8	16	2	>32	>16	>16	32
	MIC range	4->16	1-4	0.25-1	1-4	0.25-8	0.12-16	0.06-32	0.016-4	1->32	0.5->16	0.5->16	2->32
	GM	24.25	3.03	0.47	2.93	2.93	2.63	0.49	0.21	4.59	3.86	6.50	11.71

Note: ITR: itraconazole, VOR: voriconazole, POS: posaconazole; ISA: isavuconazole, TEB: Tebuconazole, DIF: Difenoconazole, PRO: Prochloraz, PYR: Pyraclostrobine, BEN: Benomyl, CAR: Carbendazim, BOS: Boscalid, FLUO: Fluopyram

Table 2 summarizes the in vitro activity of six fungicides against 198 *A. fumigatus* isolates. It defines the wild-type (WT) population's susceptibility range and calculates the percentage of isolates that fall outside this range (non-Wild-Type, NWT). Prochloraz shows the highest percentage of Non-Wild-Type isolates (43.2%), even when using the 99% cut-off. Tebuconazole also shows a notable percentage of NWT isolates (8.4%). Pyraclostrobin and Benomyl have the lowest percentages of NWT isolates (2.1% and 3.4% respectively at the 97.5% cut-off). For Difenoconazole and Carbendazim, the percentage of NWT isolates is lower when using the 99% cut-off (0.9% and 1.6%) compared to the 97.5% cut-off (3.2% and 14.3%).

Table 2. MIC and UL-WT distribution of *Aspergillus fumigatus* isolates against fungicides.

Fungicides	No. of isolates	Range (µg/mL)	Modal MIC	UL-WT 97.5%	UL-WT 99%	% NWT 97.5%	% NWT 99%
Tebuconazole	198	0.03->16	0.25	1	1	8.4	8.4
Difenoconazole	198	0.016->16	0.5	4	8	3.2	0.9
Prochloraz	198	0.016->16	0.03	0.06	0.06	43.2	43.2
Pyraclostrobine	198	0.016->16	0.03	0.5	0.5	2.1	2.1
Benomyl	198	0.12->16	1	4	4	3.4	3.4
Carbendazim	198	0.016->16	1	2	4	14.3	1.6

MICs distribution for medical azoles between the pre-FE and FE wildtype isolates

The Pre-FE group, representing a baseline with no historical azole exposure, displays a tight distribution of low MIC values for itraconazole (0.06-0.25µg/ml), voriconazole (0.25-0.5µg/ml), posaconazole (0.016-0.06µg/ml), isavuconazole (0.5-1µg/ml), indicating uniform susceptibility (Figure 1). In contrast, the FE-WT group exhibits a distinct rightward shift in its MIC distribution, particularly visible for itraconazole (0.12-1µg/ml, $p<0.001$), posaconazole (0.03-0.12µg/ml, $p<0.001$) and voriconazole (0.5-2µg/ml, $p<0.001$), where a subset of isolates shows MIC values that are 2- to 4-fold higher than the Pre-FE mode, with more subtle but observable shifts for isavuconazole (0.5-1µg/ml, $p>0.05$) (Figure 1). This rightward shift demonstrates a statistically significant decrease in itraconazole, posaconazole and voriconazole susceptibility among FE-WT isolates compared to the pre-fungicide era baseline.

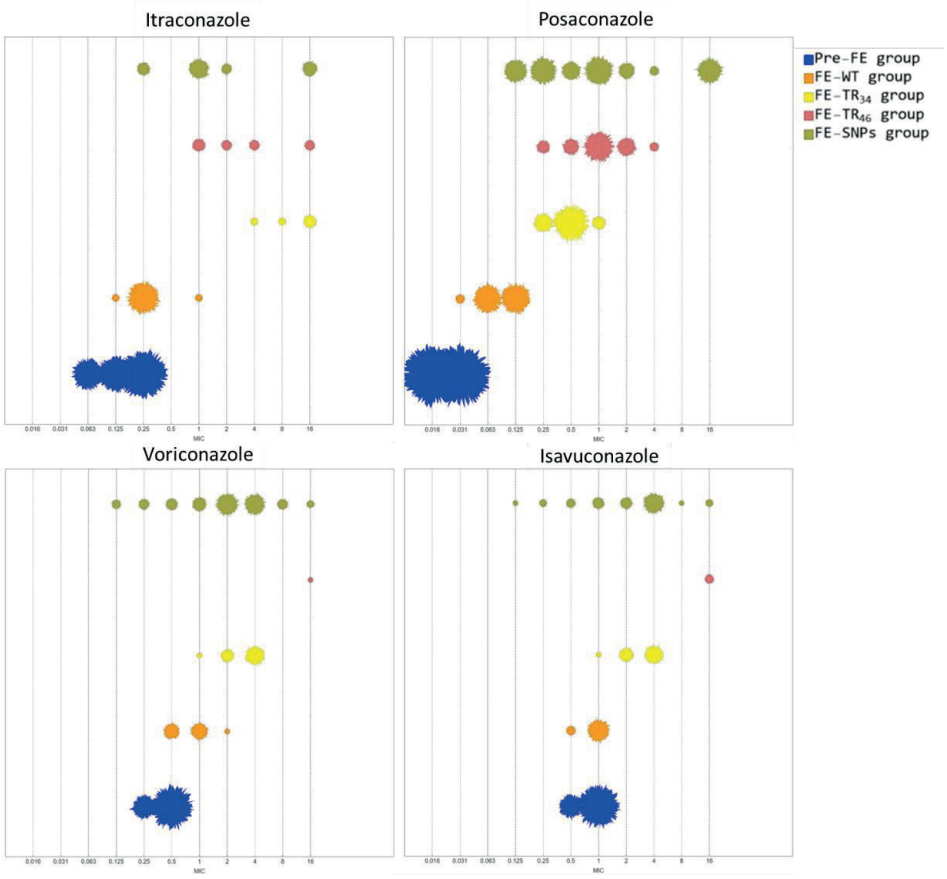

Figure 1. Medical azoles phenotypes distribution of five *A. fumigatus* groups.

MICs distribution for agricultural fungicides between the pre-FE and FE-WT groups

The Pre-FE isolates exhibit consistently low MIC values across in these agricultural fungicides tebuconazole (0.03-2 mg/L), difenoconazole (0.016-0.5 mg/L), prochloraz (0.03-0.06 mg/L) and pyraclostrobine (0.016-0.5 mg/L), indicating high activity with minimal variability, while benomyl (0.12-8 mg/L) and carbendazim (0.12-8 mg/L) show broad ranges. In contrast, the FE-WT group demonstrates a rightward shift in MIC distributions, particularly noticeable for tebuconazole (0.06-8 mg/L), difenoconazole (0.016-8 mg/L), prochloraz (0.016-16 mg/L), and pyraclostrobine (0.016-16 mg/L), where the MIC values are broadly elevated compared to the Pre-FE baseline (Figure 2, $P<0.001$). This shift reflects a decrease in susceptibility among contemporary wild-type isolates.

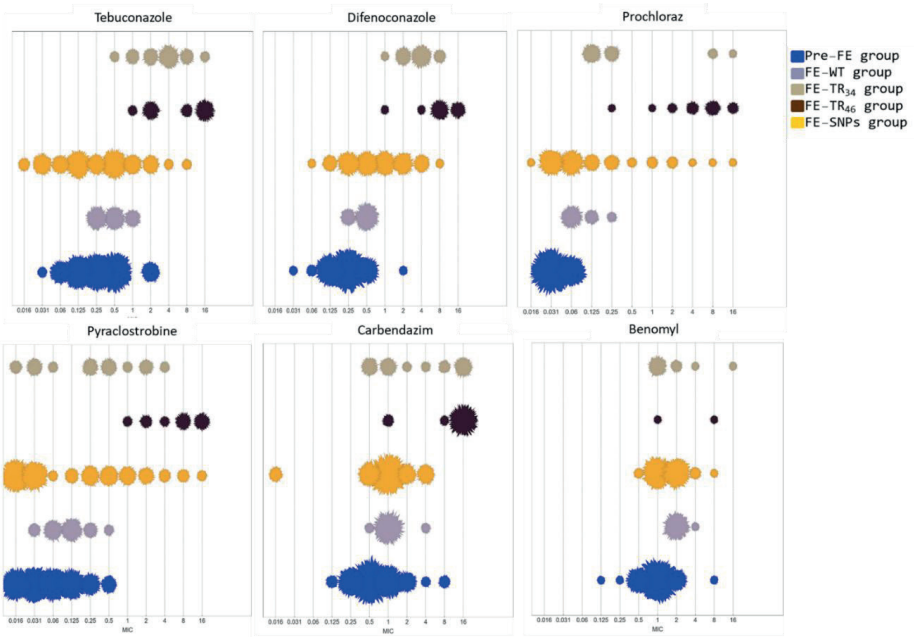

Figure 2. Agricultural fungicides phenotypes distribution of five *A. fumigatus* groups.

Correlation coefficient analysis

A correlation analysis of the GM MIC values across all groups and compounds reveals the strong internal consistency among the medical and agricultural azoles in TRs groups, and significant positive correlations were detected between specific phenotypes of voriconazole and posaconazole and resistance to multiple fungicides ($p < 0.001$). In addition, extensive and significant positive correlations were found among most fungicides, especially within the BEN-CAR-BOS-FLUO group (e.g., BOS vs. FLUO, $r = 0.839$, $p < 0.001$).

Phylogenetic analysis of *cyp51A* gene in Pre-FE and FE groups of *A. fumigatus*

A phylogenetic tree constructed from the *cyp51A* gene sequences of 129 *A. fumigatus* isolates (Figure 3). Unlike a whole-genome tree that reflects the organism's overall genetic history, this tree reveals how resistance-associated alleles of the *cyp51A* gene itself have evolved and spread. The clear, distinct clustering of isolates by genotype—particularly the tight clades formed by TR_{34} and TR_{46} mutants. The very small tree scale (0.0007) indicates recent origin and minimal genetic divergence among these alleles. Furthermore, the intermingling of clinical and environmental isolates within the same resistant clades provides direct genetic evidence that resistance originates in the environment and subsequently spreads to

infect humans. This tree also allows for the identification of potential horizontal transfer or genetic recombination events if identical resistant alleles are found in genetically distant backgrounds.

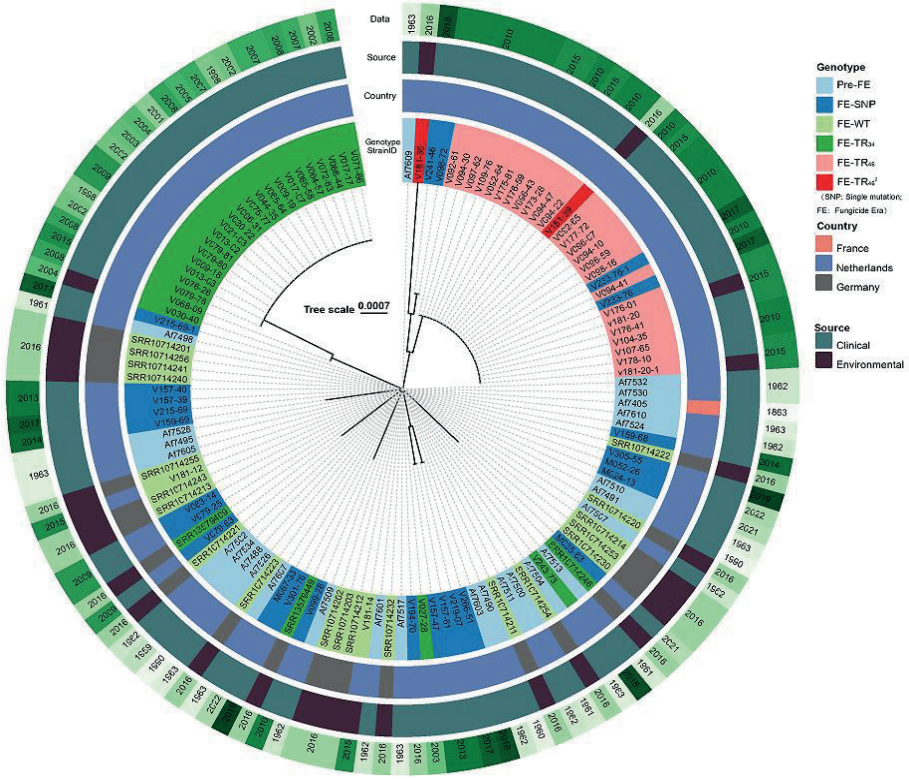

Figure 3 *Cyp51A* gene phylogenetics tree of 128 triazole- susceptible and triazole-resistant *A. fumigatus* isolates

Phylogenomics analysis of Pre-FE and FE groups in *A. fumigatus*

Based on whole-genome sequencing of 129 triazole-susceptible and resistant *A. fumigatus* isolates, Figure 4 presents a phylogenetic tree revealing population structure and evolutionary relationships. The isolates are color-coded by genotype, showing clear genetic clustering of key resistant genotypes: TR_{34} and TR_{46} isolates each form distinct, tight clades, indicating that these major resistance mechanisms likely emerged through clonal expansion from a limited number of successful genetic ancestors rather than through independent mutation events. The analysis further incorporates country of origin (France, Netherlands, Germany) and source (clinical or environmental), demonstrating that identical resistance clones are found across

national borders. Crucially, clinical and environmental resistant isolates are intermingled within the same clonal clusters, providing strong support for the hypothesis that resistance originated in the environment—driven by agricultural azole exposure—and subsequently spread to infect humans. The tree scale (0.05) denotes genetic distance, corresponding to 5% nucleotide divergence.

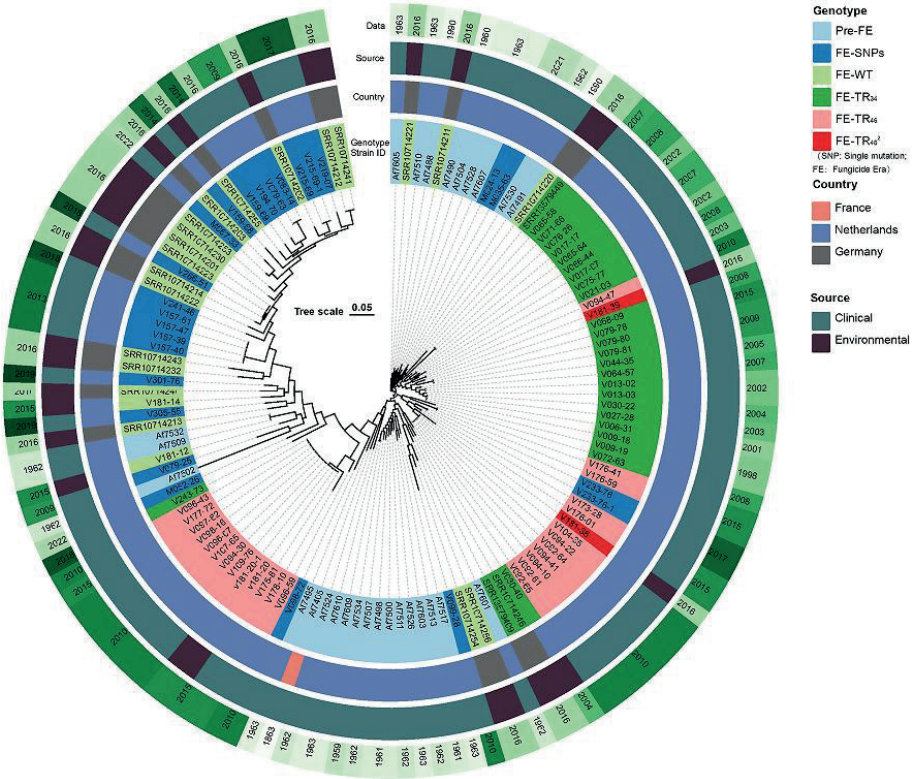

Figure 4 Whole-genome sequencing of 128 triazole- susceptible and triazole-resistant *A. fumigatus* isolate

Discussion

This study provides robust phylogenetic and phenotypic evidence that the widespread deployment of agricultural triazole fungicides has been the primary driver of the emergence and global spread of pan-azole-resistant *A. fumigatus* lineages. Our analysis of isolates collected before and after the introduction of these compounds demonstrates not only a significant decrease in susceptibility to both medical and agricultural azoles among post-exposure wild-type isolates, but also the convergent evolution of multi-fungicide resistance in strains

harboring the TR_{34} and TR_{46} mutations. These resistance lineages emerged monophyletically in the late 20th century, contemporaneous with the intensive agricultural use of triazoles, and have since disseminated rapidly across clinical and environmental reservoirs through both clonal expansion and horizontal genetic transfer (Snelders et al., 2012; EFSA J. 2025).

Several key findings support this conclusion. First, the reduced azole susceptibility in contemporary wild-type isolates (FE-WT) compared to pre-fungicide era strains (Pre-FE) suggests that background resistance levels in the global *A. fumigatus* population have risen in response to fungicide pressure. This shift may be due to the accumulation of cryptic resistance variants or compensatory mutations in genes beyond *cyp51A*, which could facilitate the eventual emergence of full resistance upon continued selection. Second, the TR_{34} and TR_{46} lineages exhibit extreme and broad-spectrum resistance profiles, including unexpectedly high resistance to non-azole classes such as SDHIs, QoIs, and MBCs. This multidrug resistance phenotype is consistent with recent reports of altered mutation rates and mismatch repair deficiency in TR-bearing strains, which may accelerate the acquisition of additional resistance alleles across the genome (Bottery et al., 2024; Rhodes et al., 2022).

The high proportion of non-wild-type isolates for prochloraz (43.2%)—far exceeding that of other fungicides—suggests either widespread pre-existing reduced susceptibility in the population or the rapid selection of resistance following exposure. This is particularly notable given prochloraz's status as an imidazole, a class widely used in both agriculture and medicine. The significant non-wild-type frequency for tebuconazole (8.4%) further underscores the selective pressure exerted by azole compounds. In contrast, the low percentages of non-wild-type isolates for pyraclostrobin (2.1%) and benomyl (3.4%) indicate that the wild-type population remains largely susceptible to these modes of action. The establishment of these epidemiological cut-off values (ECVs) is crucial, as they provide an essential baseline for future resistance surveillance and highlight significant differences in resistance development across fungicide classes.

Phylogenomic analysis revealed strong phylogeographic structure and temporal signal within the TR clades, indicating that these genotypes originated in Northwestern Europe before spreading internationally (Rhodes et al., 2022; Snelders et al., 2025). The high evolutionary rate and strong correlation between sampling year and genetic divergence ($R^2 = 0.81$) suggest that fungicide selection has dramatically accelerated the molecular clock within these lineages. Furthermore, the discordance between the whole-genome phylogeny and the *cyp51A* gene tree

indicates that resistance alleles have been horizontally transferred among genetically distant backgrounds, likely through parasexual recombination or other mechanisms of genetic exchange (Snelders et al., 2025). This process may be facilitated in agricultural settings where diverse strains co-occur under strong fungicide selection.

The convergence of resistance across chemical classes has serious implications for clinical management and agricultural disease control (Kanellopoulos et al., 2025; Dieste-Pérez et al., 2025). The fact that TR mutants show co-resistance to benzimidazoles and SDHIs—compounds widely used in crop protection—underscores the role of agricultural co-selection in shaping multidrug-resistant pathogens. This phenomenon limits treatment options in both fields and suggests that resistance management must extend beyond single-mode-of-action strategies.

Our study has several limitations. The historical isolates are skewed toward European origins, and broader global sampling would help clarify the geographic origins of resistance mechanisms. In addition, functional validation of the putative resistance variants outside *cyp51A* identified in this study would provide deeper mechanistic insights.

In conclusion, this work solidifies the link between agricultural fungicide use and clinical azole resistance in *A. fumigatus*, demonstrating that selection in the environment has given rise to successful, multidrug-resistant clonal lineages capable of infecting humans. These findings argue urgently for an integrated One Health approach to antifungal stewardship, including tighter regulation of high-risk fungicides, enhanced surveillance of resistance in both environmental and clinical isolates, and increased investment in alternative disease management strategies that reduce reliance on chemical controls.

Reference

Barber AE, Riedel J, Sae-Ong T, et al. Effects of agricultural fungicide use on *Aspergillus fumigatus* abundance, antifungal susceptibility, and population structure. *mBio.* 2020; 11: e02213-20.

Ballard E, Melchers WJG, Zoll J, Brown AJP, Verweij PE, Warris A. In-host microevolution of *Aspergillus fumigatus*: A phenotypic and genotypic analysis. *Fungal Genet Biol*. 2018; 113:1-13.

Beckerman J, Palmer C, Tedford E, Ypema H. Fifty Years of Fungicide Development,

Deployment, and Future Use. *Phytopathology*. 2023; 113:694-706.

Bottery MJ, van Rhijn N, Chown H, Rhodes JL, Celia-Sanchez BN, Brewer MT, Momany M, Fisher MC, Knight CG, Bromley MJ. Elevated mutation rates in multi-azole resistant *Aspergillus fumigatus* drive rapid evolution of antifungal resistance. *Nat Commun*. 2024; 15:10654.

Castro-Ríos K, Buri MCS, Ramalho da Cruz AD, Ceresini PC. *Aspergillus fumigatus* in the Food Production Chain and Azole Resistance: A Growing Concern for Consumers. *J Fungi (Basel)*. 2025; 11:252.

Chowdhary A, Sharma C, Meis JF. Azole-resistant aspergillosis: epidemiology, molecular mechanisms, and treatment. *J Infect Dis*. 2017;216: S436–S444.

Chowdhary A, Kathuria S, Xu J, Meis JF. Emergence of azole-resistant Aspergillus fumigatus strains due to agricultural azole use creates an increasing threat to human health. *PLoS Pathog*. 2013;9: e1003633.

Chowdhary A, Sharma C, Hagen F, Meis JF. Exploring azole antifungal drug resistance in *Aspergillus fumigatus* with special reference to resistance mechanisms. *Future Microbiol*. 2014;9:697–711.

Dieste-Pérez L, Holstege MMC, de Jong JE, Heuvelink AE. Azole resistance in *Aspergillus* isolates from animals or their direct environment (2013-2023): a systematic review. *Front Vet Sci*. 2025; 12:1507997.

European Food Safety Authority (EFSA); European Centre for Disease Prevention and Control (ECDC); European Chemicals Agency (ECHA); European Environment Agency (EEA); European Medicines Agency (EMA); European Commission's Joint Research Centre (JRC). Impact of the use of azole fungicides, other than as human medicines, on the development of azole-resistant *Aspergillus* spp. EFSA J. 2025; 23(1): e9200.

Felsenstein J. (1985). Confidence limits on phylogenies: An approach using the bootstrap. *Evolution.* 39:783-791.

Feys S, Carvalho A, Clancy CJ, Gangneux JP, Hoenigl M, Lagrou K, Rijnders BJA, Seldeslachts L, Vanderbeke L, van de Veerdonk FL, Verweij PE, Wauters J. Influenza-associated and COVID-19-associated pulmonary aspergillosis in critically ill patients. *Lancet Respir Med*. 2024; 12:728-742.

Fisher MC, Alastruey-Izquierdo A, Berman J, Bicanic T, Bignell EM, Bowyer P, Bromley

M, Brüggemann R, Garber G, Cornely OA, Gurr SJ, Harrison TS, Kuijper E, Rhodes J, Sheppard DC, Hagiwara D, Watanabe A, Kamei K, Goldman GH. Epidemiological and genomic landscape of azole resistance mechanisms in Aspergillus fungi. *Front Microbiol*. 2016; 7:1382.

Kanellopoulos SG, Snelders E. Moving beyond multi-triazole to multi-fungicide resistance: Broader selection of drug resistance in the human fungal pathogen *Aspergillus fumigatus*. *PLoS Pathog*. 2025;21:e1012851.

Kang SE, Sumabat LG, Melie T, Mangum B, Momany M, Brewer MT. Evidence for the agricultural origin of resistance to multiple antimicrobials in Aspergillus fumigatus, a fungal pathogen of humans. *G3 (Bethesda)*. 2022;12: jkab427.

Kumar S., Stecher G., Li M., Knyaz C., and Tamura K. (2018). MEGA X: Molecular Evolutionary Genetics Analysis across computing platforms. *Molecular Biology and Evolution.* 35:1547-1549.

Lavergne RA, Chouaki T, Hagen F, et al., Home environment as a source of life-threatening azole-resistant *Aspergillus fumigatus* in immunocompromised patients. *Clin Infect Dis.* 2017; 64: 76-8.

Lestrade PP, Bentvelsen RG, Schauwvlieghe AFAD, Schalekamp S, van der Velden WJFM, Kuiper EJ, van Paassen J, van der Hoven B, van der Lee HA, Melchers WJG, de Haan AF, van der Hoeven HL, Rijnders BJA, van der Beek MT, Verweij PE. Voriconazole resistance and mortality in invasive aspergillosis: A multicenter retrospective cohort study. *Clin Infect Dis*. 2019; 68:1463-1471.

Paluch M, Lejeune S, Hecquet E, Prévotat A, Deschildre A, Fréalle E. High airborne level of *Aspergillus fumigatus* and presence of azole-resistant TR_{34}/L98H isolates in the home of a cystic fibrosis patient harbouring chronic colonisation with azole-resistant H285Y *A. fumigatus*. *J Cyst Fibros.* 2019; 18: 364-7.

Rhodes J, Abdolrasouli A, Dunne K, et al., Population genomics confirms acquisition of drug-resistant *Aspergillus fumigatus* infection by humans from the environment. *Nat Microbiol*. 2022;7:663-674.

Schoustra SE, Debets AJM, Rijs AJMM, et al. Environmental hotspots for azole resistance selection of *Aspergillus fumigatus*, the Netherlands. *Emerg Infect Dis* 2019; 25: 1347–53.

Saitou N. and Nei M. The neighbor-joining method: A new method for reconstructing phylogenetic trees. *Molecular Biology and Evolution*.1987; 4:406-425.

Shelton JMG, Collins R, Uzzell CB, et al. Citizen science surveillance of triazole-resistant *Aspergillus fumigatus* in United Kingdom residential garden soils. *Appl Environ Microbiol.* 2022; 88: e0206121.

Singh A, Singh J, Kumar S. Aspergillosis: A comprehensive review of pathogenesis, drug resistance, and emerging therapeutics. *J Food Drug Anal*. 2025; 33:75-96.

Sparks TC, Lorsbach BA, Sparks JM, Duke SO. Origins of new modes of action for fungicides, herbicides and insecticides: a review and analysis. *Pest Manag Sci*. 2025 Jun 18. doi: 10.1002/ps.8962.

Tamura K., Nei M., and Kumar S. (2004). Prospects for inferring very large phylogenies by using the neighbor-joining method. Proceedings of the National Academy of Sciences (USA) 101:11030-11035.

Steinberg G, Gurr SJ. Fungi, fungicide discovery and global food security. *Fungal Genet Biol*. 2020; 144:103476.

Ullmann AJ, Aguado JM, Arikan-Akdagli S, et al. Diagnosis and management of *Aspergillus* diseases: executive summary of the 2017 ESCMID-ECMM-ERS guideline. *Clin Microbiol Infect.* 2018; 24: Suppl 1: e1-e38.

van de Veerdonk FL, Carvalho A, Wauters J, Chamilos G, Verweij PE. *Aspergillus fumigatus* biology, immunopathogenicity and drug resistance. *Nat Rev Microbiol*. 2025 May 2. doi: 10.1038/s41579-025-01180-z.

Verweij PE, Brüggemann RJM, Azoulay E, Bassetti M, Blot S, Buil JB, Calandra T, Chiller T, Clancy CJ, Cornely OA, et al. Taskforce report on the diagnosis and clinical management of COVID-19 associated pulmonary aspergillosis. *Intensive Care Med*. 2021; 47:819–834.

Verweij PE, Rijnders BJA, Brüggemann RJM, Azoulay E, Bassetti M, Blot S, Calandra T, Clancy CJ, Cornely OA, Chiller T, et al. Review of influenza-associated pulmonary aspergillosis in ICU patients and proposal for a case definition: an expert opinion. *Intensive Care Med*. 2020; 46:1524–1535.

Warris A, White PL, Xu J, Zwaan B, Verweij PE. Tackling the emerging threat of antifungal resistance to human health. *Nat Rev Microbiol*. 2022; 20:557-571.

Zhang J, Verweij PE, Rijs AJMM, Debets AJM, Snelders E. Flower Bulb Waste Material is a Natural Niche for the Sexual Cycle in *Aspergillus fumigatus*. *Front Cell Infect Microbiol*. 2022; 11:785157.

CHAPTER 5

Accelerated mutator phenotype in the human fungal pathogen *Aspergillus fumigatus* contributes to adaptive evolution

Yinggai Song • Margriet W. J. Hokken • Jan Zoll • Hanka Venselaar • Paul E Verweij • Willem J G Melchers • Johanna Rhodes

Manuscript submitted

Abstract

The opportunistic pathogen *Aspergillus fumigatus* represents a major threat to immunocompromised individuals and is increasingly resistant to antifungal therapies. Resistance selection primarily takes place through environmental selection to azole fungicides, but in-host resistance may develop in patients with chronic aspergillosis receiving azole therapy. In this study, we examine clinical *A. fumigatus* isolates that exhibit irregular growth and accumulated mutations rapidly during antifungal treatment. Whole-genome sequencing of serial isolates revealed an accelerated mutation rate as the likely driver of the observed phenotype. The mutation frequency of this isolate was approximately 15-times higher than other *A. fumigatus* strains. We identified non-synonymous single nucleotide polymorphisms (SNPs) as potential loci involved in the increased mutation rate. Using CRISPR/Cas9 gene editing and comprehensive genomic analysis, we show that a mutation in *mre11*, a gene critical for genomic stability during DNA replication, is responsible for this elevated mutation rate. Mutations within *mre11* results in a 27% reduction in radial growth, highlighting the fitness cost associated with the higher mutation rate. All *mre11*-mutant isolates in this study belong to clade B, a lineage that rarely carries environmental azole-resistance mutations, potentially supporting in-host adaptation. The Phe332Leu allele was observed both in clinical and environmental isolates, suggesting that the mutator phenotype may represent a general adaptive strategy, allowing *A. fumigatus* to persist under prolonged azole pressure. We hypothesize that this heightened mutation background could facilitate the rapid spread of antifungal resistance alleles within *A. fumigatus* populations.

Key words: *Aspergillus fumigatus*, Antifungal resistance, Mutator phenotype, *mre11* gene, In-host adaptation

Introduction

The human fungal pathogen *Aspergillus fumigatus* poses a significant public health threat on a global scale and has emerged as the predominant etiological agent of *Aspergillus*-related diseases worldwide (Latgé et al., 2019; Verweij et al., 2020). *A. fumigatus* is capable of causing a wide range of diseases in at-risk individuals, and in excess of 2 million people develop invasive aspergillosis (IA) annually in the context of chronic obstructive pulmonary disease, intensive care, lung cancer, or hematological malignancy, with a crude annual mortality of 85.2% (Denning et al., 2024). Prior to the introduction of the azole class, resistance to clinical antifungals in *A. fumigatus* was rarely reported, however, rates of resistance to the mold-active azoles, is reported as high as 10% (Buil et al., 2019).

Azole resistance in clinical *A. fumigatus* isolates is primarily associated with environmental fungicide exposure (Rhodes et al., 2022); indeed, the first isolates with the TR_{34}/L98H polymorphism conferring azole resistance were observed in environmental and clinical isolates, supporting the theory of environmental selection of resistance ((Verweij et al., 2007; Verweij et al., 2009). Spores of azole-resistant *A. fumigatus* strains are easily dispersed from environmental niches through air, travelling long distances before being inhaled by at-risk patients and causing invasive lung infection (Kanj et al., 2018).

Population genomic analyses of *A. fumigatus* have shown pronounced genetic clustering into two highly supported populations, A and B, with the majority of azole-resistance polymorphisms clustering in isolates within population A (Verweij et al., 2007), and azole-susceptible isolates mostly identified in population B. In addition to signature *cyp51A* mediated mutations associated with environmental resistance selection (e.g. TR_{34}/L98H and TR_{46}/Y121F/T289A), isolates within population A were found to have an increased propensity to develop resistance to antifungal compounds because of mutations in the DNA mismatch repair system (MMR) through elevated mutation rates (Bottery et al., 2024).

Elevated mutation rates have been implicated in driving rapid evolution and adaptation in human fungal pathogens, such as *Candida* and *Aspergillus* species (Bottery et al., 2024; dos Reis et al., 2019; Healey et al., 2016; Vale-Silva et al., 2017). Resulting in 'mutator' fungi, these elevated mutation rates can confer evolutionary advantages but are often associated with fitness costs when deleterious mutations accumulate. In *A. fumigatus*, the pervasive use of agricultural azoles has led to the selection of mutator fungi that harbour the *cyp51A* azole resistance allelic variant TR_{34}/L98H (Bottery et al., 2024; dos Reis et al., 2019). This has resulted in a lineage of

A. fumigatus that is not only multi-azole resistant but also multi-fungicide resistant, with strong selection pressure influencing adaptation. However, fungi can also utilise this strategy to successfully and rapidly adapt to other environmental challenges, such as temperature and pH changes to generate phenotypic variability.

We have previously shown isogenic *A. fumigatus* strains isolated from a patient over a two-year period developed resistance-conferring mutations *in vivo* during long term antifungal therapy (Ballard et al., 2018). Analysis of these strains displayed a varying morphology and sectors within the mycelium. Here, we identify a novel variant in *mre11*, encoding a protein in the MMR in *A. fumigatus*, and characterise the corresponding elevated mutation rates.

Methods

Culture and morphology of clinical isolates

Three azole-susceptible *A. fumigatus* clinical isolates (V130-14, V147-03, V155-40) were cultured from a patient with x-linked chronic granulomatous disease between Nov 25, 2011 and Oct 23, 2013 at Radboud University Medical Centre, Nijmegen, the Netherlands (Table 1). Isolates were cultured on Sabouraud Dextrose Agar (SDA) (Oxoid) (1% peptone, 4% glucose, 1.5% agar, pH 5.6) or in a tissue culture flask with semi-permeable lid (Nunc EasYflask, ThermoScientific, Massachusetts, USA) with Aspergillus Minimal Medium (AMM) 1.5% agar containing per liter: 10 g glucose, 5.95 g $NaNO_3$, 0.522 g KCl, 1.5 g KH_2PO_4, 50 mg $MgSO_4{\cdot}7H_2O$, 1 mL trace elements). Trace elements contained (per 200 mL): 10 g EDTA, 4.4 g $ZnSO_4{\cdot}7H_2O$, 1.01 g $MnCl_2{\cdot}4H_2O$, 0.315 g $CuSO_4{\cdot}5H_2O$, 0.22 g $(NH_4)6Mo7O_2{\cdot}4H_2O$, 1.0 g Fe (II)$SO_4{\cdot}7H_2O$, and 2.2 g H_3BO_3. All compounds were produced by Merck (Darmstadt, Germany). Isolates were stored in 20% glycerol at −80°C, and subcultured on SDA at 37 °C for 4–5 days. Conidia were harvested with a wet cotton swab and resuspended in Milli-Q containing 0.1% Tween 20. Approximately 2.6×10^5 CFU/mL of conidia were used to inoculate each fresh tissue culture flask. Conidia of each isolate were inoculated in triplicate.

To assess the possibility of isolate V130-14 being a mutator (Verweij et al., 2016), approximately 2.6×10^5 conidia per isolate were spotted and grown on solid AMM supplemented with 0.02% Methyl Methane Sulfonate (MMS) (Merck Millipore, USA), and grown at 37 °C for 4 days. Isolates were grown in triplicate on AMM as a control. Colony width was measured after 4 days and compared to control growth of *A. fumigatus* CEA10.

Table 1: Three azole susceptible clinical isolates were used for serial passaging on AMM for 10 weeks.

Isolate	Date of isolation	ICZ	VCZ	PCZ
V130-14	25/11/2011	1	1	0.25
V147-03	25/03/2013	0.5	1	0.25
V155-40	23/10/2013	1	1	0.25

Note: ICZ=itraconazole; VCZ=voriconazole; PCZ=posaconazole

Serial passaging of clinical isolates and microsatellite genotyping

We conducted a serial passaging experiment in triplicate with the potential mutator isolate V130-14 and two other isolates from the same patient (V147-03 and V155-40) that were azole susceptible, to investigate if the potential mutator isolate V130-14 would accumulate more mutations over time. After 7 days of growth, conidia from the outer edge of the mycelium were transferred with a wet Q-tip to a new tissue culture flask containing 20 ml AMM 1% agar. After 10 weeks, isolates were harvested, grown for 24 hours in an Erlenmeyer flask containing liquid AMM. Genomic DNA was prepared from mycelial bulbs as described previously (Tang et al., 1992) by using phenol/chloroform/isopropanol. As a control, Short Tandem Repeat (STR) analysis was performed to confirm isogeneity of T=0 and T=10 isolates. Multiplex PCR was performed for *A. fumigatus* STR loci; three trinucleotide (STRAf3A-C) and three tetranucleotide loci (STRAf4A-C) were amplified using corresponding primers containing the dye carboxyfluorescein (FAM), hexachlorofluorescein (HEX), or tetrachlorofluorescein (TET) at the 5' end, respectively. Cleaned PCR products were analyzed together with a GeneScan500 LIZ size standard (Applied Biosystems, UK) and fluorescence was detected on a Genetic Analyzer (Applied Biosystems, USA). The number of repeats were determined using the Peak Scanner Software v1.0 (Applied Biosystems, USA).

Whole genome sequencing of clinical isolates

Genomic DNA was extracted from serial passaging of the three clinical isolates from the same patient, V130-14, V147-03 and V155-40 (Tang et al., 1992). For the first analysis of putative mutator isolate V130-14, a DNA library was prepared using the Nextera XT DNA sample preparation kit (Illumina, USA). Subsequent sequencing was conducted in a paired end 2 × 150 bp mode using an Illumina NextSeq 500 machine (Illumina, USA) at the Department of Genetics in Radboudumc (Nijmegen,

Netherlands). For the WGS analysis of these three azole susceptible isolates the serial passaging experiments were (re)sequenced at BGI genomics (Hong Kong) and sequenced on the BGIseq-500 sequencing platform in a 2 x 100 bp paired-end mode.

Mapping of all reads and SNP calling was performed using CLC genomics workbench V19-22 (Qiagen). Mapping was performed using the 'Map Reads to Reference' tool, and reads were mapped against the Af293 ENSEMBL CADRE 30 reference genomes. SNPs were identified using the 'Low Frequency Variant Detection tool with the following parameters: Required significance (%) = 1,0, Ignore positions with coverage above = 100.000, Restrict calling to target regions = Not set, Ignore broken pairs = Yes, Ignore non-specific matches = Reads, Minimum coverage = 10, Minimum count = 2, Minimum frequency (%) = 80,0, Base quality filter = No, Read direction filter = No, Relative read direction filter = Yes, Significance (%) = 1,0, Read position filter = No, Remove pyro-error variants = No. The total list of 292 unique amino acid changes that were unique to putative mutator V130-14 was filtered by searching the descriptions of the Gene Ontology 'Biological Process', 'cellular component' and 'molecular function' with the words 'repair', 'polymerase', 'nuclease' and 'helicase'. Normalised coverage was calculated for each of the three isolates.

Calculations determining the mutational rate

To correct for growth speed, which differed between isolates, we made an estimation of cellular division events by measuring colony growth every 7 days and by measuring the approximate length of a hyphal cell. Hyphal cells were stained with BlankoPhor and observed through fluorescence microscopy. Mutational rate was determined by the number of mutations per generations per base pair and calculated by amount of SNPs/number of divisions/genome size (29.4 MB; Supplementary Table 1).

Creation of a protein 3D model

Modelling and calculation of a 3D protein model of the wildtype and mutated protein of AFUA_6G11410 (*mre11*) was completed in CLC genomics workbench, by creating an alignment to the template structure of the catalytic domain of MRE11 (PDB ID: 4YKE) from *Chaetomium thermophilum*, the only available crystal structure of this protein from a filamentous fungus, as the crystal structure of AfMRE11 has not been elucidated. In addition, Mre11 structures were constructed using AlphaFold for *A. fumigatus* Mre11 wild-type and Mre11 F332L (Jumper et al., 2021; Varadi et al., 2024). Yasara (version 25.1.13) was also used to construct alignments for *A. fumigatus* Mre11 structures and X-ray Mre11 structure from other related fungal

species *S. pombe, S. cerevisiae,* and *T thermophila* (Krieger et al., 2014).

CRISPR-Cas9 gene modification

A highly conserved mutation, Phe332Leu (F332L) in *mre11* was constructed in *A. fumigatus* wild-type strain A1160^{+}, a member of the CEA10 laboratory lineage lacking a functional ku80 gene, for the transformations. The hygromycin resistance cassette was used as a selectable marker and amplified from the pAN7.1 plasmid. Target specific crRNAs as well as oligos to prepare a repair template were designed using a web-based guide RNA designing tool EuPaGDT (Nicolas et al., 2014), and the program was executed with default settings to design gRNAs to the *mre11* loci. crRNAs closest to the target integration sites with the highest QC scores were manually selected for the transformation experiments (Supplementary Table 2). Homology directed repair (HDR) templates were amplified using primers that incorporated microhomology arms (Supplementary Table 2). The repair templates were amplified from mutator strain V130-14 by PCR with a corresponding pair of primers (Supplementary Table 2) using Phusion Flash Master Mix (Thermo Fisher Scientific). The amplified MHA templates were gel purified (Qiagen PCR purification kit) and used for transformation. The guide RNAs and primers used for the CRISPR-Cas9 mediated transformation are listed in Supplementary Table 2. RNP complexes were assembled using Alt-R S.p. Cas9 Nuclease V3, Alt-R®CRISPR-Cas9 tracrRNA and locus-specific Alt-R® CRISPR crRNA (Integrated DNA Technologies) by heating to 95 °C for 5 mins and cooling to room temperature in a thermal cycler for 10 mins.

Our CRISPR-Cas9 transformation protocol is based upon methodology from Zhao *et al.* (Zhao et al., 2019). The transformation mixture was plated over Sorbitol Minimal Medium selection plates (AMM supplemented with 1 M sorbitol and 1.5% [wt/vol] agar) containing hygromycin B (150µg/ml)). The plates were incubated at room temperature for the first 24 hours and then moved to 37°C for 48-72 hours. Spores from purified colonies were harvested and DNA was extracted for PCR to validate successful incorporation of cassettes using Phusion Flash Master Mix (Thermo Fisher Scientific) and relevant primer pairs (Supplementary Table 2) as previously described (Tang et al., 1992). PCR products were assessed by gel electrophoresis. Sanger sequencing was performed for three independent isolates. The genomic regions subjected to sequencing analysis and the primers used for the analysis are listed in Supplementary Table 2. Transformation efficiency was calculated by dividing the number of PCR positive strains from the total number of strains assessed. Reversal of the F332L mutation in putative mutator isolates V130-14 with the WT repair template was carried out in the same procedure.

Growth testing assays and serial passaging of recombinants genome analysis

Radial growth rates of *mre11*-F332L transformants were conducted by spotting 10^3 spores per strain on AMM agar plates. Plates were incubated for 6 days, and the radius of the colonies were measured every 24 hours. Three biological replicates were conducted for each strain. Growth measurements of the recombinants were compared to parental isolate.

mre11-F332L transformants and wild-type transformants were cultured on AMM and AMM supplemented with 0.1 µg/ml itraconazole (ICZ) for 10 weeks, and genomic DNA was extracted as previously described (15). Genome sequencing was performed using high-quality DNA samples (OD 260/280 = 1.8-2.0, > 10 µg) on the Illumina HiSeq platform (Novogene, Beijing, China).

Paired-end reads were aligned using the Burrows-Wheeler Aligner v0.7.17 (Li, 2013) MEM to the Af293 reference genome GCF_000002655.1 (ASM265v1). Post-processing was conducted using SAMtools v1.16.1 (Li et al., 2009) and Picard v2.27.4 (Institute B, 2019), and variant calling was performed using GATK HaplotypeCaller v4.2 (McKenna et al., 2010; Auwera et al., 2013), excluding repetitive regions (identified using RepeatMasker v4.0.6 (Smit et al., 2013-2015), generating GVCFs. Low-confidence variants were labelled as such if they met at least one of the parameters QD < 2.0, FS > 60.0, DP < 5, GQ < 50, MQ < 40, MQRankSum < -12.5, ReadPosRankSum < -8.0, SOR > 4.0. In addition, alternate variants must be present in at least 90% of reads covering that position. Variant annotation and functional effect were completed using snpEff v5.1 (Cingolani et al., 2012).

Results

Mycelial morphology and growth phenotypes of clinical isolates

This study includes three isolates (V130-14, V147-03 and V155-40) from a single patient, where the morphology of an azole-susceptible isolate (V130-14) on AMM plates revealed phenotypic variability, often characterized by distinct sectors within the mycelium. This was accompanied by discoloration of the conidia or a partial loss of conidiophore development in certain areas of the mycelium (Figure 1). V130-14 also displayed a growth impairment on MMS, experiencing a 27% reduction in mycelial growth relative to the control (Figure 2). In comparison, V147-03 exhibited a growth ratio of 0.92, and the reference strain CEA10 exhibited a growth ratio of 1.01. We therefore sought to understand the genetic basis of the phenotypic variability displayed by V130-14.

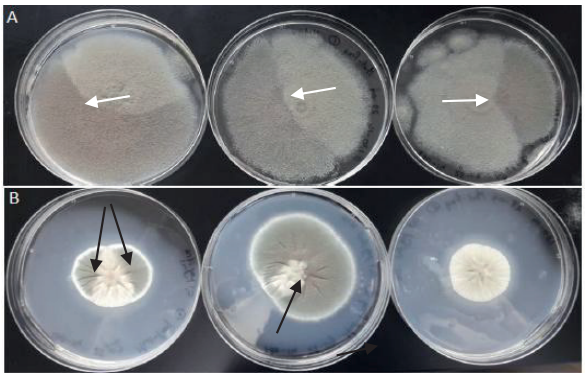

Figure 1: Morphology of clinical isolate V130-14 in triplo. A. Growth on AMM for 4d. B. Growth on AMM supplemented with 0.1 µg/ml ICZ for 4d. (Sectors were shown in arrows)

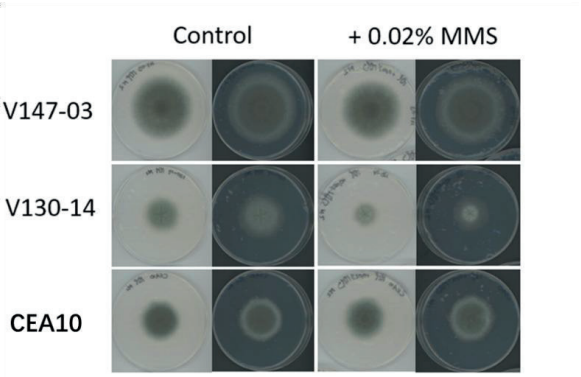

Figure 2: Typical growth of three *A. fumigatus* isolates on AMM and on AMM supplemented with 0.02% MMS. The same plate is shown on a white and on a black background.

Calculation of mutation rate and accumulated SNPs over a ten-week period through serial passaging

To be able to approximate the mutational rate in the potential mutator isolate V130-14 and two other clinical isolates (V147-03 and V155-40), an estimation was made of the number of generations that passed between timepoints T=0 weeks and T=10 weeks. After ten weeks, STR analysis showed the three isolates were still isogenic to the original inoculum (Supplementary Table 3) ruling out contamination during the passaging experiments. We approximated the mutation rate by dividing the total radial growth per ten weeks by the average length of a hyphal cell. We found that the average length of a hyphal cell was 44 µm, which corresponds to 23 cells per mm (Supplementary Figure 1). We found an average mutation rate of 5.49^{-11} for putative

mutator V130-14, and 3.73^{-12} for wild-type isolate V147-03. Due to the lack of mutations found in isolate V155-40, it was not possible to calculate a mutation rate for this isolate (Supplementary Table 1). This data suggests that the mutation rate of isolate V130-14 is approximately 15 times higher than in wild-type isolate V147-03. Therefore, we proposed V130-14 possessed an elevated mutation rate and a mutator phenotype.

Table 2: Mapping results and coverage calculations

Isolate	Timepoint	# of reads	# of uniquely mapped reads	% of mapped reads	Coverage
V130-14	T=0	8.144.108	7.877.323	96.72	54.70
V130-14-R1	T=10	9.538.322	9.421.213	98.77	65.43
V130-14-R2	T=10	9.416.724	9.301.258	98.77	64.59
V130-14-R3	T=10	8.029.006	7.928.114	98.74	55.06
V147-03	T=0	8.161.422	8.007.741	98.11	55.61
V147-03-R1	T=10	9.562.998	9.399.991	98.29	65.28
V147-03-R2	T=10	9.583.926	9.405.596	98.13	65.32
V147-03-R3	T=10	8.022.818	7.883.839	98.26	54.75
V155-40	T=0	9.585.250	9.391.427	97.97	65.22
V155-40-R1	T=10	8.129.532	7.965.578	97.98	55.32
V155-40-R2	T=10	8.144.218	7.975.049	97.92	55.38
V155-40-R3	T=10	8.172.148	8.013.115	98.05	55.65
CEA10	-	8.151.018	7.916.266	97.12	59.02
V34-78	-	7.986.954	7.857.552	98.38	54.57
V48-46	-	9.542.894	8.751.341	91.71	60.77

* Coverage is calculated as: ((# of uniquely mapped reads) *200)/28.800.000

Genome analysis of mutator isolate V130-14

After comparing all isolates of T=10 to their T=0 original inoculum, a total of 102.570.244 sequence reads were obtained, with an average unique mapping percentage of 98.1% to the reference genome Af293, and average coverage of 59.11x

(Table 2). We found on average 12 SNPs for the mutator isolate V130-14, 0.33 SNPs for isolate V147-03 and 0 SNPs for isolate V155-40 after ten weeks of serial passaging (Table 3). Whereas only 1 SNP was found in the progeny of V147-03, the other 36 SNPs were found in the progeny of putative mutator isolate V130-14, confirming that this isolate is indeed a mutator isolate.

Table 3: SNPs and corresponding amino acid changes counted after 10 weeks of serial passaging.

Isolate	# SNPs	# AA changes
V130-14-R1	14	7
V130-14-R2	15	4
V130-14-R3	7	3
V147-03-R1	1	0
V147-03-R2	0	0
V147-03-R3	0	0
V155-40-R1	0	0
V155-40-R2	0	0
V155-40-R3	0	0

In total, we found 56.472 mutations in the genome compared to reference Af293. We filtered mutations that were also present in other isolates, which therefore cannot be the causal mutations for the potential mutator phenotype seen in this isolate, to identify unique SNPs. SNPs and indels were filtered against five other genomes that were sequenced in this experiment, V147-03, V155-40, CEA10, and two additional clinical isolates V34-78 and V46-48 (Table 2).

In total, we found 1837 unique mutations, consisting of 70 deletions, 45 insertions, 101 multi nucleotide variances, 8 replacements and 1613 SNPs. Of these mutations, 292 were found to be missense mutations conferring amino acid changes. We observed 15 missense SNPs and indels in 14 genes proven or predicted to be involved in DNA damage repair (Table 4). One of these SNPs, a T994C mutation in *mre11*, resulted in a Phe332Leu substitution; *mre11* is a protein that is part of the highly conserved Mre11-Rad50-Xrs2 (MRX) complex, which plays an important role in double-strand break repair and telomere stability (Tisi et al., 2020).

No SNPs causing known mutations conferring resistance to azole antifungal drugs were present in *cyp51A*. Two missense SNPs were present in only isolates V130-14_1 and Fa1_1; one missense SNP caused Phe35Leu (F35L) in AFUA_1G00950, encoding a protein of unknown function, and the other missense SNP caused Phe332Leu (F332L) in AFUA_6G11410 (*mre11*).

Analysis of publicly available A. fumigatus genomes determined that 22 clade B isolates were found to contain this F332L-*mre11* mutation, with seven of these isolates also being from environmental sources (Table 5). The clinical isolate in this study harbouring F332L-*mre11* belongs to clade B, which rarely contains isolates with signature environmental resistance mutations commonly associated with the clade A population. All the three susceptible isolates in this study were also *cyp51A* wildtype (and present on the Clade B background), with ITR susceptible MIC data, whereas later isolates from the same patient were itraconazole, voriconazole and/or posaconazole resistant, which contained P216L, G54R, G54V and M220R, and had an MIC of 4 mg/L or >16 mg/L for ITR (Ballard et al., 2018).

Table 4: List of 14 candidate genes with unique amino acid changes in genes that are predicted or proven to be involved in DNA mismatch repair

Gene	Name	SNP	AA change	Product description
Afu3g13260	-	1967C>T	Ser656Leu	Has domain(s) with predicted nuclease activity and role in DNA repair
Afu4g03020	-	421G>T	Val141Leu	Ortholog(s) have role in chromatin remodeling and Ino80 complex, cytosol localization
Afu4g06490	*mih3*	490C>T	Pro164Ser	Ortholog(s) have role in meiotic mismatch repair, reciprocal meiotic recombination and MutLgamma complex, nucleus localization
Afu5g02570	-	9798G>T	Gln3266His	Ortholog(s) have histone acetyltransferase activity
Afu5g06260	*ino80*	3012G>T	Met1004Ile	Chromatin-remodeling ATPase INO80, putative
Afu6g11410	*mre11*	994T>C	Phe332Leu	Ortholog(s) have manganese ion binding, nuclease activity
Afu6g13290	-	917G>A	Gly306Asp	SNF2 family helicase/ATPase, putative
Afu5g01600	-	1268C>G	Thr423Ser	Has domain(s) with predicted DNA binding, DNA-directed DNA polymerase activity, catalytic activity and role in DNA replication
Afu5g06590	-	2831C>T	Thr944Met	Has domain(s) with predicted ATP binding, DNA binding, helicase activity, hydrolase activity, acting on acid anhydrides, in phosphorus-containing anhydrides and nucleic acid binding, more
Afu5g06600	-	2336G>A, 298G>A	Arg779His, Val100Met	Has domain(s) with predicted ATP binding, DNA binding, helicase activity, nucleic acid binding activity
Afu8g04740	-	5795G>A	Arg1932His	Ortholog(s) have role in spliceosomal conformational changes to generate catalytic conformation and U5 snRNP, cytosol, spliceosomal complex localization

Afu4g07290	-	442A>G	Arg148Gly	Ortholog(s) have Y-form DNA binding, crossed form four-way junction DNA binding, crossover junction endodeoxyribonuclease activity, flap-structured DNA binding activity and role in mitochondrial DNA metabolic process
Afu5g04010	*sen2*	772G>A	Glu258Lys	Putative tRNA-splicing endonuclease subunit
Afu5g04070	*spo11*	1075A>C	Met359Leu	Ortholog(s) have role in meiotic DNA double-strand break formation, reciprocal meiotic recombination, synapsis and cytosol, nucleus localization

Table 5: Metadata associated with Clade B isolates from publicly available *A. fumigatus* genomes also found to contain the *mre11* F332L mutation responsible for an accelerated mutation rate, and mutator isolate identified in this study.

Isolate ID	Country	Year	Source	ITR MIC (if known)	Accession
C16	Japan	2009	Clinical		PRJDB1541
C18	Japan	2009	Clinical		PRJDB1541
C416	Japan	2009	Clinical	1	PRJDB3064
C417	Japan	2009	Clinical	1	PRJDB3064
C58	Ireland	2010	Clinical	0.12	PRJEB27135
C59	Ireland	2010	Clinical	0.06	PRJEB27135
C418	Japan	2011	Clinical	4*	PRJDB3064
C72	Ireland	2011	Clinical	0.12	PRJEB27135
C73	Ireland	2011	Clinical	0.03	PRJEB27135
C505	USA	2015	Clinical		PRJNA632561
C531	USA	2015	Clinical		PRJNA632561
C532	USA	2015	Clinical		PRJNA632561
E427	USA	2015	Environment		PRJNA632561
E429	USA	2015	Environment		PRJNA632561
C446	USA	2016	Clinical		PRJNA632561
C470	USA	2016	Clinical		PRJNA632561
C481	USA	2016	Clinical		PRJNA632561
E594	USA	2017	Environmental	1	PRJNA742769
E606	USA	2017	Environmental	1	PRJNA742769
E372	UK	2018	Environmental		PRJEB51237
E377	UK	2018	Environmental		PRJEB51237
E547	USA	2018	Environmental	1	PRJNA742769
V130-14	Netherlands	2011	Clinical	1	

Note: ITR = itraconazole. *caused by P216L in *Cyp51A*.

Protein 3D model

Sequence alignment of this region of the gene for *A. fumigatus*, *S. pombe*, *S. cerevisiae* and *H. sapiens* shows a highly conserved tyrosine or phenylalanine on this location for all species (Figure 3A). We constructed a 3D model of the mutation based on the crystal structure of MRE11 from *S. cerevisiae* for the wildtype and the mutated sequence of MRE11. The F332L mutation results in a change on the surface of the MRE11 interface, as the aromatic phenylalanine is replaced by leucine (Figure 3B). Additionally, alignments for *A. fumigatus* Mre11 wild-type and Mre11 F332L were constructed using the EMBL-EBI MAFFT-tool. Both the phenylalanine and leucine fit into the alpha-helical structure, suggesting the mutation does not cause significant structural differences.

RMSD values were calculated using Yasara (Figure 4). RMSD values of *A. fumigatus* Mre11 versus Mre11 structures from *T. thermophila*, *S. pombe*, and *S. cerevisiae* were 0.725 Å, 0.938Å, and 1.011Å respectively.

Morphology and growth testing of *mre11*-F332L Transformants

The *mre11*-F332L transformants were subjected to detailed morphological and growth assessments. The mutation frequency of these transformants was found to be comparable to that of the original mutator strain, indicating a similar propensity for genetic alterations.

Figure 3: Alignment and predicted protein structure of wildtype and mutated MRE11 in A. fumigatus. Position 332 is located on the outside of an alpha helix.

In terms of growth, the *mre11*- F332L transformants exhibited a phenotype like the mutator strain, though the impact on growth was less pronounced. Specifically, while

the original mutator strain V130-14 showed a significant reduction in growth rate, the *mre11*- F332L mutation had a minimal effect on the growth of the strains (Supplementary Figure 2). No sectors were observed in the *mre11*- F332L transformants, which is consistent with the original mutator strain, where sector formation was not always present.

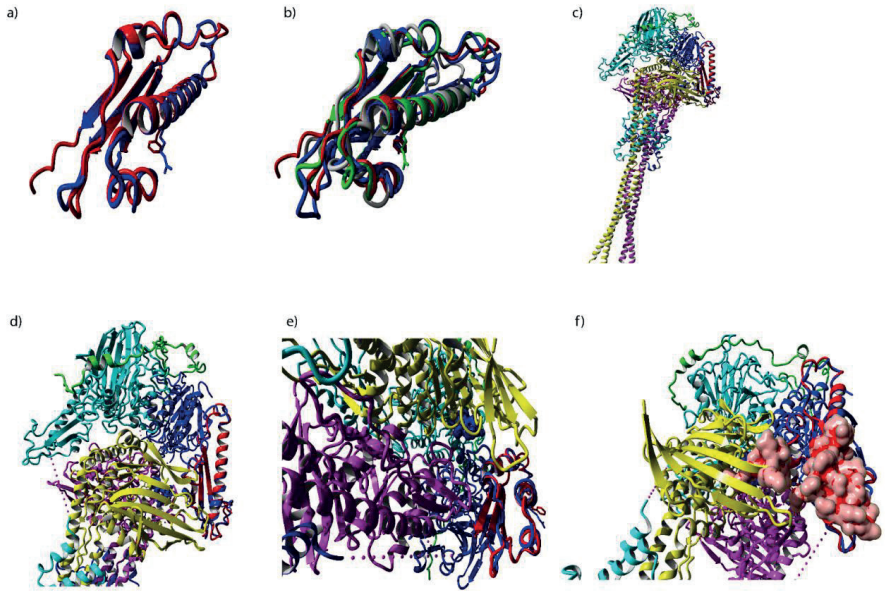

Figure 4: Figures created in Yasara a) Alignment of *A. fumigatus* (red) and *T. thermophila* (blue) MRE11. The animo acid side-chain of residue 332 is shown. b) Alignment of five MRE11 structures c) *C. themophila* Mre11-Rad50-Nbs1 complex aligned with region of interest (red) d) Alignment of *C. thermophila* region of interest (red) in Mre11 complex (blue) e) Zoomed in view of alignment of *C. thermophila* region of interest (red) in Mre11 complex (blue) f) *C. thermophila* Mre11-Rad50-Nbs1 complex with region of interest

Discussion

We investigated the mutation rate of a putative mutator isolate through WGS and found that it had a 15-fold increase in SNPs that persisted in the population after ~7000 generations compared to wild-type strains. The average mutational rate found for isolate V130-14 (5.49^{-11}) is five times higher than the mutational rate found in an *A. fumigatus* mutator isolate recently studied, which had a mutation rate of

approximately 1.1×10^{-11} (Álvarez-Escribano et al., 2019). The radial growth of the putative mutator isolate was diminished by 27% compared to the control strain, whereas wild-type isolate V147-03 only had a reduction of radial growth by 8%. These results suggest a fitness defeat associated with elevated mutation rates and are similar to the growth reduction found in literature, which shows a growth reduction in *A. fumigatus* isolates with diminished genetic stability, as compared to the wild-type (dos Reis et al., 2019; dos Reis et al., 2018).

We identified a T994C mutation in the *mre11* gene of V130-14, resulting in a Phe332Leu (F332L) substitution. The *mre11* gene encodes a protein that is a component of the highly conserved Mre11-Rad50-Xrs2 (MRX) complex, which plays a crucial role in double-strand break repair and telomere stability (Zha et al., 2009). However, we did not find any SNPs in gene *mre11* in any of the other five sequenced isolates when compared to the reference genome of Af293, which was not the case for any other candidate gene. A mutation in *mre11* gene could have consequences on the functionality of this complex: a previous study confirmed that a Phe328Leu mutation, which is a similar amino acid change in a nearby codon, causes a growth defect on medium supplemented with MMS in *S. cerevisiae* (Lammens et al., 2021). This mutation destabilizes the binding of MRE11p with RAD50p, resulting in a defect in DNA damage repair. The 3D model indicates that this region of the gene contains a highly conserved tyrosine or phenylalanine at this location across all species. The crystal structure of MRE11 from *S. cerevisiae* shows that position 332 is located on the outside of an alpha helix that forms a bonding interface with RAD50. As the aromatic phenylalanine is replaced by leucine, it is possible that this mutation also leads to decreased binding of AfMRE11 to AfRAD50 in *A. fumigatus*, thereby causing a defect in DNA double-strand break repair.

In our study, we aimed to validate the observed increase in SNPs by restoring the wildtype MRE11 locus through CRISPR/Cas9 transformation in the same genetic background. The results indicated that the mutation had a significant effect on the mutational rate, suggesting that the genetic alterations observed were indeed due to the presence of the mutation. Additionally, the mutation had a slight but measurable effect on the growth rate, indicating that while the mutator phenotype is primarily characterized by an increased mutational rate, it also has subtle effects on growth dynamics. The absence of sector formation, while informative, is not always a consistent feature in the original strain, suggesting that other genetic or environmental factors may influence this phenotype.

The clinical isolate harbouring the *mre-11* mutation belongs to clade B, a clade that

rarely possesses azole resistance mutations. Recently, elevated mutation rates were reported for (clade A) isolates harbouring TR_{34}/L98H, likely exposed to agricultural azole fungicides (Bottery et al., 2024). Together with our finding of the F332L allele in both clinical and environmental isolates, we hypothesize that the mutator genotype represents a general adaptive strategy in *A. fumigatus* to withstand prolonged azole stress.

The continued selection pressure exerted by the environmental and medical azoles could drive the expansion of these mutator backgrounds in the global *A. fumigatus* populations. This expansion, in turn, leads to opportunities for sexual recombination with isolates containing antifungal resistance alleles, further expanding the genomic variation and complicating the management of drug-resistant disease. Given the high recombination rates inherent in *A. fumigatus*, these resistance polymorphisms are likely to spread rapidly through populations if crossed on to a mutator background (Auxier et al., 2023). This not only facilitates the acquisition of resistance but also accelerates its dissemination, posing a significant challenge to public health efforts aimed at controlling fungal infections. The mutator background, therefore, represents a critical factor in the evolution of drug resistance in *A. fumigatus*, and understanding its mechanisms and impacts is essential for developing effective strategies to mitigate the spread of resistant strains.

In conclusion, our study highlights the complex interplay between genetic mutations, recombination rates, and environmental factors in the evolution of antifungal drug resistance in *A. fumigatus*. The findings underscore the need for continued research into the genetic and environmental drivers of resistance, as well as the development of novel therapeutic and preventive strategies to address this growing public health concern.

Funding

This study was supported by National Natural Science Foundation of China [82272354] supporting YS.

Data availability

All raw reads have been submitted to the European Nucleotide Archive (ENA) under accession number PRJEB63121.

References

Auxier B, Debets AJM, Stanford FA, et al. The human fungal pathogen *Aspergillus fumigatus* can produce the highest known number of meiotic crossovers. PLoS Biol.

2023;21(9): e3002278.

Auwera GAV der, Carneiro MO, Hartl C, Poplin R, Angel G del, Moonshine AL, et al. From FastQ data to high confidence variant calls: the Genome Analysis Toolkit best practices pipeline. Curr Protoc Bioinforma Ed Board Andreas Baxevanis Al. 2013;11(1110):11.10.1-11.10.33.

Álvarez-Escribano I, Sasse C, Bok JW, Na H, Amirebrahimi M, Lipzen A, et al. Genome sequencing of evolved aspergilli populations reveals robust genomes, transversions in A. flavus, and sexual aberrancy in non-homologous end-joining mutants. BMC Biol. 2019;17(1):1–17.

Bottery MJ, van Rhijn N, Chown H, Rhodes JL, Celia-Sanchez BN, Brewer MT, et al. Elevated mutation rates in multi-azole resistant *Aspergillus fumigatus* drive rapid evolution of antifungal resistance. Nat Commun. 2024;15(1):10654.

Buil JB, Snelders E, Denardi LB, Melchers WJG, Verweij PE. Trends in Azole Resistance in *Aspergillus fumigatus*, the Netherlands, 1994-2016. Emerg Infect Dis. 2019;25(1):176-178. doi:10.3201/eid2501.171925

Ballard E, Melchers WJG, Zoll J, Brown AJP, Verweij PE, Warris A. In-host microevolution of *Aspergillus fumigatus*: A phenotypic and genotypic analysis. Fungal Genet Biol. 2018;113:1-13.

Cingolani P, Platts A, Wang LL, Coon M, Nguyen T, Wang L, et al. A program for annotating and predicting the effects of single nucleotide polymorphisms, SnpEff: SNPs in the genome of Drosophila melanogaster strain w 1118; iso-2; iso-3. Fly (Austin). 2012 Apr;6(2):80–92.

Denning DW. Global incidence and mortality of severe fungal disease. Lancet Infect Dis. 2024;24(7):e428-e438. doi:10.1016/S1473-3099(23)00692-8

dos Reis TF, Silva LP, de Castro PA, de Lima PBA, do Carmo RA, Marini MM, et al. The influence of genetic stability on *Aspergillus fumigatus* virulence and azole resistance. G3 Genes, Genomes, Genet. 2018;8(1):265–78.

dos Reis TF, Pereira Silva L, Alves de Castro, Patrícia Andrade do Carmo R, Mendes Marini M, Franco da Silveira J, Ferreira BH, et al. The *Aspergillus fumigatus* Mismatch Repair MSH2 Homolog Is Important for Virulence and Azole Resistance. mSphere. 2019;4(4):416–9.

Healey KR, Zhao Y, Perez WB, Lockhart SR, Sobel JD, Farmakiotis D, et al. Prevalent mutator genotype identified in fungal pathogen *Candida glabrata* promotes multi-drug resistance. Nat Commun. 2016; 7:1–10.

Institute B. Picard Toolkit. 2019.

Jumper J. et al. 2021. Highly accurate protein structure prediction with AlphaFold. Nature 596, 583-589.

Krieger E and Vriend G. 2014. YASARA View. Bioinformatics 30, 2981-2982.

Kanj A, Abdallah N, Soubani AO. The spectrum of pulmonary aspergillosis. Respir Med. 2018;141(March):121–31.

Latgé JP, Chamilos G. *Aspergillus fumigatus* and Aspergillosis in 2019. Clin Microbiol Rev. 2019;33(1):e00140-18. doi: 10.1128/CMR.00140-18.

Li H. Aligning sequence reads, clone sequences and assembly contigs with BWA-MEM. 2013.

Li H, Handsaker B, Wysoker A, Fennell T, Ruan J, Homer N, et al. The Sequence Alignment/Map format and SAMtools. Bioinformatics. 2009;25(16):2078–9.

Lammens K, Bemeleit DJ, Möckel C, Clausing E, Schele A, Hartung S, et al. The Mre11:Rad50 structure shows an ATP-dependent molecular clamp in DNA double-strand break repair. Cell. 2011;145(1):54–66.

McKenna A, Hanna M, Banks E, Sivachenko A, Cibulskis K, Kernytsky A, et al. The Genome Analysis Toolkit: A MapReduce framework for analyzing next-generation DNA sequencing data. Genome Res. 2010;20(9):1297–303.

Nicolas AG, Serero A, Legoix-Né P, Jubin C, Loeillet S. Mutational landscape of yeast mutator strains. Proc Natl Acad Sci. 2014;111(5):1897–902.

Rhodes J, Abdolrasouli A, Dunne K, et al. Population genomics confirms acquisition of drug-resistant *Aspergillus fumigatus* infection by humans from the environment [published correction appears in Nat Microbiol. 2022 Nov;7(11):1944. doi: 10.1038/s41564-022-01160-6.]. Nat Microbiol. 2022;7(5):663-674. doi:10.1038/s41564-022-01091-2

Smit A, Hubley R, Green P, 2015. RepeatMasker Open-4.0. 2013–2015.

Tang CM, Cohen J, Holden DW. An *Aspergillus fumigatus* alkaline protease mutant constructed by gene disruption is deficient in extracellular elastase activity. Mol Microbiol. 1992;6(12):1663–71.

Tisi R, Vertemara J, Zampella G, Longhese MP. Functional and structural insights into the MRX/MRN complex, a key player in recognition and repair of DNA double-strand breaks. Comput Struct Biotechnol J. 2020; 18:1137–52.

Verweij PE, Rijnders BJA, Brüggemann RJM, et al. Review of influenza-associated pulmonary aspergillosis in ICU patients and proposal for a case definition: an expert opinion. Intensive Care Med 2020;46(08):1524–1535. doi: 10.1007/s00134-020-06091-6.

Verweij PE, Mellado E, Melchers WJ. Multiple-triazole-resistant aspergillosis. N Engl J Med. 2007;356(14):1481-1483. doi:10.1056/NEJMc061720

Verweij PE, Snelders E, Kema GH, Mellado E, Melchers WJ. Azole resistance in *Aspergillus fumigatus*: a side-effect of environmental fungicide use?. Lancet Infect Dis. 2009;9(12):789-795. doi:10.1016/S1473-3099(09)70265-8

Vale-Silva L, Beaudoing E, Tran VDT, Sanglard D. Comparative Genomics of Two Sequential Candida glabrata Clinical Isolates. G3 (Bethesda). 2017;7(8):2413-2426.

Verweij PE, Zhang J, Debets AJM, Meis JF, van de Veerdonk FL, Schoustra SE, Zwaan BJ, Melchers WJG. In-host adaptation and acquired triazole resistance in *Aspergillus fumigatus*: a dilemma for clinical management. Lancet Infect Dis. 2016;16(11):e251-e260.

Varadi M. et al. 2024. AlphaFold protein structure database in 2024: providing structure coverage for over 214 million protein sequences. NAR 52, D368-D375.

Zhao C, Fraczek MG, Dineen L, Lebedinec R, Macheleidt J, Heinekamp T, et al. High-Throughput Gene Replacement in Aspergillus fumigatus. Curr Protoc Microbiol. 2019;54(1): e88.

Zha S, Boboila C, Alt FW. Mre11: roles in DNA repair beyond homologous recombination. Nat Struct Mol Biol. 2009;16(8):798-800.

Supplemental tables and figures

Supplemental table 1. Mutation rate calculation and data on cell lengths

Isolate	1	2	3	4	5	6	7	8	9	10	Total distance (mm)	# of mitotic divisions	AVG	AVG SNPs	Mutation rate
130-14: 1	18	31	17	37	36	30	18	29	47	22	285	6555			
130-14: 2	22	38	28	45	44	32	33	33	49	21	345	7935	7115	12	5.73^{-11}
130-14: 3	17	29	28	30	44	25	30	32	43	20	298	6854			
147-03: 1	60	23	37	43	27	44	40	41	47	21	383	8809			
147-03: 2	60	24	40	41	20	45	38	22	35	32	357	8211	8725	0.33	1.29^{-12}
147-03: 3	60	30	49	35	21	41	39	45	43	35	398	9154			
155-40: 1	60	60	15	53	48	25	49	50	50	50	460	10580			
155-40: 2	60	60	52	48	46	19	50	34	49	48	466	10718	10258	0	-
155-40: 3	60	60	12	52	19	30	51	45	44	39	412	9476			

Measurements of growth per week in mm.

Supplemental table 2. gRNA and primers to generate F332L transformants.

Name	Sequence (5'-3')	Application
mre11_crRNA_F332L_up	ACTTAAGCTCTTGCTGCTCTT	guide RNA for generation of F332L
mre11_crRNA_F332L_down	ACATGGCGTTCAGGCAATTGC	guide RNA for generation of F333L
mre11_F	CACACACTTAAGCTCTTGCTGCTCTTTCGCACTTTAAGAAGTCCA	Forward primer to generate the front half of repair template
mre11_R	ATTGCCTGAACGCCATGTAGATGCAATACAGCTGATAAGACGCTC	Reverse primer to generate the front half of repair template
Hgy_F	ACATGGCGTTCAGGCAATACGGCGTAACCAAAAGTCACACAACACA	Forward primer to generate the second half of repair template containing HgyR
Hgy_R	TTCCTTAAACCGTAAGACCTGCATCTTGACGACCGTTGATCTGCTT	Reverse primer to generate the second half of repair template containing HgyR
2Temp_F	AGCAGTTGTCCTCCGTAGTTCACACACTTAAGCTCTTGCT	Forward primer to generate the whole length of repair template
2Temp_R	GTTGTGAAGAATGGCTGAAATTCCTTAAACCGTAAGACCT	Reverse primer to generate the whole length of repair template
PCR_Front_F1	TGGCTGTGTTTGTTGTCTCC	PCR for examination of recombination
PCR_Front_R1	CTTGTCACCCAAGCAGTTCA	PCR for examination of recombination
PCR_Mid_F2	CTGGTCGGGAGTTCAAATGT	PCR for examination of recombination
PCR_Mid_R2	AGCTGCTCCACCTTGACTGT	PCR for examination of recombination
PCR_Back_F	GCTTTCGAGCCTATGCAGAC	PCR for examination of recombination
PCR_Back_R	ATCTACGGGCTGTGCATTTC	PCR for examination of recombination

Supplemental table 3. Each parental isolate is marked in grey.

Isolate	Timepoint	STRaF3A	STRaF3B	STRaF3C	STRaF4A	STRaF4B	STRaF4C
V130-14	T=0	22	6	14	6	10	5
V130-14-R1	T=10	23	6	15	5	9	5
V130-14-R2	T=10	23	6	15	6	9	5
V130-14-R3	T=10	23	6	14	6	9	5
V147-03	T=0	23	6	14	6	5	5
V147-03-R1	T=10	25	7	15	5	3	4
V147-03-R2	T=10	26	8	15	5	4	5
V147-03-R3	T=10	23	6	14	5	4	4
V155-40	T=0	32	6	8	5	7	18
V155-40-R1	T=10	31	5	6	5	6	17
V155-40-R2	T=10	31	5	6	4	6	15
V155-40-R3	T=10	31	5	6	4	6	16

Supplemental Figure 1: Typical growth of hyphal cells, observed and measured after Blancophor staining under fluorescence microscopy, 200x magnification. A total of 134 cells were measured and the average cell length was calculated to be 44 µm.

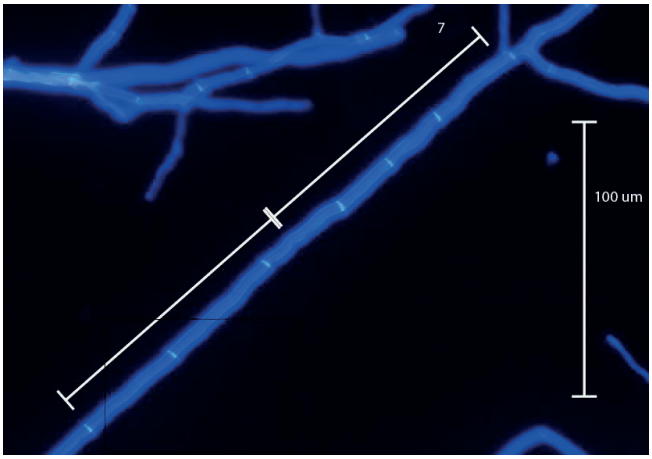

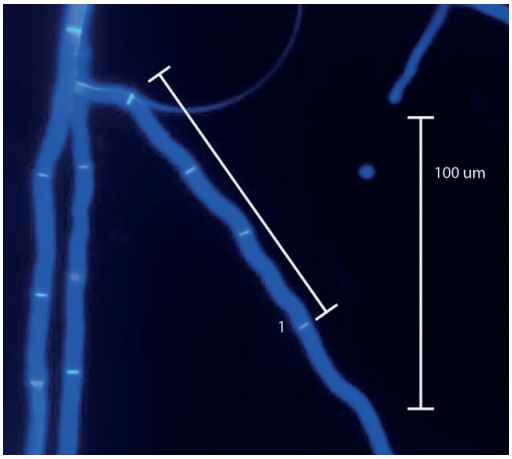

Supplemental Figure 2: Comparison of growth rates

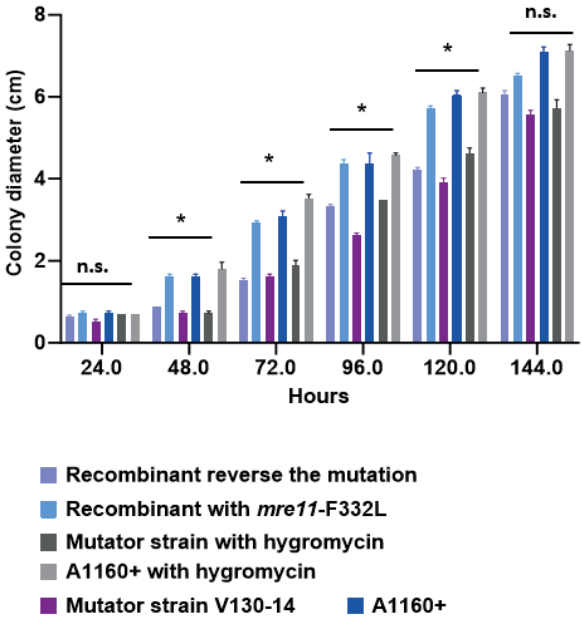

CHAPTER 6

Analysis of susceptibility and drug resistance of antifungal agents in Aspergillosis and Mucormycosis patients: A systematic review

Yinggai Song • Paul E Verweij • Jochem B Buil • Sybren de Hoog • Jie Liu • Jiaxian Guo • Wei Liu • Ruoyu Li

Mycoses. 2025;68(10):e70118.

Abstract

Objectives: To review the susceptibility and resistance of *Aspergillus* and Mucorales isolates to antifungal agents.

Methods: Studies in susceptibility or resistance of *Aspergillus* and Mucorales isolates to antifungal agents published between January 2010 to June 2023 were systematically searched in PubMed, EMBASE, and the Cochrane Library. The minimum inhibitory concentration (MIC), susceptibility, and resistance data were analyzed using CLSI or EUCAST methods.

Results: After following the systematic review processes, 96 studies were included. The total number of isolates was 16,258. Compared with existing MIC distributions and breakpoints or epidemiological cutoff values (ECVs) established by CLSI or EUCAST, for *A. flavus*, the posaconazole and voriconazole MIC values were at or below the ECV, indicating that the isolates were wild-type (WT) strains; however, the amphotericin B, isavuconazole, and itraconazole MIC values were elevated. For *A. fumigatus*, the isavuconazole MIC values were within ECV limits, indicating that the isolates were WT strains; however, the amphotericin B, posaconazole, and voriconazole MIC values were elevated. For *A. niger*, the isavuconazole and voriconazole MIC values were within ECV limits, indicating that the isolates were WT strains; however, the amphotericin B and posaconazole MIC values were elevated. *A. flavus* had consistently high in vitro susceptibility to voriconazole, and *A. fumigatus* and *A. niger* had consistently high in vitro susceptibility to amphotericin B. For Mucorales, the resistance to amphotericin B was consistently at the lowest level. The subgroup analysis indicated that the resistance among the strains in the environment was higher than that of the clinical isolates.

Conclusion: Trends in susceptibility and resistance of *Aspergillus* and Mucorales isolates should be adequately considered in antifungal therapy. The evaluation of drug resistance is beneficial in that it enables clinicians to choose suitable drugs and appropriate doses.

Keywords: antifungal agents, susceptibility, resistance, *Aspergillus*, Mucorales

Introduction

Invasive fungal diseases, especially aspergillosis and mucormycosis, are associated with high morbidity and mortality among a wide variety of immunocompromised patients, such as those receiving solid organ or stem cell transplants, those with hematological malignancies, and those taking immunosuppressive agents [1].
It is estimated that over 2,113,000 people develop invasive aspergillosis each year globally [2]. The mortality rate for aspergillosis ranges from 30% to 90%, with the rate depending on the patient population and the severity and duration of immunosuppression [3]. The incidence of mucormycosis is rising globally. The Leading International Fungal Education (LIFE) portal has estimated that the annual prevalence of mucormycosis has increased to 910,000 cases globally [4]. All-cause mortality rates for mucormycosis range considerably from 40% to 80% and vary with the underlying condition and site of infection [5]. The landscape of invasive fungal diseases is progressively changing. A successful clinical outcome generally requires early diagnosis and effective antifungal therapy. However, antifungal options for aspergillosis and mucormycosis are few, with the chemical classes available for treating invasive diseases limited to azoles (isavuconazole, itraconazole, posaconazole, voriconazole) and polyenes (amphotericin B).
Over the past decade, due to the expansion of antifungal use for prophylaxis, and empirical and directed therapy in patients with various conditions, the epidemiology of invasive fungal infections has changed, which has led to increased drug resistance [6]. Additionally, the use of medically related antifungal drugs in agriculture has contributed to environmental reservoirs for some drug-resistant pathogens [7 8]. There is increasing concern about the global emergence of antifungal resistance among both clinical and environmental isolates, for which optimal therapies are not well defined. Factors related to antifungal agents, such as in vitro susceptibility and drug resistance, have an important bearing on the ultimate outcome of treatment and can help to predict the clinical response to therapy. In addition, the susceptibility of *Aspergillus* and Mucorales isolates to antifungal agents varies geographically.

Currently, there is no systematic review or meta-analysis on the susceptibility and resistance of *Aspergillus* and Mucorales isolates to antifungal agents in aspergillosis and mucormycosis patients despite the large amount of data in the literature. A better understanding of the clinical impact of antifungal resistance is essential for the prompt and efficient treatment of patients with aspergillosis and mucormycosis and for improving the outcome of such infections. As reported in this article, we systematically collected susceptibility and drug resistance data of *Aspergillus* isolates (specifically *Aspergillus fumigatus*, *A. flavus*, and *A. niger*) and Mucorales isolates

(specifically *Rhizopus* spp., *Mucor* spp., and *Rhizomucor* spp.) for different types of antifungal agents (specifically amphotericin B, isavuconazole, itraconazole, posaconazole, and voriconazole).

Methods

This study followed the Preferred Reporting Items for Systematic Reviews and Meta-Analyses (PRISMA 2020) extension for scoping reviews [9]. The protocol was registered on Inplasy (registration number: INPLASY202470069).

Data sources and literature search

An electronic database search for PubMed, EMBASE, and the Cochrane Library was conducted on June 13, 2023. The included studies focused on antifungal susceptibility and were published between January 2010 to June 2023. The search strategy is provided in Appendix 1.

Study selection

The studies comprised in vitro studies that reported the susceptibility data of *Aspergillus* and Mucorales isolates to antifungal agents used to treat aspergillosis and mucormycosis. Moreover, molecular tests must be performed before the analysis according to standardized classification for fungus. Articles that did not use molecular test will be excluded. Detailed inclusion criteria were as follows:

Population: Studies on *A. fumigatus*, *A. flavus*, or *A. niger* and studies on *Rhizopus* spp., *Mucor* spp., or *Rhizomucor* spp.
Intervention: Studies on antifungal agents including amphotericin B, isavuconazole, itraconazole, posaconazole, and voriconazole.
Comparator: No limitation.
Outcome: Susceptibility, drug resistance, and minimum inhibitory concentration (MIC) determined by broth dilution methods.
Study design: In vitro studies.

Data extraction

Data from each study was extracted independently by two reviewers using a standardized data extraction form. Any disagreements were resolved by discussion, with assistance from a third party if necessary. Where information relating to a potentially included study was lacking, we contacted the authors and requested further information. We extracted all relevant characteristics of the included studies, including:

1) General study characteristics: First author's name, publication year, country, study

design, funding sources

2) Pathogens: Type, sources (environmental or clinical)

3) Interventions: Types of antifungal agents (amphotericin B, isavuconazole, itraconazole, posaconazole, and voriconazole)

4) Outcomes: Susceptibility, drug resistance, and MIC value (MIC range and MIC50)

Data synthesis and analysis

We summarized the susceptibility and resistance data of *Aspergillus* and Mucorales isolates to antifungal agents. The MIC, susceptibility, and resistance data were presented with the MIC_{50} defined as the MIC at which 50% of the isolates of a particular microorganism are inhibited by a given antimicrobial agent and the range. When clinical breakpoints values were proposed based on the Clinical & Laboratory Standards Institute (CLSI) or the European Committee on Antimicrobial Susceptibility Testing (EUCAST) guidelines, MIC values were interpreted in accordance with them. The MIC data in our study were compared with the cutoff values proposed by CLSI or EUCAST guidelines, and the therapy outcome was predicted based on these results. In the absence of clinical breakpoints, in accordance with Astvad 2022 [10], after ascertaining that the species was correctly identified, we compared the MIC values with existing MIC distributions for that drug and species to determine whether the MIC was “normal” or “elevated”. CLSI defines the epidemiological cutoff value (ECV) as the MIC or zone diameter value that separates microbial populations into those with and without acquired and/or mutational resistance. EUCAST introduced the concept of the epidemiological cutoff value (ECOFF-the official EUCAST abbreviation) to describe the MIC above which microbial isolates have phenotypically detectable acquired resistance mechanisms. If the MIC values were at or below the epidemiological cutoff value (ECV for CLSI method and ECOFF for EUCAST method), the isolates were defined as wild-type (WT). In this article, susceptibility denotes the proportion of isolates with WT MICs, and the resistance denotes the proportion of isolates with non-WT MICs. This is a narrative evidence synthesis, and we performed subgroup analyses to susceptibility and drug resistance data between environmental and clinical isolates.

Results

Results of study selection

The trial search identified 2,779 records, 1,717 of which remained after removing duplicates. Next, 1,168 records were excluded after screening the title and abstract.

Subsequently, 27 reports were not retrieved, leaving 522 reports with the full text to be assessed for eligibility. Finally, 426 reports were excluded following screening of the full text, leaving the 96 studies[11-106] included in this review. The study-screening process and the reasons for exclusion at the full-text screening stage are presented in Figure 1.

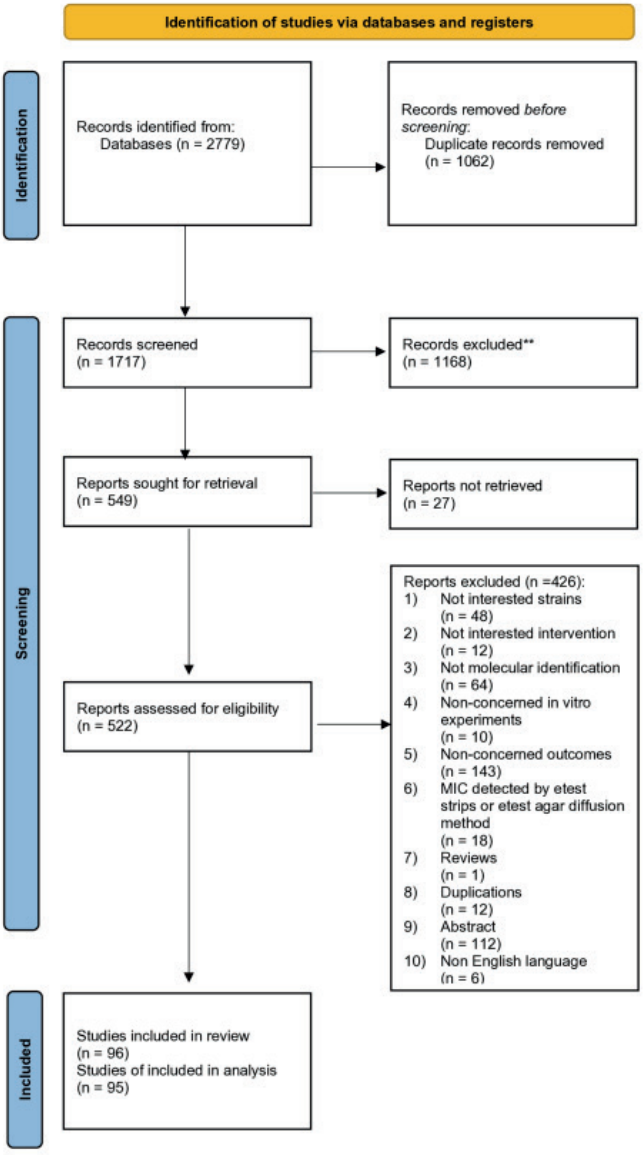

Figure 1. Flow of study review and selection process.

Summary of characteristics of included studies

We included 96 studies from multiple countries or regions. The total number of isolates was 16,258. The strains isolated from patients, or the environment were *A. fumigatus*, *A. flavus*, *A. niger*, *Rhizopus* spp., *Mucor* spp., and *Rhizomucor* spp. - Strains were isolated from patients in 79 studies (including 14,993 isolates), the environment in five studies (including 269 isolates), both patients and the environment in 8 studies (including 971 isolates), and the laboratory in two studies. One study did not report the strain source. To determine the MIC, 76 studies used the CLSI method, 18 used the EUCAST method, one used both methods, and two did not report the method. The general characteristics of the included studies, including the MIC determination methods, are summarized in Appendix Table 1.

MIC_{50} of antifungal agents for *Aspergillus* isolates

For *A. flavus*, the MIC_{50} values (CLSI method) were as follows: amphotericin B 1 (0.125–4) mg/L (21 studies), isavuconazole 1 (0.5–2) mg/L (9 studies), itraconazole 0.375 (0.12–16) mg/L (20 studies), posaconazole 0.25 (0.12–0.5) mg/L (15 studies), and voriconazole 0.5 (0.125–1) mg/L (21 studies). The MIC_{50} values using the EUCAST method were higher for amphotericin B, ranging from 1 to 32 mg/L (7 studies); those of isavuconazole (5 studies), itraconazole (7 studies), posaconazole (7 studies), and voriconazole (9 studies) obtained using the EUCAST method were 1 (0.5–1), 0.25 (0.12–1), 0.125 (0.12–1), and 0.5 (0.5–1) mg/L, respectively (Figure 2A, Table 1). Based on ECVs established by CLSI for *A. flavus*, the ECVs for WT strains were as follows: amphotericin B (ECVs WT≤4), isavuconazole (ECVs WT≤1), itraconazole (ECVs WT≤1), posaconazole (ECVs WT≤0.5), voriconazole (ECVs WT≤2) [107]. Based on antifungal ECOFFs and clinical breakpoints (mg/L) established by EUCAST for *A. flavus*, the ECOFFs and breakpoints were amphotericin B (ECOFFs WT≤4), isavuconazole (ECOFFs WT≤2, S [susceptible]≤1, R [resistant]>2, ATU [area of technical uncertainty]=2), itraconazole (ECOFFs WT≤1, S≤1, R>1, ATU=2), posaconazole (ECOFFs WT≤0.5), and voriconazole (ECOFFs WT≤2) [108]. Overall, for *A. flavus*, the MIC values of posaconazole and voriconazole were at or below the ECV (≤0.5 mg/L for posaconazole, ≤2 mg/L for voriconazole); thus, it can be assumed that the isolates were WT strains. However, the MIC values of amphotericin B, isavuconazole, and itraconazole exceeded the ECV (≤4 mg/L for amphotericin B, ≤1 or 2 mg/L for isavuconazole, ≤1 mg/L for itraconazole) and were elevated compared with existing MIC distributions.

For *A. fumigatus*, the CLSI method yielded MIC_{50} values for amphotericin B (26 studies), isavuconazole (10 studies), itraconazole (29 studies), posaconazole (25

studies), and voriconazole (32 studies) of 1 (0.0625–4) mg/L, 0.5 (0.25–1) mg/L, 0.5 (0.125–1) mg/L, 0.25 (0.03–1) mg/L, and 0.5 (0.125–4) mg/L, respectively. Using the EUCAST method, the MIC_{50} values were 0.5 (0.25–2) mg/L, 1 (0.5–1) mg/L, 0.375 (0.125–0.5) mg/L, 0.0925 (0.06–0.5) mg/L, and 0.5 (0.25–4) mg/L, respectively (Figure 2B, Table 1). CLSI ECVs for *A. fumigatus* indicated WT cutoffs for amphotericin B, isavuconazole, and itraconazole of ≤2 mg/L, ≤1 mg/L, and ≤1 mg/L, respectively. EUCAST ECOFFs and breakpoints showed slight variations, with WT cutoffs of ≤1 mg/L for amphotericin B, ≤2 mg/L for isavuconazole, ≤1 for itraconazole, ≤0.25 for posaconazole and ≤1 for voriconazole. MICs for isavuconazole and itraconazole were within ECV limits, so that the isolates were WT strains. However, the MICs for amphotericin B, posaconazole, and voriconazole exceeded the established ECVs.

For *A. niger*, the MIC_{50} values (CLSI method) were as follows: amphotericin B 0.5 (0.0312–8) mg/L (19 studies), isavuconazole 2 (1–2) mg/L (6 studies), itraconazole 1 (0.032–4) mg/L (17 studies), posaconazole 0.25 (0.063–2) mg/L (12 studies), and voriconazole 1(0.125–2) mg/L (19 studies); the corresponding values obtained with the EUCAST method were 0.25 (0.12–0.5), 1.25 (1–1.5), 0.5 (0.5–1), 0.125 (0.12–1), and 1 (0.5–1) mg/L, respectively (Figure 2C, Table 1). CLSI ECVs for *A. niger* showed WT cutoffs for amphotericin B, isavuconazole, itraconazole, posaconazole, and voriconazole of ≤2 mg/L, ≤4 mg/L, ≤4 mg/L, ≤2 mg/L, and ≤2 mg/L, respectively [107]. EUCAST ECOFFs and clinical breakpoints indicated some variations, with WT cutoffs of ≤0.5 mg/L for amphotericin B, ≤4 mg/L for isavuconazole, ≤2 for itraconazole, ≤0.5 for posaconazole and ≤2 for voriconazole[108] . The MIC values for isavuconazole, itraconazole, voriconazole, and posaconazole were at or below the ECV, thus, it can be assumed that the isolates were WT strains. The MIC values for amphotericin B exceeded the ECV and were elevated compared with existing MIC distributions.

Susceptibility to antifungal agents of *Aspergillus* isolates

For *A. flavus*, the susceptibility to amphotericin B (12 studies), isavuconazole (4 studies), itraconazole (10 studies), posaconazole (10 studies), and voriconazole (reported in 10 studies) , based on the CLSI method, was 96.75% (6.5–100%), 97.9% (83.2–100%), 100% (7.1–100%), 97.7% (59.7–100%), and 100% (95.8–100%); the corresponding values for amphotericin B (3 studies), isavuconazole (2 studies), itraconazole (4 studies), posaconazole (4 studies), and voriconazole (3 studies), using the EUCAST method, were 96% (30–100%), 98.45% (98–98.9%), 98.55% (80–100%), 99.75% (35–100%), and 100% (60–100%), respectively (Appendix Figure 1A and Appendix Table 2). The resistance is provided in Appendix Figure 2A and Appendix Table 3.

For *A. fumigatus*, the susceptibility (CLSI method) to amphotericin B (12 studies), isavuconazole (5 studies), itraconazole (15 studies), posaconazole (10 studies), and voriconazole (16 studies) was 100% (95.7–100%), 95.1% (88.7–96.2%), 93.7% (83.3–100%), 98% (79.4–100%), and 96.8% (83.3–100%); the corresponding values (EUCAST method) for amphotericin B (2 studies), isavuconazole (1 study), itraconazole (3 studies), posaconazole (2 studies), and voriconazole (reported in 2 studies) were 100% (100%), 91.7% (91.7%), 66.7% (52–100%), 33.3% (33.3%), and 100% (100%), respectively (Appendix Figure 1B and Appendix Table 2). The resistance is provided in Appendix Figure 2B and Appendix Table 3.

For *A. niger*, the susceptibility (CLSI method) to amphotericin B (6 studies), isavuconazole (3 studies), itraconazole (7 studies), posaconazole (7 studies), and voriconazole (8 studies) was 100% (100%), 97.75% (95.7–100%), 96.9% (86–100%), 100% (11–100%), and 98.05% (71–100%); the corresponding values (EUCAST method) for amphotericin B (1 study), itraconazole (1 study), posaconazole (1 study), and voriconazole (1 study) were 80% (80%), 67.5% (67.5%), 50% (50%), and 87.5% (87.5%), respectively (Appendix Figure 1C and Appendix Table 2). The resistance is provided in Appendix Figure 2C and Appendix Table 3.

MIC ranges of antifungal agents for *Aspergillus* isolates

For *A. flavus*, the MIC ranges (CLSI method) were as follows: amphotericin B 0.0125–32 mg/L (32 studies), isavuconazole 0.06–16 mg/L (13 studies), itraconazole 0.03–64 mg/L (31 studies), posaconazole 0.03–4 mg/L (29 studies), and voriconazole 0.03–16 mg/L (33 studies) ; the corresponding ranges (EUCAST method) were as follows: amphotericin B 0.5–32 mg/L(10 studies), isavuconazole 0.125–16 mg/L (8 studies), itraconazole 0.031–16 mg/L (9 studies), posaconazole 0.03–4 mg/L (9 studies), and voriconazole 0.063–16 mg/L (11 studies) (Appendix Table 4).

For *A. fumigatus*, the MIC ranges (CLSI method) were as follows: amphotericin B 0.016–8 mg/L (37 studies), isavuconazole 0.06–32 mg/L (12 studies), itraconazole 0.015–128 mg/L (54 studies), posaconazole 0.008–32 mg/L (46 studies), and voriconazole 0.03–32 mg/L (62 studies) ; the corresponding ranges (EUCAST method) were as follows: amphotericin B 0.015–2 mg/L (8 studies), isavuconazole 0.06–32 mg/L (20 studies), itraconazole 0.015–128 mg/L (54 studies), posaconazole 0.008–32 mg/L (46 studies), and voriconazole 0.03–32 mg/L (62 studies) , respectively (Appendix Table 4).

For *A. niger*, the MIC ranges (CLSI method) were as follows: amphotericin B 0.016–16 mg/L (31 studies), isavuconazole 0.06–16 mg/L (16 studies), itraconazole 0.015–16

mg/L (25 studies), posaconazole 0.002–4 mg/L (18 studies), and voriconazole 0.03–16 mg/L (28 studies); the corresponding ranges (EUCAST method) were as follows: amphotericin B 0.016–16 mg/L (31 studies), isavuconazole 0.06–16 mg/L (16 studies), itraconazole 0.06–16 mg/L (4 studies), posaconazole 0.002–4 mg/L (23 studies), and voriconazole 0.25–2 mg/L (6 studies), respectively (Appendix Table 4).

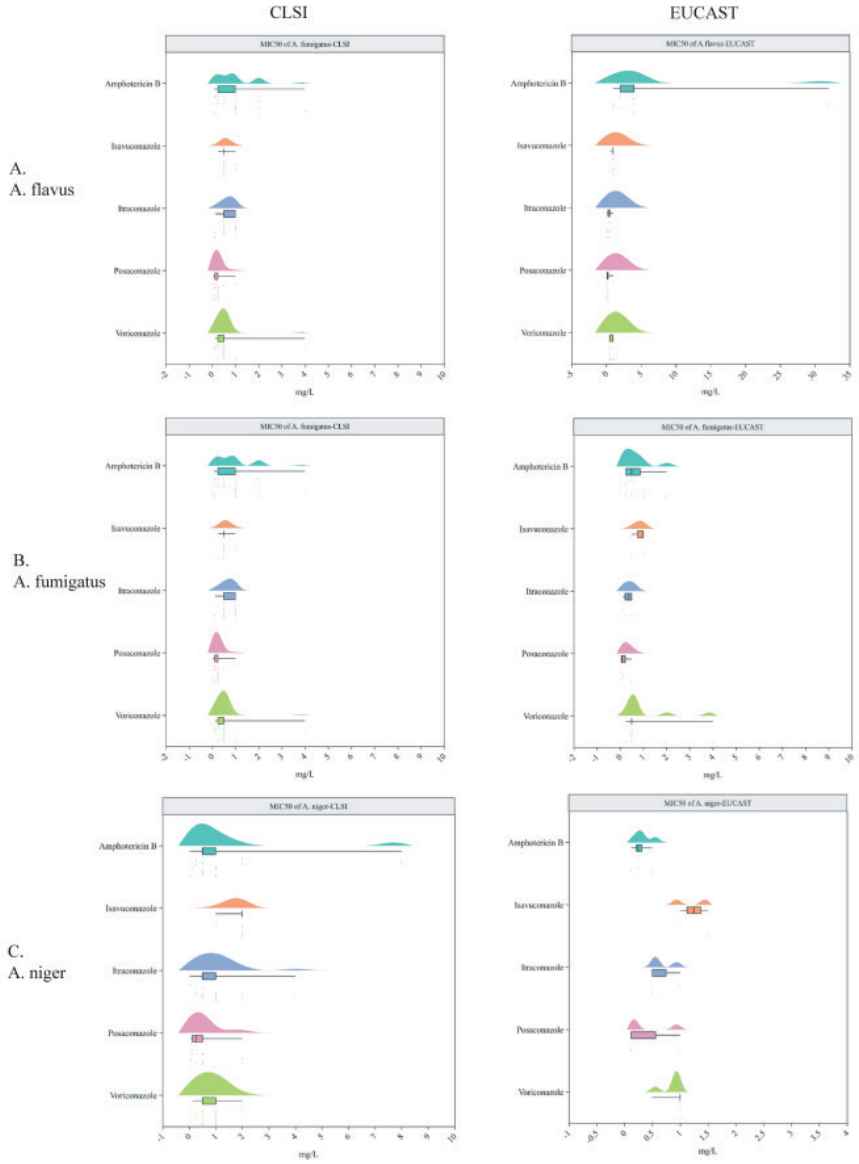

Figure 2. MIC50 (median and range, mg/L) of antifungal agents for *Aspergillus* isolates

Abbreviations: *A. flavus*, *Aspergillus flavus*; *A. fumigatus*, *Aspergillus fumigatus*; *A. niger*, *Aspergillus niger*; CLSI, Clinical and Laboratory Standards Institute; EUCAST, European Committee on Antimicrobial Susceptibility Testing; MIC50, 50% minimun inhibitory concentration.

MIC_{50} of antifungal agents for Mucorales isolates

For *Mucor* spp., the MIC_{50} values of amphotericin B (4 studies), isavuconazole (5 studies), itraconazole (5 studies), posaconazole (6 studies), and voriconazole (5 studies), based on the CLSI method, were 0.375 (0.125–0.5) mg/L, 8 (4–8) mg/L, 4 (0.25–4) mg/L, 1 (0.25–4) mg/L, and 16.25 (0.5–32) mg/L, respectively (Figure 3 A, Table 1). No breakpoints or ECVs have been established for Mucorales, making it challenging to assess WT and non-WT classifications from this data.

For *Rhizomucor* spp., the MIC_{50} values (CLSI method) of amphotericin B (3 studies), isavuconazole (4 studies), itraconazole (2 studies), and posaconazole (4 studies) were 0.375 (0.125–0.5) mg/L, 2 (2) mg/L, 0.5 (0.5–1) mg/L, and 0.5 (0.25–0.5) mg/L, respectively (Figure 3 B, Table 1).

For *Rhizopus* spp., the MIC_{50} values (CLSI method) of amphotericin B (5 studies), isavuconazole (6 studies), itraconazole (5 studies), posaconazole (6 studies), and voriconazole (6 studies) were 0.5 (0.25–1) mg/L, 1 (0.5–2) mg/L, 1 (0.25–2) mg/L, 0.5 (0.25–0.5) mg/L, and 8 (0.5–8) mg/L, respectively (Figure 3 C, Table 1).

MIC ranges of antifungal agents for Mucorales isolates

For *Mucor* spp., the MIC ranges (CLSI method) were as follows: amphotericin B 0.03–8 mg/L (7 studies), isavuconazole 0.5–32 mg/L (6 studies), itraconazole 0.03–32 mg/L (7 studies), posaconazole 0.008–8 mg/L (9 studies), and voriconazole 0.031–32 mg/L (9 studies), respectively (Appendix Table 6).

For *Rhizomucor* spp., the MIC ranges (CLSI method) were as follows: amphotericin B 0.03–1 mg/L (5 studies), isavuconazole 0.06–8 mg/L (6 studies), itraconazole 0.03–4 mg/L (5 studies), posaconazole 0.03–4 mg/L (7 studies), and voriconazole 2–16 mg/L (7 studies), respectively (Appendix Table 6).

For *Rhizopus* spp., the MIC ranges (CLSI method) were as follows: amphotericin B 0.032–32 mg/L (9 studies), isavuconazole 0.125–32 mg/L (7 studies), itraconazole 0.031–32 mg/L (7 studies), posaconazole 0.008–32 mg/L (11 studies), and voriconazole 0.03–32 mg/L (13 studies), respectively (Appendix Table 7). The

corresponding ranges (EUCAST method) were as follows: amphotericin B 0.25–16 mg/L (2 studies), itraconazole 0.25–16 mg/L (2 studies), and voriconazole 2–16 mg/L (2 studies) respectively (Appendix Table 6).

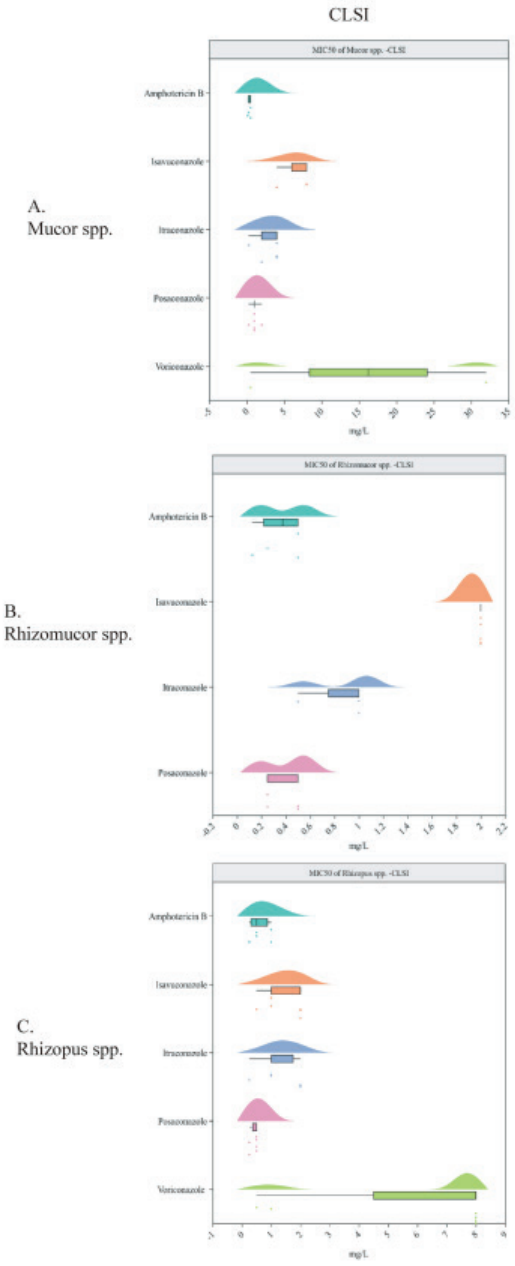

Figure 3. MIC50 (median and range, mg/L) of antifungal agents for Mucorales isolates

Abbreviations: CLSI, Clinical and Laboratory Standards Institute; MIC50, 50% minimun inhibitory concentration.

Susceptibility data among different subgroups

MIC_{50} of antifungal agents for *Aspergillus* spp. and susceptibility of *Aspergillus* spp. isolated from clinical isolates

For *A. flavus*, the MIC_{50} values (CLSI method) were as follows: amphotericin B 2 (0.125–4) mg/L (19 studies), isavuconazole 1 (0.5–2) mg/L (12 studies), itraconazole 0.5 (0.125–16) mg/L (18 studies), posaconazole 0.25 (0.125–0.5) mg/L (19 studies), and voriconazole 0.5 (0.125–1) mg/L (19 studies); the corresponding values (EUCAST method) were as follows: amphotericin B 2.5 (1–32) mg/L (6 studies), isavuconazole 1 (1–1) mg/L (2 studies), itraconazole 0.25 (0.12–1) mg/L (3 studies), posaconazole 0.125 (0.12–1) mg/L (1 study), and voriconazole 0.5 (0.5–1) mg/L (7 studies), respectively (Appendix Figure 3A and Appendix Table 7). For *A. flavus*, the susceptibility (CLSI method) was as follows: amphotericin B 98.55% (6.5–100.0%) (8 studies), isavuconazole 97.9% (83.2–100%) (2 studies), itraconazole 100% (7.1–100%) (9 studies), posaconazole 97.8% (57.9–100%) (9 studies), and voriconazole 100% (95.8–100%) (9 studies), respectively (Appendix Figure 4A and Appendix Table 8). The resistances to the drugs are provided in Appendix Figure 5A and Appendix Table 9.

For *A. fumigatus*, the MIC_{50} values (CLSI method) were as follows: amphotericin B 1 (0.0625–4) mg/L (24 studies), isavuconazole 0.5 (0.25–1) mg/L (14 studies), itraconazole 0.5 (0.125–1) mg/L (34 studies), posaconazole 0.25 (0.03–1) mg/L (31 studies), and voriconazole 0.5 (0.25–4) mg/L (38 studies); the corresponding values (EUCAST method) were as follows: amphotericin B 0.5 (0.25–3.12) mg/L (6 studies), isavuconazole 1 (1–1) mg/L (3 studies), itraconazole 0.5 (0.12–1) mg/L (2 studies), posaconazole 0.125 (0.06–0.5) mg/L (5 studies), and voriconazole 0.75 (0.5–4) mg/L (7 studies), respectively using (Appendix Figure 3B and Appendix Table7). For *A. fumigatus*, the susceptibility (CLSI method) was as follows: amphotericin B 99.85% (95.7–100.0%) (11 studies), isavuconazole 95.1% (88.7–96.2%) (5 studies), itraconazole 93.35% (83.3–100.0%) (14 studies), posaconazole 98% (79.4–100.0%) (10 studies), and voriconazole 96.8% (91.1–100.0%) (15 studies), respectively (Appendix Figure 4B and Appendix Table 8). The resistances are provided in Appendix Figure 5B and Appendix Table 9.

For *A. niger*, the MIC_{50} values (CLSI method) were as follows: amphotericin B 0.5 (0.0312–8) mg/L (18 studies), isavuconazole 2 (1–2) mg/L (6 studies), itraconazole 1

(0.032–4) mg/L (16 studies), posaconazole 0.5 (0.063–2) mg/L (11 studies), and voriconazole 1(0.125–2) mg/L (18 studies); the corresponding values (EUCAST method) were as follows: amphotericin B 0.25 (0.12–6.25) mg/L (4 studies), isavuconazole 1.25 (1–1.5) mg/L (2 studies), itraconazole 0.5 (0.5–1) mg/L (2 studies), posaconazole 0.125 (0.12–1) mg/L (3 studies), and voriconazole 1(0.5–1) mg/L (5 studies) respectively (Appendix Figure 3C and Appendix Table 7). For *A. niger*, the susceptibility (CLSI method) was as follows: amphotericin B 100% (100.0%) (6 studies), isavuconazole 97.75% (95.7–100.0%) (3 studies), itraconazole 96.9% (93.3–100.0%) (7 studies), posaconazole 100% (95.5–100.0%) (7 studies), and voriconazole 99.15% (76.2–100%) (8 studies), respectively (Appendix Figure 4C and Appendix Table 8). The resistances are provided in Appendix Figure 5C and Appendix Table 9.

MIC_{50} of antifungal agents for *Aspergillus* spp. and susceptibility of *Aspergillus* spp. isolated from from environment

The MIC_{50} values of antifungal agents for *Aspergillus* spp. isolated from the environment are provided in Appendix Table 10. Susceptibility and resistance data for these isolates are provided in Appendix Tables 11 and 12, respectively. Analysis with small number of studies on environmental isolates indicated that environmental strains were resistant to itraconazole or posaconazole, but clinical strains were still highly sensitive to itraconazole or posaconazole.

MIC_{50} of antifungal agents for Mucorales and susceptibility of Mucorales isolated from from clinical isolates

For *Mucor* spp., the MIC_{50} values (CLSI method) were as follows: amphotericin B 0.375 (0.125–0.5) mg/L (4 studies), isavuconazole 8 (4–8) mg/L (4 studies), itraconazole 4 (0.25–4) mg/L (2 studies), posaconazole 1 (0.25–2) mg/L (4 studies), and voriconazole 16.25 (0.5–32) mg/L (2 studies), respectively (Appendix Figure 6A and Appendix Table 13).

For *Rhizomucor* spp., the MIC_{50} values (CLSI method) were as follows: amphotericin B 0.375 (0.125–0.5) mg/L (4 studies), isavuconazole 2 (2) mg/L (4 studies), itraconazole 1 (0.5–1) mg/L (2 studies), and posaconazole 0.5 (0.25–0.5) mg/L (4 studies) respectively (Appendix Figure 6B and Appendix Table 13).

For *Rhizopus* spp., the MIC_{50} values (CLSI method) were as follows: amphotericin B 0.5 (0.25–1) mg/L (4 studies), isavuconazole 1 (0.5–2) mg/L (5 studies), itraconazole 1 (0.25–2) mg/L (5 studies), posaconazole 0.5 (0.25–0.5) mg/L (6 studies), and voriconazole 8 (0.5–8) mg/L (6 studies) respectively (Appendix Figure 6C and Appendix Table 13).

For *Mucor* spp., *Rhizomucor* spp., and *Rhizopus* spp., two studies reported resistances to amphotericin B, isavuconazole, itraconazole, posaconazole, and voriconazole. The results were as described previously in "Susceptibility to antifungal agents against Mucorales isolates" (Appendix Table 7).

Discussion

This review included 96 studies from multiple countries or regions. This study comprehensively summarized the MIC_{50}, susceptibility, and resistance of *Aspergillu*s isolates and Mucorales isolates to antifungal agents, including amphotericin B, isavuconazole, itraconazole, posaconazole, and voriconazole, for clinical and environmental *Aspergillu*s isolates and Mucorales isolates, which were most common opportunistic fungal pathogens in clinical practice [109]and a major threat to various patient groups especially those with immunosuppression or immune deficiency [2]. With these data, we provided some detailed important information about antifungal treatment which could be referred to when necessary. MIC_{50} is more commonly used and has been adopted by more studies compared with MIC_{90}. The choice of MIC_{50} can greatly contribute to the estimation of pharmacodynamic target in clinical application. For *A. flavus* and *A. niger*, the MIC values of voriconazole was below the ECV indicating these two fungi were WT strains, while for all three species of *Aspergillus* isolates, a small percentage of the MIC values of amphotericin B exceeded the ECV. However, the existing data was insufficient to compare the MIC_{50} with ECV for Mucorales isolates. We believed that these MIC data for *Aspergillus* isolates would be helpful for clinician to choose reasonable antifungal drugs when facing aspergillosis infection [110].

In this study, it is very interesting and notable that bimodal distributions of MIC for antifungal agents were found in *Aspergillus* isolates and Mucorales isolates. On the Raincloud plots (Figure 2 and Figure 3), bimodal distributions of MIC is significant, especially in *A. niger* isolates, indicating that isolates with a higher MIC are a natural part of the fungus population or a subpopulation with reduced susceptibility to antifungal agents within our collection[111 112]. While *A. fumigatus* distributions are likely to consist predominantly of *A. fumigatus* sensu stricto isolates, given the low prevalence of cryptic species, the distributions of *A. niger* may include larger proportions of other species within the *A. niger* species complex, such as *A. tubingensis*, which are indistinguishable using conventional mycological methods and exhibit differing antifungal susceptibility profiles. As previous study reported, the bimodal distributions may be caused by the methodological differences in the

EUCAST and CLSI MIC, and also generated in the detection procedure by reader to reader and centre to centre variation [113]. Given these observations, further work is required to determine if bimodal MIC patterns is related to the differences in genetic background led to distinct variations and if it is related to the difficulty in clinical treatment.

Breakpoints can categorize an isolate as either susceptible or resistant while the ECVs/ECOFFs can distinguish the WT (no known resistance mechanisms) from the non-WT (harboring resistant mechanisms). There has been a recent rise in non-WT *Aspergillus* isolates, particularly in relation to azoles [114]. Drug resistance is a worrisome and widespread phenomenon which can result in treatment failure and a high fatality rate. A group of experts recommended that changes in treatment practices including prolonging treatment time or multi-drugs combination should be used in areas where the resistance is prevalent [115].

Breakpoints are used to predict whether an antifungal agent will be clinically effective against a particular fungal isolate. They are based on a combination of MIC distributions, ECV or ECOFFs, preclinical and clinical PK/PD, Monte Carlo simulations and PK/PD breakpoints and clinical data, especially from a clinical trial. However, for many fungus-antifungal combinations, these data might never be available. For these combinations, ECVs can provide a methodology for categorizing isolates either WT or non-WT and provide some guidance for treatment [116]. According to the procedures for the development of ECV for antifungal susceptibility testing, for each ECV, data must be acquired from a minimum of three different laboratories, and the data from all three laboratories must meet the criteria for inclusion. Then, Weighting is performed by converting each MIC within each dataset, such that the total in each dataset equals 100 (to be performed by the program used to generate the ECVs). After weighing, the data can then be pooled. For each ECV, a minimum of 100 MIC/minimal effective concentration (MEC) values from 100 individual isolates are needed [107]. There is, to date, no international standard method for selecting ECV or ECOFFs. The definitions of ECOFF by EUCAST are similar but not identical to ECV, where the EUCAST approach is more prescriptive about the analysis. The setting of ECOFFs codifies its approach in the EUCAST Standard Operating Procedure SOP 10.2 [117].

When there are no breakpoints or ECVs established for some antifungal agents, whether the MIC is within the WT population of that specific species or not can only be a reference for clinicians. We should identify the isolates and search relevant literature combing with the patient's clinical symptoms, other etiological results and therapeutic drugs to determine the clinical significance and importance of the species and adjust the medication regimen.

Drug resistance is a major problem in clinical practice for patients with infection [6 118]. As for fungi, the molecular mechanisms of drug resistance mainly involved 1) Target modification: fungi altered the target site to reduce the binding of drugs, 2) Target overexpression: fungi produced more of the binding-receptor to dilute the effect of the drugs, 3) Efflux pumps: individuals actively pumped out the antifungal agent to reduce intracellular concentration, 4) Biochemical target alteration: fungi produced alternative enzymes that can replace the target of the antifungal, and 5) Metabolic inactivation: infected patients break down the antifungal agent through metabolic pathways [118-121]. In the present study, we listed susceptibility and resistance according to both CLSI method or EUCAST method. These two methods have significant difference in their approaches and methodologies [122 123]. CLSI currently only defined a clinical breakpoint for voriconazole for *A. fumigatus* and reports ECVs for the other Aspergillus species and drugs to differentiate between wild-type and non-wild-type strains, while EUCAST has set breakpoints for several *Aspergillus* species that classify isolates as susceptible or resistant. The conditions for antifungal susceptibility testing, such as temperature and incubation times are different between CLSI and EUCAST. Meanwhile, EUCAST breakpoints are often more stringent than CLSI' s, leading to differences in susceptibility classification. Unlike CLSI, EUCAST has eliminated the intermediate category for some drugs, which might impact the agreement between the two [124 125]. In our study, the data of susceptibility and resistance were slightly different between these two different methods especially in MIC values and MIC ranges. However, the results of variation trends in susceptibility and resistance and the identification of non-WT and WT were basically consistent. The summary also showed that the general susceptibility of *Aspergillus* isolates to antifungal agents using CLSI method or EUCAST method were similar, and the resistance rate of *Aspergillus* isolates to amphotericin B was probably the lowest when compared with other drugs. However, we found no qualified data reporting drug sensitivity in Mucorales isolates as there are no clinical breakpoints for either CLSI or EUCAST.

We also presented the MIC ranges of antifungal agents for *Aspergillus* isolates and Mucorales isolates in detail. From the results we listed, we can see that the ranges were wide with upper limit as hundreds or thousands of times of lower limit, indicating that even for the same kind of fungus, the MIC might be significantly different due to different studies, isolates, population, and laboratory conditions. These results of MIC ranges provided references for clinicians and investigator to evaluate the performance of a specific antifungal agent.

Further, we summarized the MIC_{50} (CLSI method and EUCAST method) of antifungal agents for clinical isolates. And the results showed that the two methods also resulted in similar MIC_{50} values which were consistent with those for whole isolates. We also summarized the susceptibility of clinical isolates (CLSI method) to antifungal agents, which was similar with general susceptibility described before. The results suggested that most clinical *Aspergillus* isolates of all three species were sensitive to the five antifungal agents, which was consistent with previous studies [126-128]. As for resistance of clinical *Aspergillus* isolates to antifungal agents, voriconazole showed better performance, especially in *A. flavus* isolates [129].

Aspergillosis or mucormycosis is an infectious disease for which person-to-person transmission seems unlikely. Patients likely become infected by inhaling strains present in the environment [130]. The environmental route probably plays an important role in the emergence of resistant strains [131]. The drug-resistant mutations were first found in environmental strains and later found in clinical strains. Indeed, no previous azole treatment was reported for 50% to 71% of aspergillosis cases caused by azole resistant strains [132 133]. We summarized the MIC_{50} of antifungal agents for *Aspergillus* isolated from environment and the susceptibility and resistance of these isolates to drugs. The limited data in our study revealed that environmental strains were resistant to itraconazole or posaconazole, but clinical strains were still highly sensitive to itraconazole or posaconazole. Previous reports had rise the hypothesis that exposure of *Aspergillus* to azole fungicides in the environment causes cross-resistance to medical triazoles, indicating environmental route of resistance selection[134 135] Notably, long-term prophylactic exposure to posaconazole showed no evidence for the emergence of resistance in patients at high risk for invasive aspergillisuis [136]. The cases of triazole resistance in this patient group are all associated with environmental resistance selection[137]. In contract, resistance selection has been described in patients with long-term treatment for chronic pulmonary aspergillosis, especially those with cavitary disease[138].The study emphasises the need of continued surveillance of resistance in environmental and clinical strains. It is thus essential to pay attention to the screening of environmental

resistant strains and the collecting of patients' personal contact history, occupation and trauma history.

This study has the following strengths: firstly, the search strategy was developed by professional information specialists; we established a study selection process with strict inclusion and exclusion criteria, then we searched both electronic databases and the references of relevant systematic reviews; secondly, the study screening and data extraction were independently conducted by two researchers to minimize bias. The efficacy of antifungal agents in treating aspergillosis and mucormycosis patients and the resistance of the isolates were first analyzed by a systematic review of the relevant field. Similarly to other studies, our systematic review also has some limitations. For example, no breakpoints or ECVs or ECOFFs have been established for any antifungal agent against Mucorales; therefore, emerging resistance and susceptibility to the agents cannot be evaluated from the descriptive data. Due to insufficient data, we failed to analyze the differences in the MIC and in vitro susceptibility of antifungal agents against *Aspergillus* spp. or Mucorales, and their resistances to the drugs, between environmental and clinical isolates. Overall, the target studies and results were heterogeneous, meaning that broad, summary conclusions could not be made.

This review provides insights into the susceptibility and resistance of fungi to different antifungal agents, which is essential for the prompt and efficient treatment of patients with aspergillosis and mucormycosis and for improving the outcome of such infections. Some of our estimates might deserve special attention, particularly the evaluation of resistance of antifungal agents against *Aspergillus* spp. or Mucorales. Although we estimated a relatively low prevalence of resistance of fungi to different antifungal agents, the rates of deaths in which resistant aspergillosis or mucormycosis infection was so much greater in immunocompromised patients. Correct detection

of resistant *Aspergillus* spp. or Mucorales isolates is for obvious reasons crucial to avoid inappropriate treatment in clinical practice. In the future, it will be imperative to bolster the development of novel diagnostic techniques to ensure early, precise, and rapid detection of clinical drug-resistant fungal strains. Further clinical breakpoints and epidemiological cutoff values must be established urgently for filamentous fungi, especially for the Mucorales, and antifungal agents. Using cutoff values, we can compare and analyze the susceptibility data and the resistance of *Aspergillus* spp. or Mucorales to antifungal agents. Sufficient data from studies with larger sample sizes will be required to compare the susceptibility profiles of

environmental and clinical isolates and to analyze their resistance to antifungal agents in different patient populations.

Conclusion

Descriptive data of MIC, susceptibility, and resistance revealed that, compared with existing MIC distributions and breakpoints or ECVs established by CLSI or EUCAST, for *A. flavus*, the posaconazole and voriconazole MIC values were at or below the ECV, indicating that the isolates were WT strains, but amphotericin B, isavuconazole, and itraconazole MIC values for a small proportion of the strains were elevated; for *A. fumigatus*, isavuconazole and itraconazole MIC values were within ECV limits, indicating that the isolates were WT strains, but amphotericin B, posaconazole, and voriconazole MIC values for a small proportion of the strains were elevated; and for *A. niger*, isavuconazole, itraconazole, voriconazole, and posaconazole MIC values were within ECV limits, indicating that the isolates were WT strains, but amphotericin B MIC values for a small proportion of the strains were elevated. In addition, *A. flavus* had consistently high in vitro susceptibility to voriconazole. *A. fumigatus* and *A. niger* had consistently high in vitro susceptibility to amphotericin B, which had low resistance to the drug.

References

1. Leroux S, Ullmann AJ. Management and diagnostic guidelines for fungal diseases in infectious diseases and clinical microbiology: critical appraisal. *Clinical microbiology and infection : the official publication of the European Society of Clinical Microbiology and Infectious Diseases* 2013;19(12):1115-21. doi: 10.1111/1469-0691.12426.
2. Denning DW. Global incidence and mortality of severe fungal disease. *The Lancet Infectious diseases* 2024;24(7):e428-e38. doi: 10.1016/s1473-3099(23)00692-8.
3. Rybak JM, Fortwendel JR, Rogers PD. Emerging threat of triazole-resistant Aspergillus fumigatus. *The Journal of antimicrobial chemotherapy* 2019;74(4):835-42. doi: 10.1093/jac/dky517.
4. Prakash H, Chakrabarti A. Global Epidemiology of Mucormycosis. *Journal of fungi (Basel, Switzerland)* 2019;5(1) doi: 10.3390/jof5010026.
5. Cornely OA, Alastruey-Izquierdo A, Arenz D, et al. Global guideline for the diagnosis and management of mucormycosis: an initiative of the European Confederation of Medical Mycology in cooperation with the Mycoses Study Group Education and Research Consortium. *The Lancet Infectious diseases* 2019;19(12):e405-e21. doi: 10.1016/s1473-3099(19)30312-3.
6. Perlin DS, Rautemaa-Richardson R, Alastruey-Izquierdo A. The global problem of antifungal resistance: prevalence, mechanisms, and management. *The Lancet Infectious diseases* 2017;17(12):e383-e92. doi: 10.1016/s1473-3099(17)30316-x.
7. Verweij PE, Snelders E, Kema GH, et al. Azole resistance in Aspergillus fumigatus: a side-effect of environmental fungicide use? *The Lancet Infectious diseases* 2009;9(12):789-95. doi: 10.1016/s1473-3099(09)70265-8.
8. Snelders E, Melchers WJ, Verweij PE. Azole resistance in Aspergillus fumigatus: a new challenge in the management of invasive aspergillosis? *Future microbiology* 2011;6(3):335-47. doi: 10.2217/fmb.11.4.
9. Tricco AC, Lillie E, Zarin W, et al. PRISMA extension for scoping reviews (PRISMA-ScR): checklist and explanation. *Annals of internal medicine* 2018;169(7):467-73.
10. Astvad KMT, Arikan-Akdagli S, Arendrup MC. A Pragmatic Approach to Susceptibility Classification of Yeasts without EUCAST Clinical Breakpoints. *Journal of fungi (Basel, Switzerland)* 2022;8(2) doi: 10.3390/jof8020141.
11. Abastabar M, Haghani I, Shokohi T, et al. Low in vitro antifungal activity of tavaborole against yeasts and molds from onychomycosis. *Antimicrob Agents Chemother* 2018;62(12) doi: 10.1128/aac.01632-18.

12. Alastruey-Izquierdo A, Alcazar-Fuoli L, Rivero-Menéndez O, et al. Molecular Identification and Susceptibility Testing of Molds Isolated in a Prospective Surveillance of Triazole Resistance in Spain (FILPOP2 Study). *Antimicrob Agents Chemother* 2018;62(9) doi: 10.1128/aac.00358-18.
13. Alastruey-Izquierdo A, Mellado E, Peláez T, et al. Population-based survey of filamentous fungi and antifungal resistance in Spain (FILPOP Study). *Antimicrob Agents Chemother* 2013;57(7):3380-7. doi: 10.1128/aac.00383-13.
14. Arendrup MC, Jensen RH, Cuenca-Estrella M. In Vitro Activity of ASP2397 against Aspergillus Isolates with or without Acquired Azole Resistance Mechanisms. *Antimicrob Agents Chemother* 2016;60(1):532-6. doi: 10.1128/aac.02336-15.
15. Assress HA, Selvarajan R, Nyoni H, et al. Azole antifungal resistance in fungal isolates from wastewater treatment plant effluents. *Environ Sci Pollut Res Int* 2021;28(3):3217-29. doi: 10.1007/s11356-020-10688-1.
16. Astvad KMT, Hare RK, Arendrup MC. Evaluation of the in vitro activity of isavuconazole and comparator voriconazole against 2635 contemporary clinical Candida and Aspergillus isolates. *Clin Microbiol Infect* 2017;23(11):882-87. doi: 10.1016/j.cmi.2017.03.023.
17. Badali H, Cañete-Gibas C, McCarthy D, et al. Epidemiology and Antifungal Susceptibilities of Mucoralean Fungi in Clinical Samples from the United States. *J Clin Microbiol* 2021;59(9):e0123021. doi: 10.1128/jcm.01230-21.
18. Badali H, Fakhim H, Zarei F, et al. In Vitro Activities of Five Antifungal Drugs Against Opportunistic Agents of Aspergillus Nigri Complex. *Mycopathologia* 2016;181(3-4):235-40. doi: 10.1007/s11046-015-9968-0.
19. Borman AM, Fraser M, Patterson Z, et al. In Vitro Antifungal Drug Resistance Profiles of Clinically Relevant Members of the Mucorales (Mucoromycota) Especially with the Newer Triazoles. *J Fungi (Basel)* 2021;7(4) doi: 10.3390/jof7040271.
20. Bustamante B, Illescas LR, Posadas A, et al. Azole resistance among clinical isolates of Aspergillus fumigatus in Lima-Peru. *Med Mycol* 2020;58(1):54-60. doi: 10.1093/mmy/myz032.
21. Carvalhaes CG, Klauer AL, Rhomberg PR, et al. Evaluation of Rezafungin Provisional CLSI Clinical Breakpoints and Epidemiological Cutoff Values Tested against a Worldwide Collection of Contemporaneous Invasive Fungal Isolates (2019 to 2020). *J Clin Microbiol* 2022;60(4):e0244921. doi: 10.1128/jcm.02449-21.
22. Carvalhaes CG, Rhomberg PR, Huband MD, et al. Antifungal Activity of Isavuconazole and Comparator Agents against Contemporaneous Mucorales

Isolates from USA, Europe, and Asia-Pacific. *J Fungi (Basel)* 2023;9(2) doi: 10.3390/jof9020241.
23. Carvalhaes CG, Rhomberg PR, Pfaller M, et al. Comparative activity of posaconazole and systemic azole agents against clinical isolates of filamentous fungi from a global surveillance programme. *JAC Antimicrob Resist* 2021;3(2):dlab088. doi: 10.1093/jacamr/dlab088.
24. Cascio GL, Bazaj A, Trovato L, et al. Multicenter Italian Study on "In Vitro Activities" of Isavuconazole, Voriconazole, Amphotericin B, and Caspofungin for Aspergillus Species: Comparison between Sensititre™ YeastOne™ and MIC Test Strip. *Infect Drug Resist* 2022;15((Cascio G.L., g.locascio@ausl.pc.it; Bazaj A.) Clinical Microbiology and Virology Unit, Azienda Ospedaliera Universitaria Integrata, Verona, Italy):5839-48. doi: 10.2147/idr.s367082.
25. Castanheira M, Messer SA, Rhomberg PR, et al. Antifungal susceptibility patterns of a global collection of fungal isolates: results of the SENTRY Antifungal Surveillance Program (2013). *Diagn Microbiol Infect Dis* 2016;85(2):200-4. doi: 10.1016/j.diagmicrobio.2016.02.009.
26. Colozza C, Posteraro B, Santilli S, et al. In vitro activities of amphotericin B and AmBisome against Aspergillus isolates recovered from Italian patients treated for haematological malignancies. *Int J Antimicrob Agents* 2012;39(5):440-3. doi: 10.1016/j.ijantimicag.2012.01.013.
27. Denardi LB, Keller JT, de Azevedo MI, et al. Comparison Between Etest and Broth Microdilution Methods for Testing Itraconazole-Resistant Aspergillus fumigatus Susceptibility to Antifungal Combinations. *Mycopathologia* 2018;183(2):359-70. doi: 10.1007/s11046-017-0208-7.
28. Deng S, Zhang L, Ji Y, et al. Triazole phenotypes and genotypic characterization of clinical Aspergillus fumigatus isolates in China. *Emerg Microbes Infect* 2017;6(12):e109. doi: 10.1038/emi.2017.97.
29. Drogari-Apiranthitou M, Mantopoulou FD, Skiada A, et al. In vitro antifungal susceptibility of filamentous fungi causing rare infections: synergy testing of amphotericin B, posaconazole and anidulafungin in pairs. *J Antimicrob Chemother* 2012;67(8):1937-40. doi: 10.1093/jac/dks137.
30. Duong TMN, Nguyen PT, Le TV, et al. Drug-Resistant Aspergillus flavus Is Highly Prevalent in the Environment of Vietnam: A New Challenge for the Management of Aspergillosis? *J Fungi (Basel)* 2020;6(4) doi: 10.3390/jof6040296.
31. Erami M, Hashemi SJ, Raiesi O, et al. COVID-19-associated pulmonary aspergillosis (CAPA) in Iranian patients admitted with severe COVID-19 pneumonia. *Infection* 2023;51(1):223-30. doi: 10.1007/s15010-022-01907-7.

32. Escribano P, Peláez T, Muñoz P, et al. Is azole resistance in Aspergillus fumigatus a problem in Spain? *Antimicrob Agents Chemother* 2013;57(6):2815-20. doi: 10.1128/aac.02487-12.
33. Espinel-Ingroff A, Chowdhary A, Gonzalez GM, et al. Multicenter study of isavuconazole MIC distributions and epidemiological cutoff values for Aspergillus spp. for the CLSI M38-A2 broth microdilution method. *Antimicrob Agents Chemother* 2013;57(8):3823-8. doi: 10.1128/aac.00636-13.
34. Fattahi A, Zaini F, Kordbacheh P, et al. In vitro susceptibility of aflatoxigenic and non-aflatoxigenic Aspergillus flavus strains to conventional antifungal agents. *Acta Med Iran* 2012;50(12):798-804.
35. Gajjar DU, Pal AK, Ghodadra BK, et al. Microscopic evaluation, molecular identification, antifungal susceptibility, and clinical outcomes in fusarium, aspergillus and, dematiaceous keratitis. *Biomed Res Int* 2013;2013((Gajjar D.U., devarshimistry@yahoo.com) Department of Microbiology and Biotechnology Centre, Faculty of Science, M. S. University of Baroda, Vadodara 390 002, India) doi: 10.1155/2013/605308.
36. Halvaeezadeh M, Jalaee GA, Fatahinia M, et al. Aspergillus welwitschiae; an otomycosis predominant agent, new epidemiological and antifungal susceptibility data from Iran. *Microb Pathog* 2023;181:106180. doi: 10.1016/j.micpath.2023.106180.
37. Hivary S, Fatahinia M, Halvaeezadeh M, et al. The potency of luliconazole against clinical and environmental Aspergillus nigri complex. *Iran J Microbiol* 2019;11(6):510-19.
38. Hsu TH, Huang PY, Fan YC, et al. Azole Resistance and cyp51A Mutation of Aspergillus fumigatus in a Tertiary Referral Hospital in Taiwan. *J Fungi (Basel)* 2022;8(9) doi: 10.3390/jof8090908.
39. Jafarian H, Amanati A, Badiee P. Antifungal activity of Taurolidine against Mucorales: An in vitro study on clinical isolates. *Curr Med Mycol* 2022;8(1):26-31. doi: 10.18502/cmm.8.1.9211.
40. Jing R, Morrissey I, Xiao M, et al. In vitro Activity of Isavuconazole and Comparators Against Clinical Isolates of Molds from a Multicenter Study in China. *Infect Drug Resist* 2022;15:2101-13. doi: 10.2147/idr.s360191.
41. Jing R, Yang WH, Xiao M, et al. Species identification and antifungal susceptibility testing of Aspergillus strains isolated from patients with otomycosis in northern China. *J Microbiol Immunol Infect* 2022;55(2):282-90. doi: 10.1016/j.jmii.2021.03.011.

42. Kachuei R, Khodavaisy S, Rezaie S, et al. In vitro antifungal susceptibility of clinical species belonging to Aspergillus genus and Rhizopus oryzae. *J Mycol Med* 2016;26(1):17-21. doi: 10.1016/j.mycmed.2015.12.002.
43. Khodavaisy S, Badali H, Hashemi SJ, et al. In vitro activities of five antifungal agents against 199 clinical and environmental isolates of Aspergillus flavus, an opportunistic fungal pathogen. *J Mycol Med* 2016;26(2):116-21. doi: 10.1016/j.mycmed.2016.01.002.
44. Khojasteh S, Abastabar M, Haghani I, et al. Five-year surveillance study of clinical and environmental Triazole-Resistant Aspergillus fumigatus isolates in Iran. *Mycoses* 2023;66(2):98-105. doi: 10.1111/myc.13535.
45. Kikuchi K, Watanabe A, Ito J, et al. Antifungal susceptibility of Aspergillus fumigatus clinical isolates collected from various areas in Japan. *J Infect Chemother* 2014;20(5):336-8. doi: 10.1016/j.jiac.2014.01.003.
46. Kirchhoff L, Braun LM, Schmidt D, et al. COVID-19-associated pulmonary aspergillosis in ICU patients in a German reference centre: Phenotypic and molecular characterisation of Aspergillus fumigatus isolates. *Mycoses* 2022;65(4):458-65. doi: 10.1111/myc.13430.
47. Kordalewska M, Guerrero KD, Garcia-Rubio R, et al. Antifungal Drug Susceptibility and Genetic Characterization of Fungi Recovered from COVID-19 Patients. *J Fungi (Basel)* 2021;7(7) doi: 10.3390/jof7070552.
48. Lei G, Dan H, Jinhua L, et al. Berberine and itraconazole are not synergistic in vitro against Aspergillus fumigatus isolated from clinical patients. *Molecules* 2011;16(11):9218-33. doi: 10.3390/molecules16119218.
49. Li Y, Wang H, Xu YC, et al. Antifungal susceptibility of clinical isolates of 23 genetically confirmed Aspergillus species collected from Taiwan and Mainland China. *Int J Antimicrob Agents* 2017;50((Li Y.; Wang H.; Xu Y.-C.) Department of Clinical Laboratory, Peking Union Medical College Hospital, Peking Union Medical College, Beijing, China):S31-S32.
50. Manikandan P, Abdel-Hadi A, Randhir Babu Singh Y, et al. Fungal Keratitis: Epidemiology, Rapid Detection, and Antifungal Susceptibilities of Fusarium and Aspergillus Isolates from Corneal Scrapings. *Biomed Res Int* 2019;2019:6395840. doi: 10.1155/2019/6395840.
51. Meletiadis J, Mavridou E, Melchers WJ, et al. Epidemiological cutoff values for azoles and Aspergillus fumigatus based on a novel mathematical approach incorporating cyp51A sequence analysis. *Antimicrob Agents Chemother* 2012;56(5):2524-9. doi: 10.1128/aac.05959-11.
52. Melhem MSC, Coelho VC, Fonseca CA, et al. Evaluation of the Sensititre YeastOne and Etest in Comparison with CLSI M38-A2 for Antifungal

Susceptibility Testing of Three Azoles, Amphotericin B, Caspofungin, and Anidulafungin, against Aspergillusfumigatus and Other Species, Using New Clinical Breakpoints and Epidemiological Cutoff Values. *Pharmaceutics* 2022;14(10) doi: 10.3390/pharmaceutics14102161.

53. Messer SA, Carvalhaes CG, Castanheira M, et al. In vitro activity of isavuconazole versus opportunistic filamentous fungal pathogens from the SENTRY Antifungal Surveillance Program, 2017-2018. *Diagn Microbiol Infect Dis* 2020;97(1):115007. doi: 10.1016/j.diagmicrobio.2020.115007.
54. Moazeni M, Aslani N, Nabili M, et al. Overexpression of Efflux Pump Genes is an Alternative Mechanism in Voriconazole Resistant Aspergillus fumigatus isolates Without Relative Mutations in CYP5A. *Infect Disord Drug Targets* 2020;20(6):860-66. doi: 10.2174/1871526519666191119123135.
55. Mohammadi F, Hashemi SJ, Zoll J, et al. Quantitative Analysis of Single-Nucleotide Polymorphism for Rapid Detection of TR34/L98H- and TR46/Y121F/T289A-Positive Aspergillus fumigatus Isolates Obtained from Patients in Iran from 2010 to 2014. *Antimicrob Agents Chemother* 2016;60(1):387-92. doi: 10.1128/aac.02326-15.
56. Monteiro C, Pinheiro D, Maia M, et al. Aspergillus species collected from environmental air samples in Portugal-molecular identification, antifungal susceptibility and sequencing of cyp51A gene on A. fumigatus sensu stricto itraconazole resistant. *J Appl Microbiol* 2019;126(4):1140-48. doi: 10.1111/jam.14217.
57. Nayak N, Satpathy G, Prasad S, et al. Molecular characterization of drug-resistant and drug-sensitive Aspergillus isolates causing infectious keratitis. *Indian J Ophthalmol* 2011;59(5):373-7. doi: 10.4103/0301-4738.83614.
58. Negri CE, Gonçalves SS, Sousa ACP, et al. Triazole Resistance Is Still Not Emerging in Aspergillus fumigatus Isolates Causing Invasive Aspergillosis in Brazilian Patients. *Antimicrob Agents Chemother* 2017;61(11) doi: 10.1128/aac.00608-17.
59. Onder S, Oz Y. In Vitro Effects of Farnesol Alone and in Combination with Antifungal Drugs Against Aspergillus Clinical Isolates. *Med Mycol J* 2021;62(1):5-10. doi: 10.3314/mmj.20-00016.
60. Osman M, Bidon B, Abboud C, et al. Species distribution and antifungal susceptibility of Aspergillus clinical isolates in Lebanon. *Future Microbiol* 2021;16(1):13-26. doi: 10.2217/fmb-2020-0141.
61. Pfaller MA, Carvalhaes CG, DeVries S, et al. Impact of COVID-19 on the antifungal susceptibility profiles of isolates collected in a global surveillance program that monitors invasive fungal infections. *Med Mycol* 2022;60(5) doi: 10.1093/mmy/myac028.

62. Pfaller MA, Carvalhaes CG, Messer SA, et al. In vitro activity of posaconazole and comparators versus opportunistic filamentous fungal pathogens globally collected during 8 years. *Diagn Microbiol Infect Dis* 2021;101(3):115473. doi: 10.1016/j.diagmicrobio.2021.115473.
63. Pfaller MA, Carvalhaes CG, Rhomberg P, et al. Antifungal susceptibilities of opportunistic filamentous fungal pathogens from the Asia and Western Pacific Region: data from the SENTRY Antifungal Surveillance Program (2011-2019). *J Antibiot (Tokyo)* 2021;74(8):519-27. doi: 10.1038/s41429-021-00431-4.
64. Pfaller MA, Castanheira M, Messer SA, et al. In vitro antifungal susceptibilities of isolates of Candida spp. and Aspergillus spp. from China to nine systemically active antifungal agents: data from the SENTRY antifungal surveillance program, 2010 through 2012. *Mycoses* 2015;58(4):209-14. doi: 10.1111/myc.12299.
65. Pfaller MA, Castanheira M, Messer SA, et al. Echinocandin and triazole antifungal susceptibility profiles for Candida spp., Cryptococcus neoformans, and Aspergillus fumigatus: application of new CLSI clinical breakpoints and epidemiologic cutoff values to characterize resistance in the SENTRY Antimicrobial Surveillance Program (2009). *Diagn Microbiol Infect Dis* 2011;69(1):45-50. doi: 10.1016/j.diagmicrobio.2010.08.013.
66. Pfaller MA, Huband MD, Rhomberg PR, et al. Activities of Manogepix and Comparators against 1,435 Recent Fungal Isolates Collected during an International Surveillance Program (2020). *Antimicrob Agents Chemother* 2022;66(11):e0102822. doi: 10.1128/aac.01028-22.
67. Pfaller MA, Messer SA, Jones RN, et al. Antifungal susceptibilities of Candida, Cryptococcus neoformans and Aspergillus fumigatus from the Asia and Western Pacific region: data from the SENTRY antifungal surveillance program (2010-2012). *J Antibiot (Tokyo)* 2015;68(9):556-61. doi: 10.1038/ja.2015.29.
68. Pfaller MA, Messer SA, Motyl MR, et al. In vitro activity of a new oral glucan synthase inhibitor (MK-3118) tested against Aspergillus spp. by CLSI and EUCAST broth microdilution methods. *Antimicrob Agents Chemother* 2013;57(2):1065-8. doi: 10.1128/aac.01588-12.
69. Pfaller MA, Rhomberg PR, Messer SA, et al. Isavuconazole, micafungin, and 8 comparator antifungal agents' susceptibility profiles for common and uncommon opportunistic fungi collected in 2013: Temporal analysis of antifungal drug resistance using CLSI species-specific clinical breakpoints and proposed epidemiological cutoff values. *Diagn Microbiol Infect Dis* 2015;82(4):303-13. doi: 10.1016/j.diagmicrobio.2015.04.008.
70. Pfaller MA, Rhomberg PR, Wiederhold NP, et al. In Vitro Activity of Isavuconazole against Opportunistic Fungal Pathogens from Two Mycology

Reference Laboratories. *Antimicrob Agents Chemother* 2018;62(10) doi: 10.1128/aac.01230-18.
71. Pinto E, Monteiro C, Maia M, et al. Aspergillus Species and Antifungals Susceptibility in Clinical Setting in the North of Portugal: Cryptic Species and Emerging Azoles Resistance in A. fumigatus. *Front Microbiol* 2018;9:1656. doi: 10.3389/fmicb.2018.01656.
72. Rath S, Das SR, Padhy RN. Bayesian analysis of two methods MALDI-TOF-MS system and culture test in otomycosis infection. *World J Otorhinolaryngol Head Neck Surg* 2019;5(1):6-13. doi: 10.1016/j.wjorl.2018.03.006.
73. Reichert-Lima F, Lyra L, Pontes L, et al. Surveillance for azoles resistance in Aspergillus spp. highlights a high number of amphotericin B-resistant isolates. *Mycoses* 2018;61(6):360-65. doi: 10.1111/myc.12759.
74. Rivero-Menendez O, Soto-Debran JC, Cuenca-Estrella M, et al. In Vitro Activity of Ibrexafungerp against a Collection of Clinical Isolates of Aspergillus, Including Cryptic Species and Cyp51A Mutants, Using EUCAST and CLSI Methodologies. *J Fungi (Basel)* 2021;7(3) doi: 10.3390/jof7030232.
75. Roohi B, Nemati S, Alipour A, et al. Otomycosis: The foremost aetiological agent causing otitis externa and the antifungal susceptibility pattern in North-Western Iran. *Mycoses* 2023;66(2):87-97. doi: 10.1111/myc.13532.
76. Rudramurthy SM, Chakrabarti A, Geertsen E, et al. In vitro activity of isavuconazole against 208 Aspergillus flavus isolates in comparison with 7 other antifungal agents: assessment according to the methodology of the European Committee on Antimicrobial Susceptibility Testing. *Diagn Microbiol Infect Dis* 2011;71(4):370-7. doi: 10.1016/j.diagmicrobio.2011.08.006.
77. Sağıroğlu P, Nedret Koç A, Atalay MA, et al. Mucormycosis experience through the eyes of the laboratory. *Infect Dis (Lond)* 2019;51(10):730-37. doi: 10.1080/23744235.2019.1645962.
78. Sarigüzel FM, Koç AN, Sağiroğlu P, et al. Molecular epidemiology and antifungal susceptibilities of Aspergillus species isolated from patients with invasive aspergillosis. *Rev Assoc Med Bras (1992)* 2023;69(1):44-50. doi: 10.1590/1806-9282.20220441.
79. Schwarz P, Djenontin E, Dannaoui E. Colistin and Isavuconazole Interact Synergistically In Vitro against Aspergillus nidulans and Aspergillus niger. *Microorganisms* 2020;8(9) doi: 10.3390/microorganisms8091447.
80. Sheba E, Sharma S, Kumar Mishra D, et al. Microbiology Profile of COVID-19-Associated Rhino-Orbital Mucormycosis Pathogens in South India. *Am J Trop Med Hyg* 2023;108(2):377-83. doi: 10.4269/ajtmh.22-0411.

81. Shivaprakash MR, Geertsen E, Chakrabarti A, et al. In vitro susceptibility of 188 clinical and environmental isolates of Aspergillus flavus for the new triazole isavuconazole and seven other antifungal drugs. *Mycoses* 2011;54(5):e583-9. doi: 10.1111/j.1439-0507.2010.01996.x.
82. Singh A, Singh P, Meis JF, et al. In vitro activity of the novel antifungal olorofim against dermatophytes and opportunistic moulds including Penicillium and Talaromyces species. *J Antimicrob Chemother* 2021;76(5):1229-33. doi: 10.1093/jac/dkaa562.
83. Soleimani M, Salehi Z, Fattahi A, et al. Ocular fungi: Molecular identification and antifungal susceptibility pattern to azoles. *Jundishapur J Microbiol* 2020;13(3) doi: 10.5812/jjm.99922.
84. Stewart AG, Isler B, Simos P, et al. Aspergillus Species Causing Invasive Fungal Disease in Queensland, Australia. *Mycopathologia* 2023 doi: 10.1007/s11046-023-00713-5.
85. Szigeti G, Sedaghati E, Mahmoudabadi AZ, et al. Species assignment and antifungal susceptibilities of black aspergilli recovered from otomycosis cases in Iran and Hungary. *Acta Microbiologica et Immunologica Hungarica* 2011;58((Szigeti G.; Kocsubé S.; Vágvölgyi C.S.; Varga J.) Department of Microbiology, Faculty of Science and Informatics, University of Szeged, Szeged, Hungary):224. doi: 10.1556/AMicr.58.2011.Suppl.2.
86. Taghizadeh-Armaki M, Hedayati MT, Ansari S, et al. Genetic Diversity and In Vitro Antifungal Susceptibility of 200 Clinical and Environmental Aspergillus flavus Isolates. *Antimicrob Agents Chemother* 2017;61(5) doi: 10.1128/aac.00004-17.
87. Takazono T, Ito Y, Tashiro M, et al. Transition of triazole-resistant Aspergillus fumigatus isolates in a Japanese tertiary hospital and subsequent genetic analysis. *J Infect Chemother* 2021;27(3):537-39. doi: 10.1016/j.jiac.2020.11.027.
88. Toyotome T, Fujiwara T, Kida H, et al. Azole susceptibility in clinical and environmental isolates of Aspergillus fumigatus from eastern Hokkaido, Japan. *J Infect Chemother* 2016;22(9):648-50. doi: 10.1016/j.jiac.2016.03.002.
89. Toyotome T, Saito S, Koshizaki Y, et al. Prospective survey of Aspergillus species isolated from clinical specimens and their antifungal susceptibility: A five-year single-center study in Japan. *J Infect Chemother* 2020;26(2):321-23. doi: 10.1016/j.jiac.2019.09.002.
90. Trovato L, Scalia G, Domina M, et al. Environmental Isolates of Multi-Azole-Resistant Aspergillus spp. in Southern Italy. *J Fungi (Basel)* 2018;4(4) doi: 10.3390/jof4040131.

91. Tsuchido Y, Tanaka M, Nakano S, et al. Prospective multicenter surveillance of clinically isolated Aspergillus species revealed azole-resistant Aspergillus fumigatus isolates with TR34/L98H mutation in the Kyoto and Shiga regions of Japan. *Med Mycol* 2019;57(8):997-1003. doi: 10.1093/mmy/myz003.
92. van Ingen J, van der Lee HA, Rijs TA, et al. Azole, polyene and echinocandin MIC distributions for wild-type, TR34/L98H and TR46/Y121F/T289A Aspergillus fumigatus isolates in the Netherlands. *J Antimicrob Chemother* 2015;70(1):178-81. doi: 10.1093/jac/dku364.
93. Vitale RG, de Hoog GS, Schwarz P, et al. Antifungal susceptibility and phylogeny of opportunistic members of the order mucorales. *J Clin Microbiol* 2012;50(1):66-75. doi: 10.1128/jcm.06133-11.
94. Walther G, Zimmermann A, Theuersbacher J, et al. Eye Infections Caused by Filamentous Fungi: Spectrum and Antifungal Susceptibility of the Prevailing Agents in Germany. *J Fungi (Basel)* 2021;7(7) doi: 10.3390/jof7070511.
95. Wang HC, Hsieh MI, Choi PC, et al. Comparison of the Sensititre YeastOne and CLSI M38-A2 Microdilution Methods in Determining the Activity of Amphotericin B, Itraconazole, Voriconazole, and Posaconazole against Aspergillus Species. *J Clin Microbiol* 2018;56(10) doi: 10.1128/jcm.00780-18.
96. Wang HC, Hsieh MI, Choi PC, et al. Species distribution and antifungal susceptibility of clinical Aspergillus isolates: A multicentre study in Taiwan, 2016-2020. *Mycoses* 2023 doi: 10.1111/myc.13593.
97. Wang Y, Zhang L, Zhou L, et al. Epidemiology, Drug Susceptibility, and Clinical Risk Factors in Patients With Invasive Aspergillosis. *Front Public Health* 2022;10:835092. doi: 10.3389/fpubh.2022.835092.
98. Wiederhold NP, Locke JB, Daruwala P, et al. Rezafungin (CD101) demonstrates potent in vitro activity against Aspergillus, including azole-resistant Aspergillus fumigatus isolates and cryptic species. *J Antimicrob Chemother* 2018;73(11):3063-67. doi: 10.1093/jac/dky280.
99. Wiederhold NP, Patterson HP, Tran BH, et al. Fungal-specific Cyp51 inhibitor VT-1598 demonstrates in vitro activity against Candida and Cryptococcus species, endemic fungi, including Coccidioides species, Aspergillus species and Rhizopus arrhizus. *J Antimicrob Chemother* 2018;73(2):404-08. doi: 10.1093/jac/dkx410.
100. Won EJ, Joo MY, Lee D, et al. Antifungal Susceptibility Tests and the cyp51 Mutant Strains among Clinical Aspergillus fumigatus Isolates from Korean Multicenters. *Mycobiology* 2020;48(2):148-52. doi: 10.1080/12298093.2020.1744955.
101. Xu Y, Chen M, Zhu J, et al. Aspergillus species in lower respiratory tract of hospitalized patients from shanghai, China: Species diversity and emerging azole

resistance. *Infect Drug Resist* 2020;13((Xu Y.) Department of Dermatology, The Third People's Hospital of Hangzhou, Hangzhou, China):4663-72.
102. Yamazaki T, Inagaki Y, Fujii T, et al. In vitro activity of isavuconazole against 140 reference fungal strains and 165 clinically isolated yeasts from Japan. *Int J Antimicrob Agents* 2010;36(4):324-31. doi: 10.1016/j.ijantimicag.2010.06.003.
103. Yang X, Chen W, Liang T, et al. A 20-Year Antifungal Susceptibility Surveillance (From 1999 to 2019) for Aspergillus spp. and Proposed Epidemiological Cutoff Values for Aspergillus fumigatus and Aspergillus flavus: A Study in a Tertiary Hospital in China. *Front Microbiol* 2021;12:680884.
104. Yousfi H, Ranque S, Rolain JM, et al. In vitro polymyxin activity against clinical multidrug-resistant fungi. *Antimicrob Resist Infect Control.* 2019;8:66.
105. Zhang H, Tan J, Kontoyiannis DP, et al. Screening the in vitro susceptibility of posaconazole in clinical isolates of Candida spp. and Aspergillus spp. and analyzing the sequence of ERG11 or CYP51A in non-wild-type isolates from China. *Diagn Microbiol Infect Dis* 2019;95(2):166-70.
106. Zhang L, Wang X, Houbraken J, et al. Molecular Identification and In Vitro Antifungal Susceptibility of Aspergillus Isolates Recovered from Otomycosis Patients in Western China. *Mycopathologia* 2020;185(3):527-35.
107. CLSI. Epidemiological Cutoff Values for Antifungal Susceptibility Testing. 4th ed. CLSI supplement M57S. Clinical and Laboratory Standards Institute; 2022.
108. The European Committee on Antimicrobial Susceptibility Testing. Overview of antifungal ECOFFs and clinical breakpoints for yeasts, moulds and dermatophytes using the EUCAST E.Def 7.4, E.Def 9.4 and E.Def 11.0 procedures. Version 4.0, 2023. http://www.eucast.org.
109. Mei-Sheng Riley M. Invasive Fungal Infections Among Immunocompromised Patients in Critical Care Settings: Infection Prevention Risk Mitigation. *Crit Care Nurs Clin North Am* 2021;33(4):395-405.
110. Espinel-Ingroff A, Fothergill A, Fuller J, et al. Wild-type MIC distributions and epidemiological cutoff values for caspofungin and Aspergillus spp. for the CLSI broth microdilution method (M38-A2 document). *Antimicrob Agents Chemother* 2011;55(6):2855-9.
111. Achi ZW, Zacchaeus SL, Gwatau DD, et al. Antifungal activity of terminalia avicennioides in drosophila melanogaster as an infectious model. *Research Journal of Medicinal Plant* 2019;13(2):64-73.
112. Allen M, Poggiali D, Whitaker K, et al. Raincloud plots: a multi-platform tool for robust data visualization. *Wellcome Open Res* 2019;4:63.
113. Arendrup MC, Lockhart SR, Wiederhold N. Candida auris MIC testing by EUCAST and clinical and laboratory standards institute broth microdilution, and gradient

diffusion strips; to be or not to be amphotericin B resistant? *Clin Microbiol Infect* 2025;31(1):108-12.
114. Hussain A, Wang Y, Mo E, et al. Epidemiology and Antifungal Susceptibilities of Clinically Isolated Aspergillus Species in Tertiary Hospital of Southeast China. *Infect Drug Resist* 2024;17:5451-62.
115. Jeanvoine A, Rocchi S, Bellanger AP, et al. Azole-resistant Aspergillus fumigatus: A global phenomenon originating in the environment? *Med Mal Infect* 2020;50(5):389-95.
116. Lockhart SR, Ghannoum MA, Alexander BD. Establishment and Use of Epidemiological Cutoff Values for Molds and Yeasts by Use of the Clinical and Laboratory Standards Institute M57 Standard. *J Clin Microbiol* 2017;55(5):1262-68.
117. European Committee on Antimicrobial Susceptibility Testing – Standard Operating Procedure 10.2 (SOP 10.2) . 2021. MIC distributions and the setting of epidemiological cut-off (ECOFF) values.
118. Revie NM, Iyer KR, Robbins N, et al. Antifungal drug resistance: evolution, mechanisms and impact. *Curr Opin Microbiol* 2018;45:70-76.
119. Wiederhold NP. Emerging Fungal Infections: New Species, New Names, and Antifungal Resistance. *Clin Chem* 2021;68(1):83-90.
120. Sanglard D, Coste A, Ferrari S. Antifungal drug resistance mechanisms in fungal pathogens from the perspective of transcriptional gene regulation. *FEMS Yeast Res* 2009;9(7):1029-50.
121. Fisher MC, Hawkins NJ, Sanglard D, et al. Worldwide emergence of resistance to antifungal drugs challenges human health and food security. *Science* 2018;360(6390):739-42.
122. Berkow EL, Lockhart SR, Ostrosky-Zeichner L. Antifungal Susceptibility Testing: Current Approaches. *Clin Microbiol Rev* 2020;33(3).
123. Salam MA, Al-Amin MY, Pawar JS, et al. Conventional methods and future trends in antimicrobial susceptibility testing. *Saudi J Biol Sci* 2023;30(3):103582.
124. Sánchez-Bautista A, Coy J, García-Shimizu P, et al. From CLSI to EUCAST guidelines in the interpretation of antimicrobial susceptibility: What is the effect in our setting? *Enferm Infecc Microbiol Clin (Engl Ed)* 2018;36(4):229-32.
125. Vasala A, Hytönen VP, Laitinen OH. Modern Tools for Rapid Diagnostics of Antimicrobial Resistance. *Front Cell Infect Microbiol* 2020;10:308.
126. Wang HC, Hsieh MI, Choi PC, et al. Species distribution and antifungal susceptibility of clinical Aspergillus isolates: A multicentre study in Taiwan, 2016-2020. *Mycoses* 2023;66(8):711-22.

127. Cadena J, Thompson GR, 3rd, Patterson TF. Aspergillosis: Epidemiology, Diagnosis, and Treatment. *Infect Dis Clin North Am* 2021;35(2):415-34.
128. Li Y, Wang H, Zhao YP, et al. Antifungal susceptibility of clinical isolates of 25 genetically confirmed Aspergillus species collected from Taiwan and Mainland China. *J Microbiol Immunol Infect* 2020;53(1):125-32.
129. Pfaller MA, Carvalhaes CG, Castanheira M. Susceptibility patterns of amphotericin B, itraconazole, posaconazole, voriconazole and caspofungin for isolates causing invasive mould infections from the SENTRY Antifungal Surveillance Program (2018-2021) and application of single-site epidemiological cutoff values to evaluate amphotericin B activity. *Mycoses* 2023;66(10):854-68.
130. Berger S, El Chazli Y, Babu AF, et al. Azole Resistance in Aspergillus fumigatus: A Consequence of Antifungal Use in Agriculture? *Front Microbiol* 2017;8:1024.
131. Snelders E, Huis In 't Veld RA, Rijs AJ, et al. Possible environmental origin of resistance of Aspergillus fumigatus to medical triazoles. *Appl Environ Microbiol* 2009;75(12):4053-7.
132. Chowdhary A, Kathuria S, Xu J, et al. Emergence of azole-resistant aspergillus fumigatus strains due to agricultural azole use creates an increasing threat to human health. *PLoS pathogens* 2013;9(10):e1003633.
133. Meis JF, Chowdhary A, Rhodes JL, et al. Clinical implications of globally emerging azole resistance in Aspergillus fumigatus. *Philos Trans R Soc Lond B Biol Sci* 2016;371(1709):20150460. doi: 10.1098/rstb.2015.0460.
134. Verweij PE, Kema GH, Zwaan B, et al. Triazole fungicides and the selection of resistance to medical triazoles in the opportunistic mould Aspergillus fumigatus. *Pest Manag Sci* 2013;69(2):165-70. doi: 10.1002/ps.3390.
135. Ribas ERAD, Spolti P, Del Ponte EM, et al. Is the emergence of fungal resistance to medical triazoles related to their use in the agroecosystems? A mini review. *Braz J Microbiol* 2016;47(4):793-99.
136. Verweij PE, Zhang J, Debets AJM, et al. In-host adaptation and acquired triazole resistance in Aspergillus fumigatus: a dilemma for clinical management. *The Lancet Infectious Diseases* 2016;16(11):e251-e60.
137. Buil JB, Hare RK, Zwaan BJ, et al. The fading boundaries between patient and environmental routes of triazole resistance selection in Aspergillus fumigatus. *PLoS Pathog* 2019;15(8):e1007858.
138. Howard SJ, Cerar D, Anderson MJ, et al. Frequency and evolution of Azole resistance in Aspergillus fumigatus associated with treatment failure. *Emerg Infect Dis* 2009;15(7):1068-76.

Table 1. MIC_{50} of antifungal agents for *Aspergillus* isolates and Mucorales isolates

Isolate	MIC method	Drug	No. of studies	Median (mg/L)	Range (mg/L)	Notes
A. flavus	CLSI	Amphotericin B	21	1	0.125-4	—
		Isavuconazole	9	1	0.5-2	—
		Itraconazole	20	0.375	0.12-16	—
		Posaconazole	15	0.25	0.12-0.5	—
		Voriconazole	21	0.5	0.125-1	—
	EUCAST	Amphotericin B	7	4	1-32	—
		Isavuconazole	5	1	0.5-1	—
		Itraconazole	7	0.25	0.12-1	—
		Posaconazole	7	0.125	0.12-1	—
		Voriconazole	9	0.5	0.5-1	—
A. fumigatus	CLSI	Amphotericin B	26	1	0.0625-4	—
		Isavuconazole	10	0.5	0.25-1	—
		Itraconazole	29	0.5	0.125-1	The MIC_{50} range of *A. fumigatus* for Itraconazole was reported to be 0.031-0.25 mg/L in Lei 2011, and this study was not shown in the figure
		Posaconazole	25	0.25	0.03-1	The MIC_{50} of *A. fumigatus* for Posaconazole

Isolate	MIC method	Drug	No. of studies	Median (mg/L)	Range (mg/L)	Notes
						was reported to ≤0.03mg/L in be Arendrup 2016, and this study was not shown in the figure
		Voriconazole	32	0.5	0.125-4	—
	EUCAST	Amphotericin B	7	0.5	0.25-2	—
		Isavuconazole	3	1	0.5-1	—
		Itraconazole	4	0.375	0.125-0.5	—
		Posaconazole	5	0.0925	0.06-0.5	The MIC_{50} of *A. fumigatus* for Posaconazole was reported to ≤0.03mg/L in be Arendrup 2016, and this study was not shown in the figure
		Voriconazole	7	0.5	0.25-4	—
A. niger	CLSI	Amphotericin B	19	0.5	0.0312-8	The MIC_{50} range of *A. niger* for Amphotericin B was reported to be 0.5-1 mg/L in Szigeti 2011, and this study was not shown in the figure
		Isavuconazole	6	2	1-2	—
		Itraconazole	17	1	0.032-4	—
		Posaconazole	12	0.25	0.063-2	—
		Voriconazole	19	1	0.125-2	—
	EUCAST	Amphotericin B	4	0.25	0.12-0.5	—
		Isavuconazole	2	1.25	1-1.5	—

Isolate	MIC method	Drug	No. of studies	Median (mg/L)	Range (mg/L)	Notes
		Itraconazole	3	0.5	0.5-1	—
		Posaconazole	3	0.125	0.12-1	—
		Voriconazole	5	1	0.5-1	—
Mucor spp.	CLSI	Amphotericin B	4	0.375	0.125-0.5	—
		Isavuconazole	5	8	4-8	The MIC_{50} of *Mucor* spp. to Isavuconazole was reported to be >16 mg/L in Borman 2021, >8 mg/L in Carvalhaes 2023, these studies were not shown in the figure
		Itraconazole	5	4	0.25-4	—
		Posaconazole	6	1	0.25-2	—
		Voriconazole	5	16.25	0.5-32	The MIC_{50} of *Mucor* spp. to Voriconazole was reported to be >16 mg/L in Borman 2021, >8 mg/L in Carvalhaes 2021 and Carvalhaes 2023, these studies were not shown in the figure
Rhizomucor spp.	CLSI	Amphotericin B	3	0.375	0.125-0.5	—
		Isavuconazole	4	2	2	—
		Itraconazole	2	0.5	0.5-1	—
		Posaconazole	4	0.5	0.25-0.5	—
		Voriconazole	2	—	—	The MIC_{50} of Rhizomucor spp. to Voriconazole was reported to be >16 mg/L in Borman 2021 and >8 mg/L in Carvalhaes 2023 and these

Isolate	MIC method	Drug	No. of studies	Median (mg/L)	Range (mg/L)	Notes
						studies were not shown in the figure
Rhizopus spp.	CLSI	Amphotericin B	5	0.5	0.25-1	—
		Isavuconazole	6	1	0.5-2	—
		Itraconazole	5	1	0.25-2	—
		Posaconazole	6	0.5	0.25-0.5	—
		Voriconazole	6	8	0.5-8	—

CLSI: Clinical and Laboratory Standards Institute; EUCAST: European Committee on Antimicrobial Susceptibility Testing

CHAPTER 7

General discussion

Future Directions in Managing Azole Resistance in *A. fumigatus*

The rising crisis of azole resistance in *A. fumigatus* represents a paradigm shift in medical mycology, highlighting the intricate connections between agricultural practices, environmental ecology, and human health. This thesis highlights the complex interplay between environmental selection pressure, pathogen evolution, and clinical outcomes, pointing toward an integrated "One Health" approach as the only viable long-term solution. Looking ahead, future work should concentrate on three critical areas to translate current findings into practical interventions.

1. Advancing Precision Diagnostics for Resistance Genotyping in Clinical Practice

The transition from phenotypic to genotypic resistance detection represents the frontier of clinical mycology. Current diagnostic limitations—including the poor sensitivity of culture-based methods and the narrow target spectrum of single-plex PCR assays—have created critical gaps in resistance detection, particularly for emerging non-cyp51A mechanisms and heteroresistant populations. Future implementation should focus on deploying next-generation sequencing technologies directly from patient specimens, including multiplexed targeted amplicon sequencing for comprehensive resistance allele profiling and metagenomic approaches for detecting polyclonal infections. These methods enable simultaneous identification of established resistance markers (TR_{34}/L98H, TR_{46}/Y121F/T289A) and novel variants (e.g., I364V, G448S), while also capturing mixed infections that complicate therapeutic decisions.

A critical parallel initiative involves establishing curated genotype-phenotype correlation databases, validated through CRISPR-Cas9 engineered isogenic strains containing specific resistance mutations. Such repositories will facilitate predictive resistance modeling, allowing clinicians to infer susceptibility profiles from genomic data alone. Furthermore, the development of rapid point-of-care molecular platforms—such as cartridge-based PCR or microfluidic systems—could revolutionize management in critical care settings where time-to-results significantly impacts outcomes. Implementation science research will be essential to integrate these advanced diagnostics into clinical pathways, addressing barriers related to cost, infrastructure, and interpretation expertise. Ultimately, these efforts will pave the way for personalized aspergillosis management, tailoring antifungal therapy based on individual pathogen genetics rather than empirical protocols.

2. Establishing a Global One Health Standardized Surveillance for Cross-Country Comparisons

The transboundary nature of antifungal resistance necessitates a coordinated international surveillance strategy that mirrors successful models in antibiotic resistance monitoring. Future efforts should establish a standardized global network integrating human, animal, and environmental surveillance through harmonized protocols for sample collection, processing, and data sharing. This network must explicitly target key fungal pathogens, prioritizing *A. fumigatus* due to its environmental prevalence and clinical significance, while also encompassing other *Aspergillus* species and major *Candida* species. The surveillance framework should combine pathogen-focused antifungal resistance surveillance (e.g., measuring resistance rates in clinical and environmental isolates) with disease surveillance to monitor the incidence and outcomes of resistant infections. This infrastructure would employ advanced environmental sampling tools including qPCR-enabled spore traps for continuous air monitoring of airborne pathogens like *Aspergillus*, soil metagenomics for tracking resistance reservoirs, and wastewater surveillance for community-level resistance assessment. The integration of satellite remote sensing data on crop treatment patterns and atmospheric spore dispersal models could further enhance predictive capabilities for pathogens with significant environmental dispersal pathways.

Key deliverables include dynamic resistance mapping dashboards visualizing temporal and spatial trends, early warning systems for emerging resistance genotypes, and risk assessment tools quantifying the impact of agricultural fungicide use on clinical resistance rates. Such a system requires robust international governance frameworks—potentially under WHO coordination—to ensure data standardization, equitable participation, and responsible data sharing. Capacity building in low- and middle-income countries will be particularly crucial, as these regions often bear the highest burden of invasive fungal diseases while having limited diagnostic resources. By creating a truly global observatory for antifungal resistance, we can move from reactive containment to proactive prediction and prevention, ultimately informing evidence-based policies on fungicide regulation and antimicrobial stewardship across human and agricultural sectors.

3. Expanding Resistance Assessment to Fungicides and Understanding Collateral Resistance Mechanisms

While azole resistance remains the immediate clinical priority, the potential role of other fungicide classes in selecting for cross-resistance demands urgent investigation. Future research must systematically evaluate the susceptibility of clinical and environmental *A. fumigatus* isolates to widely used non-azole fungicides, including

succinate dehydrogenase inhibitors (SDHIs), quinone outside inhibitors (QoIs), and benzimidazoles. Comprehensive mechanistic studies should identify potential shared resistance pathways, such as efflux pump overexpression mutations that may confer reduced susceptibility to both agricultural fungicides and medical antifungals. Of particular concern is the possibility of collateral resistance—where selection pressure from one fungicide class inadvertently enhances resistance to unrelated compounds through pleiotropic effects or co-selection of resistance determinants.

Expanded environmental monitoring should quantify non-azole fungicide residues in soils, composts, and waterways, correlating these levels with resistance genotypes in adjacent *A. fumigatus* populations. These data are critical for developing and validating environmental risk assessment protocols that can dynamically account for the consequences of fungicides with new modes of action. Advanced molecular techniques, including whole-genome sequencing and transcriptomic profiling, can reveal adaptation signatures specific to different fungicide exposures, thereby supporting the scientific basis for such risk assessments. Insights gained should directly inform registration requirements for fungicide use and strengthen stewardship programs by identifying high-risk combinations of compound use and environmental settings. This integrated approach, aligning with frameworks such as those outlined by the European Food Safety Authority (EFSA), will help shape sustainable agricultural practices that minimize resistance selection while maintaining crop protection efficacy. Furthermore, understanding non-azole resistance mechanisms may reveal novel therapeutic targets for drug development, particularly for pan-resistant isolates that escape current antifungal classes. Adopting this broader ecological and regulatory perspective is essential for developing comprehensive resistance management strategies that address the full spectrum of selection pressures shaping fungal adaptation.

Conclusion: Toward an Integrated Eco-Clinical Framework

The challenge of azole resistance in *A. fumigatus* epitomizes the complex interplay between human activity, environmental change, and pathogen evolution. This thesis provides not merely a description of the problem but a roadmap for transformative action through precision diagnostics, global surveillance, and comprehensive environmental assessment. By implementing these three strategic pillars in a coordinated manner, we can shift from reactive treatment to proactive containment, creating a resilient system capable of adapting to the continuing evolution of fungal pathogens. The success of this endeavor will require unprecedented collaboration across disciplines and sectors, uniting clinicians, microbiologists, agricultural

scientists, policy makers, and public health experts in a common mission to preserve antifungal efficacy for future generations.

REFERENCE

Alanio A, Dellière S, Fodil S, Bretagne S, Mégarbane B. Prevalence of putative invasive pulmonary aspergillosis in critically ill patients with COVID-19. *Lancet Respir Med.* 2020; 8: e48-e49.

Bader O, Weig M, Reichard U, Lugert R, Kuhns M, Christner M, et al. Cyp51A-based mechanisms of aspergillus fumigatus azole drug resistance present in clinical samples from Germany. *Antimicrob Agents Chemother*. 2013;57:3513–7.

Barber AE, Riedel J, Sae-Ong T, et al. Effects of agricultural fungicide use on *Aspergillus fumigatus* abundance, antifungal susceptibility, and population structure. *mBio.* 2020; 11: e02213-20.

Ballard E, Melchers WJG, Zoll J, Brown AJP, Verweij PE, Warris A. In-host microevolution of Aspergillus fumigatus: A phenotypic and genotypic analysis. *Fungal Genet Biol*. 2018; 113:1-13.

Castro-Ríos K, Buri MCS, Ramalho da Cruz AD, Ceresini PC. *Aspergillus fumigatus* in the Food Production Chain and Azole Resistance: A Growing Concern for Consumers. *J Fungi (Basel)*. 2025; 11:252.

Chowdhary A, Sharma C, Meis JF. Azole-resistant aspergillosis: epidemiology, molecular mechanisms, and treatment. *J Infect Dis*. 2017;216: S436–444.

Chowdhary A, Kathuria S, Xu J, Meis JF. Emergence of azole-resistant *Aspergillus fumigatus* strains due to agricultural azole use creates an increasing threat to human health. *PLoS Pathog*. 2013;9: e1003633.

Chowdhary A, Sharma C, Hagen F, Meis JF. Exploring azole antifungal drug resistance in *Aspergillus fumigatus* with special reference to resistance mechanisms. *Future Microbiol*. 2014;9:697–711.

Dieste-Pérez L, Holstege MMC, de Jong JE, Heuvelink AE. Azole resistance in *Aspergillus* isolates from animals or their direct environment (2013-2023): a systematic review. *Front Vet Sci*. 2025; 12:1507997.

European Food Safety Authority (EFSA); European Centre for Disease Prevention and Control (ECDC); European Chemicals Agency (ECHA); European Environment Agency

(EEA); European Medicines Agency (EMA); European Commission's Joint Research Centre (JRC). Impact of the use of azole fungicides, other than as human medicines, on the development of azole-resistant *Aspergillus* spp. EFSA J. 2025; 23(1): e9200.

Feys S, Carvalho A, Clancy CJ, Gangneux JP, Hoenigl M, Lagrou K, Rijnders BJA, Seldeslachts L, Vanderbeke L, van de Veerdonk FL, Verweij PE, Wauters J. Influenza-associated and COVID-19-associated pulmonary aspergillosis in critically ill patients. *Lancet Respir Med*. 2024; 12:728-742.

Fisher MC, Alastruey-Izquierdo A, Berman J, Bicanic T, Bignell EM, Bowyer P, Bromley M, Brüggemann R, Garber G, Cornely OA, Gurr SJ, Harrison TS, Kuijper E, Rhodes J, Sheppard DC, Hagiwara D, Watanabe A, Kamei K, Goldman GH. Epidemiological and genomic landscape of azole resistance mechanisms in Aspergillus fungi. *Front Microbiol*. 2016; 7:1382.

Paluch M, Lejeune S, Hecquet E, Prévotat A, Deschildre A, Fréalle E. High airborne level of *Aspergillus fumigatus* and presence of azole-resistant TR_{34}/L98H isolates in the home of a cystic fibrosis patient harbouring chronic colonisation with azole-resistant H285Y *A. fumigatus*. *J Cyst Fibros.* 2019; 18: 364-367.

Rhodes J, Abdolrasouli A, Dunne K, Sewell TR, Zhang Y, Ballard E, Brackin AP, van Rhijn N, Chown H, Tsitsopoulou A, Posso RB, Chotirmall SH, McElvaney NG, Murphy PG, Talento AF, Renwick J, Dyer PS, Szekely A, Bowyer P, Bromley MJ, Johnson EM, Lewis White P, Warris A, Barton RC, Schelenz S, Rogers TR, Armstrong-James D, Fisher MC. Population genomics confirms acquisition of drug-resistant Aspergillus fumigatus infection by humans from the environment. *Nat Microbiol*. 2022;7:663-674.

Schoustra SE, Debets AJM, Rijs AJMM, et al. Environmental hotspots for azole resistance selection of *Aspergillus fumigatus*, the Netherlands. *Emerg Infect Dis.* 2019; 25: 1347–53.

Lavergne RA, Chouaki T, Hagen F, et al. Home environment as a source of life-threatening azole-resistant *Aspergillus fumigatus* in immunocompromised patients. *Clin Infect Dis.* 2017; 64: 76-78.

Shelton JMG, Collins R, Uzzell CB, et al. Citizen science surveillance of triazole-resistant *Aspergillus fumigatus* in United Kingdom residential garden soils. *Appl Environ Microbiol.* 2022; 88: e0206121.

Singh A, Singh J, Kumar S. Aspergillosis: A comprehensive review of pathogenesis, drug resistance, and emerging therapeutics. *J Food Drug Anal*. 2025;33:75-96.

Ullmann AJ, Aguado JM, Arikan-Akdagli S, et al. Diagnosis and management of

Aspergillus diseases: executive summary of the 2017 ESCMID-ECMM-ERS guideline. *Clin Microbiol Infect.* 2018; 24: Suppl 1: e1-e38.

van de Veerdonk FL, Carvalho A, Wauters J, Chamilos G, Verweij PE. *Aspergillus fumigatus* biology, immunopathogenicity and drug resistance. *Nat Rev Microbiol*. 2025 May 2. doi: 10.1038/s41579-025-01180-z.

Verweij PE, Brüggemann RJM, Azoulay E, Bassetti M, Blot S, Buil JB, Calandra T, Chiller T, Clancy CJ, Cornely OA, et al. 2021. Taskforce report on the diagnosis and clinical management of COVID-19 associated pulmonary aspergillosis. *Intensive Care Med.* 47:819–834.

Verweij PE, Rijnders BJA, Brüggemann RJM, Azoulay E, Bassetti M, Blot S, Calandra T, Clancy CJ, Cornely OA, Chiller T, et al. Review of influenza-associated pulmonary aspergillosis in ICU patients and proposal for a case definition: an expert opinion. *Intensive Care Med*. 2020; 46:1524–1535.

Verweij PE, Song Y, Buil JB, Zhang J, Melchers WJG. Antifungal Resistance in Pulmonary Aspergillosis. *Semin Respir Crit Care Med*. 2024; 45:32-40.

Warris A, White PL, Xu J, Zwaan B, Verweij PE. Tackling the emerging threat of antifungal resistance to human health. *Nat Rev Microbiol*. 2022;20:557-571.

World Health Organization. WHO fungal priority pathogens list to guide research, development and public health action [Internet]. 2022. Available from: https://www.who.int/publications/i/item/9789240060241.

Song Y, Buil JB, Rhodes J, Zoll J, Tehupeiory-Kooreman M, Ergün M, Zhang J, Li R, Bosch T, Melchers WJG, Verweij PE. Triazole-resistant *Aspergillus fumigatus* in the Netherlands between 1994 and 2022: a genomic and phenotypic study. Lancet Microbe. 2025; 6:101114.

Zhang J, Verweij PE, Rijs AJMM, Debets AJM, Snelders E. Flower Bulb Waste Material is a Natural Niche for the Sexual Cycle in *Aspergillus fumigatus*. *Front Cell Infect Microbiol*. 2022; 11:785157.

APPENDIX

SAMENVATTING SUMMARY

RESEARCH DATA MANAGEMENT

CURRICULUM VITAE

PORTFOLIO

LIST OF PUBLICATIONS ACKNOWLEDGEMENTS

SAMENVATTING

Dit proefschrift is opgezet om de kernaspecten van het azoleresistentieprobleem bij *Aspergillus fumigatus* systematisch te onderzoeken. Het gaat verder dan louter documentatie van resistentie en ontleedt de oorsprong, mechanismen, dynamiek en klinische impact ervan. We confronteren nieuwe uitdagingen die voortkomen uit deze evoluerende situatie, met name de milieu-gedreven selectiedruk en de opmerkelijke aanpassingscapaciteit van het pathogeen. Het centrale doel is een dieper, geïntegreerd begrip van azoleresistentie te bieden dat effectieve surveillance, diagnostiek, therapie en milieu-stewardship kan ondersteunen.

Hoofdstuk 1 biedt een uitgebreid overzicht van de opportunistische schimmel *A. fumigatus* en zijn belangrijkste klinische manifestatie, invasieve aspergillose. Het analyseert systematisch de toenemende opkomst van triazoleresistentie, schetst de milieu-oorsprong, de moleculaire en genomische mechanismen achter verminderde azolegevoeligheid en de wereldwijde verspreiding van resistente klonale lijnen. Het hoofdstuk eindigt met een beschrijving van de diagnostische, therapeutische en One Health-uitdagingen die een doeltreffende surveillance en bestrijding van deze bedreiging belemmeren.

Hoofdstuk 2 presenteert een longitudinale genomische en fenotypische analyse van triazoleresistente *A. fumigatus*-isolaten uit Nederland (1994-2022). De studie volgt het ontstaan, de evolutie en de verspreiding van resistentiemechanismen door de tijd en belicht het opkomen van milieu-gebonden resistentiegenotypes.

Hoofdstuk 3 richt zich op de functionele impact van genetische variatie binnen dominante resistentie-achtergronden. Het onderzoekt hoe individuele SNPs en combinaties daarvan het resistentiefenotype beïnvloeden in stammen die de wijdverbreide TR_{34}/L98H-allel dragen, en onthult nuances die de klinische resistentiegraad bepalen.

Hoofdstuk 4 legt de directe link tussen landbouw-fungicidengebruik en klinische resistentie bloot. Door het “landbouw-fungicideresistentieprofiel” in resistente isolaten te karakteriseren, levert dit hoofdstuk bewijs voor de milieu-selectiehypothese en verkent het pad van agrochemische blootstelling naar humane ziekte.

Hoofdstuk 5 bekijkt een intrinsieke factor in de aanpasbaarheid van het pathogeen: een versneld mutator-fenotype. Het onderzoekt hoe verhoogde mutatiesnelheden in specifieke *A. fumigatus*-stammen snelle adaptieve evolutie bevorderen, wat de ontwikkeling van resistentie tegen azolen en andere stressfactoren in zowel milieu-

als klinische niches kan versnellen.

Hoofdstuk 6 biedt een systematische review die gevoeligheidspatronen en resistentie analyseert bij zowel aspergillose- als mucormycosepatiënten. Deze vergelijkende studie benadrukt de specifieke uitdagingen van *Aspergillus*-resistentie binnen het bredere spectrum van moeilijk te behandelen schimmelinfecties.

Hoofdstuk 7 bundelt de bevindingen in een algemene discussie, evalueert kritisch de nieuwe uitdagingen in azoleresistentie, bespreekt implicaties voor klinische praktijk en volksgezondheidsbeleid, en formuleert toekomstgerichte onderzoeksagenda's om deze urgente dreiging het hoofd te bieden.

In breder perspectief beoogt dit proefschrift ons begrip van de complexe krachten achter azoleresistentie in *A. fumigatus* te verdiepen, met nadruk op de nieuwe uitdagingen van milieu-selectie en pathogene evolutie. Door genomische, fenotypische, milieu-, evolutionaire en klinische perspectieven te integreren, draagt het bij aan de wereldwijde inspanning om de werkzaamheid van ons kostbare antifungale arsenaal te behouden.

Summary

This thesis is structured to systematically investigate key facets of the azole resistance challenge in *A. fumigatus*, delves into the multifaceted nature of this crisis, moving beyond simply documenting resistance to dissecting its origins, mechanisms, dynamics, and clinical impact. We confront the novel challenges presented by this evolving landscape, particularly the environmental selection pressure and the remarkable adaptability of the pathogen itself. The central aim is to provide a deeper, more integrated understanding of azole resistance selection to inform effective surveillance, diagnostic, therapeutic, and environmental stewardship strategies.

Chapter 1 a comprehensive overview of the opportunistic filamentous fungus *A. fumigatus* and its principal clinical manifestation, invasive aspergillosis. It systematically examines the escalating emergence of triazole resistance, delineating its environmental genesis, the molecular and genomic mechanisms that underlie reduced azole susceptibility, and the worldwide dissemination of resistant clonal lineages. The chapter culminates by articulating the critical diagnostic, therapeutic, and One Health challenges that currently impede effective surveillance and management of this evolving public-health threat.

Chapter 2 presents a comprehensive genomic and phenotypic analysis of triazole-resistant *A. fumigatus* isolates collected in the Netherlands over nearly three decades (1994-2022). This longitudinal study tracks the emergence, evolution, and dissemination of resistance mechanisms, providing crucial insights into temporal trends and the rise of environmentally linked resistance genotypes.

Chapter 3 shifts focus to the functional impact of genetic variation within predominant resistance backgrounds. It specifically investigates how individual single nucleotide polymorphisms (SNPs) and combinations thereof modulate the azole resistance phenotype in strains harboring the widespread TR_{34}/L98H allele, revealing nuances beyond the core mutation that influence clinical resistance levels.

Chapter 4 directly addresses the critical link between agricultural fungicide use and clinical resistance. By characterizing the "agricultural fungicide resistance signature" in resistant isolates, this chapter provides evidence for the environmental selection hypothesis and explores the potential pathways connecting agrochemical use to human disease.

Chapter 5 explores an intrinsic factor contributing to the pathogen's adaptability: an accelerated mutator phenotype. This chapter investigates how increased mutation rates in specific *A. fumigatus* strains facilitate rapid adaptive evolution, potentially

accelerating the development of resistance to azoles and other stressors within both environmental and clinical niches.

Chapter 6 broadens the perspective through a systematic review, analyzing susceptibility patterns and drug resistance not only in aspergillosis but also in mucormycosis patients. This comparative analysis highlights the specific challenges posed by Aspergillus resistance within the broader context of difficult-to-treat mold infections.

Chapter 7 integrates the findings from the preceding chapters into a General Discussion, critically evaluating the new challenges in azole resistance selection, discussing the implications for clinical practice and public health policy, and proposing directions for future research to combat this urgent threat.

Overall, this thesis aims to advance our understanding of the complex forces driving azole resistance in *A. fumigatus*, emphasizing the novel challenges posed by environmental selection and pathogen evolution. By integrating genomic, phenotypic, environmental, evolutionary, and clinical perspectives, it strives to contribute significantly to the global effort to preserve the efficacy of our vital antifungal armamentarium.

RESEARCH DATA MANAGEMENT

Ethics and privacy

This thesis is based on the results of research that involve fungal isolates, which are cultured from the patient strain collection of the MMB-Mycology diagnostic group. The Radboud University Medical Centre (RUMC) has collected and stored clinical A. fumigatus isolates that contribute to the national Aspergillus resistance surveillance program. The surveillance protocol was submitted to the institutional Medical Research Ethics Committee of RUMC (CMO) who indicated that the study was waived from the evaluation procedure as anonymous information was used (December 2020). The treatment data collection from electronic patient files was performed by personnel with a treatment relationship with the patient. The privacy of the participants in these studies was warranted using fully anonymous data. For chapter 2 data was used that was previously collected in the context of healthcare. The reuse of healthcare data is aligned with applicable laws, regulations and the national Code of Conduct for Health Research.

Data collection and storage

Data for chapter 3 to 5 was obtained through laboratory experiments involving anonymous or non-human materials. Data for chapter 2 was extracted, by using the Cliniquest application (CliniQuest (radboudumc.nl)), from (electronic) health records (EPIC). Data for chapter 6 is based on existing data which was obtained from published literature. All raw data, as well as its interpretation and protocols, are saved on the MMB-Mycology research department external hard drive, and the university servers belonging to the department of Medical Microbiology of the RadboudUMC. To ensure interpretability of the data, all filenames, primary and secondary data, metadata, descriptive files and program code and scripts used to provide the final results are documented along with the data.

Data sharing according to the FAIR principles

Chapters 2 and 6 are published open access. The sequencing data have been submitted to the European Nucleotide Archive (ENA) under accession number PRJEB63121. Chapters 3, 4, 5 have been submitted for publication and are currently under review. The data used in the unpublished chapter 3,4 and 5 are archived at the MMB-Mycology research department external hard drive, and the university servers belonging to the department of Medical Microbiology of the RadboudUMC. Upon publication of the chapter the data will be published with open access.

LIST OF PUBLICATIONS

1. **Song Y**, Buil JB, Rhodes J, Zoll J, Tehupeiory-Kooreman M, Ergün M, Zhang J, Li R, Bosch T, Melchers WJG, Verweij PE. Triazole-resistant *Aspergillus fumigatus* in the Netherlands between 1994 and 2022: a genomic and phenotypic study. *Lancet Microbe*. 2025;6(8):101114.

2. Liang T, Meng X, Liu X, de Hoog GS, **Song Y***, Li R*****. Disseminated cutaneous mucormycosis resembling multiple panniculitis. *Int J Dermatol*. 2025;64(8):1485-1487.

3. Li Y, **Song Y***, Wang A*****. Successful Treatment of Chromoblastomycosis caused by *Cladophialophora carrionii* with Itraconazole: Clinicopathology, Susceptibility, and Molecular Identification of a Case in Northern China. *Am J Trop Med Hyg*. 2024;112(4):865-867.

4. Shao Y, Shao J, de Hoog S, Verweij P, Bai L, Richardson R, Richardson M, Wan Z, Li R*, Yu J*, **Song Y***. Emerging antifungal resistance in *Trichophyton mentagrophytes*: insights from susceptibility profiling and genetic mutation analysis. *Emerg Microbes Infect*. 2025;14(1):2450026.

5. Liu X, Zhou S, Yan R, Xia C, Xue R, Wan Z, Li R, de Hoog S, Ahmed SA, Wang Q*, **Song Y***. Evaluation of metagenomic next-generation sequencing (mNGS) combined with quantitative PCR: cutting-edge methods for rapid diagnosis of non-invasive fungal rhinosinusitis. *Eur J Clin Microbiol Infect Dis*. 2025;44(1):17-26.

6. Liang T, Chen X, de Hoog GS, Li L, Wang L, Wan Z, Yu J, Li R*, **Song Y***. Antifungal Resistance Patterns of *Microsporum canis*: A 27-Year MIC Study in Mainland China. *Mycoses*. 2025;68(1): e70020.

7. Ji Y, Li Y, Wu W, de Hoog S, Wan Z, Wang Q, Zhang H, Yu J, Niu X, Li R, Liu W, **Song Y**. Antifungal Susceptibility of Melanized Fungi Isolated from CARD9 Deficient Patients: Implications for Treatment of Refractory Infections. *Mycopathologia*. 2025;190(2):29.

8. Verweij PE, **Song Y**, Buil JB, Zhang J, Melchers WJG. Antifungal Resistance in Pulmonary Aspergillosis. *Semin Respir Crit Care Med*. 2024;45(1):32-40.

9. Liu X, Li R, **Song Y***, Wang A*. Eumycetoma with Atypical Manifestation Caused by Fusarium: First Case Diagnosed by PCR and Next-Generation Sequencing in China. *Mycopathologia*. 2024;189(2):18.

10. **Song Y**, Hu S, de Hoog G S, Liu X, Meng X, Xue R, van Diepeningen A D, Fokkens

L, Li R Y, Gao S. Medical Fusarium: novel species or uncertain identifications? *Mycosphere*. 2023, 14(1): 2263-2283.

11. **Song Y#**, Wang X#, Li Q, Zhang R, de Hoog S, Li R. Fatal dermatophytic pseudomycetoma in a patient with non-HIV CD4 lymphocytopenia. *Emerg Microbes Infect*. 2023;12(1):2208685.

12. Wang Q#, **Song Y#**, Han D, et al. The first suspected disseminated Hormographiella aspergillata infection in China, diagnosed using metagenomic next-generation sequencing: a case report and literature review. *Emerg Microbes Infect*. 2023;12(1):2220581.

13. Wang R, Liu W, Liu X, Wan Z, Sybren de Hoog, G, Li R*, **Song, Y***. Comparative analysis of whole genomes and transcriptomes of Microsporum canis from invasive dermatophytosis and tinea capitis. *Emerg Microbes Infect*. 2023;12(1):2219346.

14. **Song Y**, Liu X, Stielow B, Sybren de Hoog G*, Li R*. Post-translational changes in *Phialophora verrucosa via* lysine lactylation during prolonged presence in a patient with a *CARD9*-related immune disorder. *Front Immunol*. 2022; 13:966457.

15. Liu X, **Song Y***, Li R*. The use of combined PCR, fluorescence in situ hybridisation and immunohistochemical staining to diagnose mucormycosis from formalin-fixed paraffin-embedded tissues. *Mycoses*. 2021;64(12):1460-1470.

16. **Song Y**, Liu X, Yang Z, Meng X, Xue R, Yu J, Al-Hatmi AMS, de Hoog GS, Li R. Molecular and MALDI-ToF MS differentiation and antifungal susceptibility of prevalent clinical Fusarium species in China. *Mycoses*. 2021;64(10):1261-1271.

17. **Song Y**, Menezes da Silva N, Vicente VA, Quan Y, Teixeira M, Gong J, de Hoog S*, Li R*. Comparative genomics of opportunistic *Phialophora* species involved in divergent disease types. *Mycoses*. 2021, 64(5):555-568.

18. **Song Y**, Chen X, Yan Y, Wan Z, Liu W, Li R*. Prevalence and antifungal susceptibility of pathogenic yeasts in china: a 10-year retrospective study in a teaching hospital. *Front Microbiol*. 2020.3; 11:1401.

19. Yang X#, **Song Y#**, Liang T, Wang Q, Li R, Liu W. Application of laser capture microdissection and PCR sequencing in the diagnosis of *Coccidioides* spp. infection: A case report and literature review in China. *Emerg Microbes Infect*. 2021. 10(1):331-341.

20. **Song Y**, Silva NM, Weiss VA, Vu Dong, Moreno LF, Vicente VA, Li Ruoyu*, de Hoog Sybren*. Comparative genomic analysis of capsule-producing black yeasts *Exophiala dermatitidis* and *Exophiala spinifera*, potential agents of disseminated mycoses. *Front Microbiol*, 2020. 8; 11: 586.

21. **Song Y**, Du M, Menezes da Silva N, Yang E, Vicente VA, Sybren de Hoog G*, Li R*. Comparative analysis of clinical and environmental strains of *Exophiala spinifera* by long-reads sequencing and RNAseq reveal adaptive strategies. *Front Microbiol*. 2020. 31; 11: 1880.

22. **Song Y**, Laureijssen-van de Sande WWJ, Moreno LF, Gerrits van den Ende B, Li R*, de Hoog Sybren*, Comparative ecology of capsular *Exophiala* species causing disseminated infection in humans, *Front Microbiol*, 2017, 8:2514.

23. **Song Y**#, Liu X#, de Hoog GS, Li R. Disseminated Cryptococcosis presenting as cellulitis diagnosed by laser capture microdissection: a case report and literature review. *Mycopathologia*. 2021.186(3), 423–433.

24. Tan J#, **Song Y**#, Liu W, Wang X, Zhang J, Chen W, Li R, Liu W. Molecular genotyping of *Candida albicans* isolated from different sites may trace the etiological infection routes: Observation in China. *Mycoses*. 2021; 64(8):841-850.

25. Jiang Y#, Luo W#, Verweij PE, **Song Y***, Zhang B, Shang Z, Al-Hatmi AMS, Ahmed SA, Wan Z, Li R, de Hoog GS. Regional differences in antifungal susceptibility of the prevalent dermatophyte Trichophyton rubrum. *Mycopathologia*. 2021; 186(1):53-70.

26. Lei Y#, **Song Y**#, Shu Y#, et al. Fungal antigenemia in patients with severe Coronavirus disease 2019 (COVID-19): The facts and challenges. *J Microbiol Immunol Infect*. 2020; S1684- 1182(20)30124-9.

27. Liu X, Li R, **Song Y***, Wang A*. Generalized tinea corporis caused by *Trichophyton verrucosum* misdiagnosed as allergic dermatitis and erythema annulare in an adult. *Int J Infect Dis*. 2021; 113:339-340.

28. Liu X#, **Song Y**#, Li R, Wang A. Diagnosis of *Aspergillus* species in paraffin-embedded tissue with low fungal loads. *Mycopathologia*. 2021; 186(2):307-308.

29. Zhu P, Shao J, Wang R, Xiao Y, Zhou Y, Li Q, Song Y, Wan Z, Li R, Yu J. Development and Clinical Detection of Rapid Molecular Diagnostic System for Pathogenic Dermatophytes of Tinea Capitis of Multiple Centres in China. *Mycoses*. 2025;68(1): e70008.

30. Shao J, **Song Y**, Zhou Y, Wan Z, Li R, Yu J. Diagnostic value of fluorescein-labeled chitinase staining in formalin-fixed and paraffin-embedded tissues of fungal disease. *Med Mycol*. 2020; 58(1):66-70.

31. Shao J, Yu J, **Song Y**, Wang A. Erythematous plaque on the left lower eyelid following trauma. *J Dtsch Dermatol Ges*. 2021; 19(3):471-474.

32. Wang R, **Song Y**, Du M, et al. Skin microbiome changes in patients with interdigital tinea pedis. *Br J Dermatol*. 2018; 179(4):965-968.

33. Jia QY, **Song YG**, Li XQ, Mu ZL, Li RY, Li HM. Simultaneous infection of the skin surface and dermal tissue with two different fungus mimicking pyoderma gangrenosum: a case report. *Clin Cosmet Investig Dermatol*. 2021; 14:163-167.

34. Shao J, Yu J, **Song Y**, Wang A. Erythematöse plaque auf dem linken unterlid nach verletzung. *J Dtsch Dermatol Ges*. 2021; 19(3):471-474. German.

35. Zhang Y, Huang C, **Song Y**, Ma Y, Wan Z, Zhu X, Wang X, Li R. Primary cutaneous aspergillosis in a patient with CARD9 deficiency and *Aspergillus* susceptibility of Card9 knockout mice. *J Clin Immunol*. 2021; 41(2):427-440.

36. Huang C, Zhang Y, **Song Y**, Wan Z, Wang X, Li R. Phaeohyphomycosis caused by *Phialophora americana* with CARD9 mutation and 20-year literature review in China. *Mycoses*. 2019; 62(10):908-919.

37. Wei LW, Wang H, **Song YG**, Yu J. Disfiguring *Mucor irregularis* infection cured by amphotericin b and itraconazole: a case report and treatment experience. *Mycopathologia*. 2019; 184(5):677-682.

38. Wu W, Zhang R, Wang X, **Song Y**, Li R. Subcutaneous infection with dematiaceous fungi in Card9 knockout mice reveals association of impair neutrophils and Th cell response. *J Dermatol Sci*. 2018; 92(2): 215 – 218.

39. Wu W, Zhang R, Wang X, **Song Y**, Liu Z, Han W, Li R. Impairment of immune response against dematiaceous fungi in Card9 knockout mice. *Mycopathologia*. 2016; 181(9-10):631-42.

40. Verweij PE, **Song Y**, Buil JB, Zhang J, Melchers WJG. Antifungal Resistance in Pulmonary Aspergillosis. Semin Respir Crit Care Med. 2024 Feb;45(1):32-40.

PhD portfolio of Yinggai Song

Department: Medical Microbiology
PhD period: 15/11/2021 – 14/11/2024
PhD Supervisor(s): prof. dr. P.E. Verweij
PhD Co-supervisor(s): dr. W.J.G. Melchers, prof. dr. G.S. de Hoog

Training activities	Hours
Courses	
- Radboudumc - Introduction day (2022)	6.00
- RIMLS - Introduction course "In the lead of my PhD" (2022)	15.00
- Radboudumc - Scientific integrity (2023)	20.00
- Radboudumc - Scientific integrity (2024)	20.00
Seminars	
- RCI Seminar with topic: Transition of Research Theme Infectious Diseases & Global Health into new Research Programs. (2023)	1.00
- Research Integrity Round (2023)	2.00
- RCI Seminar with topic: CD8 T cell imaging in covid patients (2023)	1.00
- 6th ECMM Educational symposium (2023)	16.00
- RCI Seminar with topic: Human SARS-CoV-2 challenge resolves local and systemic response dynamics. (2023)	1.00
- Research Community Infectious Diseases (2024)	1.00
Conferences	
- NVMy Fungal Update Meeting 2022 (2022) (oral)	8.00
- The 21st Congress of the International Society for Human and Animal Mycology (ISHAM) (2022) (oral)	32.00
- 33rd European Congress of Clinical Microbiology and Infectious Diseases (2023) (oral)	24.00
- NVMy Fungal Update Meeting (2023) (oral)	8.00
- 11th Trends in Medical Mycology 2023 (TIMM-11) (2023) (poster)	20.00
- 11th Advances Against Aspergillosis and Mucormycosis Conference 2024 (2024) (poster)	20.00
- 34th ESCMID Global: ESCMID Global 2024 (2024) (poster)	24.00
- 12th International mycology conference (2024) (poster)	20.00
- The 8th Congress secretariat of Asia-Pacific Society for Medical Mycology-APSMM2024 (2024) (oral)	40.00
- FungalDx24 (Fungal Diagnostics in Clinical Practice) (2024)	16.00
- The 22nd ISHAM Congress 2025 (2025) (oral)	40.00
- ASM Microbe 2025 (2025) (oral)	30.00
- 12th Congress on Trends in Medical Mycology (TIMM-12) (2025) (poster)	24.00
Teaching activities	
Supervision of internships / other	
- Supervision of Bachelor Student Trang Nguyen (6 mths) (2022)	60.00
Total	**449.00**

CURRICULUM VITAE

Yinggai Song, born on December 5, 1986, in Henan Province, China, earned her Bachelor of Medicine (2006–2011) in the five-year clinical medicine program at Henan Medical University. She then completed a Master's degree in Pathogenic Microbiology (2012–2015) at Capital Medical University, Beijing, before pursuing a Ph.D. in Dermatology and Venereology (2015–2018) at Peking University. During her doctoral studies she spent 2017 as a joint-training Ph.D. student under Professor Sybren de Hoog at the Westerdijk Fungal Biodiversity Institute in Utrecht, the Netherlands, specializing in medical mycology. After obtaining her Ph.D. in 2018, she joined the Department of Dermatology and Venereology at Peking University First Hospital as an attending physician and researcher. In 2021, supported by the China Scholarship Council's Young Faculty Overseas Training Program, she moved to Radboud University Medical Center, Nijmegen, the Netherlands, to conduct research on azole resistance in Aspergillus species. She is a Young Council Member of the International Society for Human and Animal Mycology (ISHAM) and Chair of the ISHAM Working Group on Chromoblastomycosis and Dematiaceous Fungi, currently leading more than ten active grants focused on cutaneous infectious diseases and invasive fungal infections.

ACKNOWLEDGEMENTS

The past few years have been an extraordinary chapter of my life, and I am deeply grateful to everyone who made this journey unforgettable. Words fall short, yet I wish to express my heartfelt thanks to those without whom this PhD would never have become a reality.

Dear Paul, long before I left China, working with you was my most cherished dream. Thank you for welcoming me into your laboratory, for your supervision, sharing your knowledge and unconditional support to me. You have shown me—once more—that with determination and vision, any goal is within reach. It has been a privilege to learn from you.

Dear Sybren, you have been my mentor and collaborator on black yeast, Fusarium and Trichophyton for more than nine years. Your constant encouragement, lightning-fast replies to every question, and steadfast faith in my potential have illuminated every step of this path. Thank you for inspiring me and most importantly always making time for me and my students, no matter how demanding your schedule.

Dear Willem, thank you for your guidance. At every group meeting you offered brilliant suggestions, and every time I reached out, your response was swift. Your humor and attentiveness have filled my Ph.D. journey with brilliance.

Dear Prof. Ruoyu Li, I know that I can't thank you enough. You made a huge contribution to my academic achievements and give me so many chances to visit international outstanding mycology centers and broad my view. I am thankful for all the values that you added in my both professional and private life. Thank you so much for supporting and trusting me. Thank you for giving me opportunities and standing by me with my decisions.

Thanks to my dear friends at Radboudumc—Shaoqin, Chao, Yu, Jianhua, Yabin, Xin, Meizhu, Xueke and Na—thank you for the laughter, the late-night conversations, and the countless memories that turned Nijmegen into a second home.

Special thanks to Jochem, Marlou, Jan, Tim, Bart, Han, Marion and Hanka: your kindness, patience, and camaraderie made the laboratory a place of both discovery and joy. I have learned so much from each of you, and your support made every challenge lighter. Thank you for your friendship and the good times we had together in Nijmegen!

My dear colleague and friends, thank you for your generosity, your collaboration, and

the warmth that turned colleagues into family. I will always remember our days in Nijmegen. It was awesome to work together with you! I will always be grateful for your kindness and helpfulness. Thank you for all!

Radboudumc
university medical center
IN DEI NOMINE FELICITER
Radboud University